Comparing the regulation and function of *FLOWERING LOCUS T* homologues in *Brassica napus*

Inaugural-Dissertation

zur

Erlangung des Doktorgrades

der Mathematisch-Naturwissenschaftlichen Fakultät

der Universität zu Köln

vorgelegt von

Juanjuan Wang

aus Jiangxi, China

Köln, March 2024

Comparing the regulation and function of *FLOWERING LOCUS T* homologues in *Brassica napus*

Inaugural-Dissertation

zur

Erlangung des Doktorgrades

der Mathematisch-Naturwissenschaftlichen Fakultät

der Universität zu Köln

vorgelegt von

Juanjuan Wang

aus Jiangxi, China

Köln, March 2024

Max Planck Institute
for Plant Breeding Research

Die vorliegende Arbeit wurde am Max-Planck-Institut für Züchtungsforschung in Köln in der Abteilung für Entwicklungsbiologie der Pflanzen (Direktor Prof. Dr. G. Coupland) angefertigt

Berichterstatter: Prof. Dr. George Coupland
Berichterstatter: Prof. Dr. Ute Höcker

Beisitzerin/ Schriftführerin: Dr. Franziska Turck
Prüfungsvorsitzender: Prof. Dr. Stanislav Kopriva

Tag der mündlichen Prüfung: 27.02.2024

MAX-PLANCK-GESELLSCHAFT

Abstract

Brassica napus, a crop that greatly contributes to global agricultural economies, originated approximately 7,500 years ago through interspecific hybridization between *Brassica rapa* and *Brassica oleracea*, resulting in a complex genome with A and C sub-genomes. Flowering time is a crucial phenological trait that directly affects the yield potential and economic sustainability of *B. napus*. In *Arabidopsis thaliana*, the *FLOWERING LOCUS T* (*FT*) gene plays a pivotal role in flowering regulation. It encodes florigen, a mobile signal that is synthesized in leaves and moves to the apical meristem to trigger the transition from vegetative to reproductive growth. Despite the well-characterized functions and regulatory mechanisms of *FT* in *A. thaliana*, knowledge about the *FT* homologues in *B. napus*, a species belonging to the same family as *A. thaliana*, is relatively limited.

To address this, we identified and characterized eight *FT* homologues in *B. napus*. Among these genes, four *BnFT* genes show synteny among *A. thaliana*, *Schrenkiella parvula* and *B. napus*, two out of the three *NEW SISTER OF FT AND TSF* (*NFT*) genes that possess synteny only among the *B. napus* and *S. parvula* were predicted to be pseudogenes, and a *C-GENOME SISTER OF FT AND TSF* (*CFT*) gene is unique to *B. napus* and the C-genome parent, *B. oleracea*, but absent from *S. parvula* and *A. thaliana*. In inter-species complementation experiments, six functional *FT* homologues all exhibited weaker complementation ability compared to *FT*, but when expressed directly in the shoot apical meristem, four *BnFTs* exhibited a similar and strong florigen function as *FT*, whereas *BnNFT.A7* and *BnCFT.C4* still showed reduced florigen activity. Furthermore, four *BnFT* genes contain conserved sequence Block A, Block C and Block E in their flanking sequences, which are known to be involved in the transcriptional regulation of *FT*. The four *BnFT* genes are expressed predominantly in long-day conditions, showing an upward parabola of diurnal expression with the lowest expression at ZT8. By contrast, *BnNFT.A7* and *BnCFT.C4* showed an irregular diurnal expression pattern, with lower levels of expression without a photoperiodic bias. Additionally, the expression level of the four *BnFT* genes was inversely proportional to the distance between Block A and Block E. A comparative analysis of the diurnal expression patterns of the *FT* gene regulatory network in *B. napus* and *A. thaliana* revealed not only similarities, but also some differences in expression patterns.

In summary, the findings of this thesis provide insights into the evolution of *FT* homologues from *A. thaliana*, *S. parvula* and *B. napu*; confirmed the conserved florigen functions of *BnFT* homologues; as well as revealed a similarities and differences in the flowering regulation network between *A. thaliana* and *B. napus*.

Zusammenfassung

Brassica napus, eine Kulturpflanze, die einen großen Beitrag zur globalen Agrarwirtschaft leistet, entstand vor etwa 7.500 Jahren durch interspezifische Hybridisierung zwischen *Brassica rapa* und *Brassica oleracea*, was zu einem komplexen Genom mit A- und C-Subgenomen führte. Die Blütezeit ist ein entscheidendes phänologisches Merkmal, das sich direkt auf das Ertragspotenzial und die wirtschaftliche Nachhaltigkeit von *B. napus* auswirkt. In *Arabidopsis thaliana* spielt das Gen *FLOWERING LOCUS T* (*FT*) eine zentrale Rolle bei der Regulierung der Blüte. Es kodiert für Florigen, ein mobiles Signal, das in den Blättern synthetisiert wird und zum apikalen Meristem wandert, um den Übergang vom vegetativen zum reproduktiven Wachstum auszulösen. Trotz der gut charakterisierten Funktionen und Regulationsmechanismen von *FT* in *A. thaliana* ist das Wissen über das *FT*-Gen in *B. napus*, einer Art, die wie *A. thaliana* zu den Brassicaceen gehört, relativ begrenzt.

Um dies zu untersuchen, haben wir acht *FT*-Homologe in *B. napus* identifiziert und charakterisiert. Unter diesen Genen zeigen vier *BnFT*-Gene Syntenie zwischen *A. thaliana*, *Schrenkiella parvula* und *B. napus*, zwei der drei *NEW SISTER OF FT AND TSF* (*NFT*)-Gene, die Syntenie nur zwischen *B. napus* und *S. parvula* aufweisen, wurden als Pseudogene vorhergesagt, und ein *C-GENOME-SISTER OF FT AND TSF* (*CFT*) ist nur bei *B. napus* und dem C-Genom-Elternteil *B. oleracea* vorhanden. In heterologen Komplementierungsexperimenten wiesen sechs funktionale *FT*-Homologe im Vergleich zu *FT* eine schwächere Komplementierungsfähigkeit in *A. thaliana ft* Mutanten auf. Wenn sie jedoch direkt im Sprossapikalmeristem exprimiert wurden, zeigten vier *BnFTs* eine ähnliche und starke florigene Funktion wie *FT*, während *BnNFT.A7* und *BnCFT.C4* immer noch eine reduzierte florigene Aktivität aufwiesen. Außerdem enthalten vier *BnFT*-Gene in ihren flankierenden Sequenzen die konservierten Sequenzen Block A, Block C und Block E, von denen bekannt ist, dass sie an der Transkriptionsregulierung von *FT* beteiligt sind. Die vier *BnFT*-Gene werden vorwiegend unter Langtagsbedingungen exprimiert und zeigen eine aufsteigende Parabel der täglichen Expression mit der niedrigsten Expression bei ZT8. Im Gegensatz dazu zeigten *BnNFT.A7* und *BnCFT.C4* ein unregelmäßiges tageszeitliches Expressionsmuster mit niedrigeren Expressionswerten ohne photoperiodische Tendenz. Darüber hinaus war das Expressionsniveau der vier *BnFT*-Gene umgekehrt proportional zum Abstand zwischen Block A und Block E. Eine vergleichende Analyse der tageszeitlichen Expressionsmuster des *FT*-Genregulationsnetzwerks in *B. napus* und *A. thaliana* ergab nicht nur Ähnlichkeiten, sondern auch einige Unterschiede in den Expressionsmustern.

Zusammenfassend lässt sich sagen, dass die Ergebnisse dieser Arbeit Einblicke in die Evolution der

FT-Homologe von *A. thaliana*, *S. parvula* und *B. napu* gewähren, die konservierten florigenen Funktionen der *BnFT*-Homologe bestätigen sowie Gemeinsamkeiten und Unterschiede im Netzwerk der Blütenregulation zwischen *A. thaliana* und *B. napus* aufzeigen.

Abstract

Table of Content

Abstract I
Zusammenfassung II
Table of Content V
1. Introduction 1
1.1 Introduction to *B. napus* 1
1.1.1 Introduction to the *Brassicaceae* 1
1.1.2 The origin and importance of *B. napus* 1
1.2 *FLOWERING LOCUS T* (*FT*) plays a central role in the promotion of flowering in the model plant *A. thaliana* 2
1.2.1 Flowering time is important for plants 2
1.2.2 FT, the *A. thaliana* florigen belongs to the PEBP family 3
1.2.3 Flowering pathways converge on the transcriptional regulation of *FT* 4
1.2.4 Induction of flowering by FT protein in the shoot apical meristem 6
1.3 The transcriptional regulation of *FT* in *A. thaliana* 7
1.3.1 The transcriptional activation of *FT* via the photoperiod-responsive pathway 7
1.3.2 The repressive transcriptional regulation of *FT* 8
1.3.3 Chromatin-mediated regulation of FT expression 9
1.4 Beyond flowering-time regulation 12
1.4.1 *FT* is a conserved activator of flowering in diverse plant species 12
1.4.2 *FT* executes multiple functions in addition to promoting flowering 13
1.5 Current flowering research in *B. napus* 14
1.5.1 Identification of *FT* homologues and their functional characterization in *B. napus* 14
1.5.2 The genome characteristics of *B. napus* 15
1.6 Aims of this study 16
2. Materials and Methods 18
2.1 Plant material and growth conditions 18
2.2 Genomic sequence collection and phylogenetic analysis 18
2.3 Online webtool analysis 19
2.4 Gene expression analysis 19
2.4.1 RNA extraction and reverse transcription 19
2.4.2 Reverse transcription-quantitative polymerase chain reaction (RT-qPCR) 20
2.5 Isolation of DNA and purification of PCR products 20

Table of Content

2.6 Plasmid construction 20
2.6.1 Plasmid for *ft-10* complementation 20
2.6.2 Plasmid for tobacco infiltration 21
2.7 Gibson assembly and *Agrobacterium*-mediated transformation 22
2.8 Transgenic plant generation and selection 23
2.9 Tobacco infiltration 24
2.9.1 Infiltration 24
2.9.2 Luciferase signal quantification 24
2.10 Transcriptome analysis 25
3. Results 26
3.1 Documentation of *B. napus* growth and development in different environmental conditions 26
3.2 Four *BnFT* genes, two *BnNFT* genes and one *BnCFT* gene exist in *B. napus* 29
3.2.1 Identification of *BnFT* homologues 29
3.2.2 Phylogenetic analysis of *BnFT* candidates 32
3.3 Preparation for expression data analysis 34
3.3.1 Sequence alignment of *FT* and BnFT-like genes 34
3.3.2 qPCR primer design 35
3.4 Tissue-specific expression data 36
3.4.1 The paraclade leaf exhibits consistently higher gene expression than other tissues 36
3.4.2 Similar tissue-specific expression patterns in Westar and ZS11 37
3.5 Protein function validation 38
3.5.1 High protein similarity among FT, BnFTs, BnNFT and BnCFT 38
3.5.2 Mutation of the last amino-acid of BnFT.A7and BnFT.C6 affects their complementation ability 39
3.5.3 The low complementation abilities of *BnFT.C6*, *BnNFT.A7* and *BnCFT.C4* were increased by expressing them from the *FD* promoter 41
3.6 Photoperiod-responsive expression analysis 42
3.6.1 Three *BnFT* homologues show vernalization- and photoperiod-responsive expression 42
3.6.2 *BnCOs* exhibit a similar expression to *CO* in LDs 44
3.7 Conservation of *cis*-regulatory regions at FT-related genes in *B. napus* 45
3.7.1 Four *BnFT* homologues all show conservation of Block C, Block A and Block E 45
3.7.2 Flowering-time motifs are generally conserved among *FT* and *BnFT* homologues 47
3.7.3 An inverse relationship exists between Block distances and the expression level of *BnFT* genes 49
3.7.4 An inverse relationship between the distances between *cis*-regulatory sequence blocks and expression level was confirmed in tobacco infiltration assay 50

3.8 Transcriptome analysis 52
3.8.1 Principal component analysis 52
3.8.2 Combinational expression analysis of key flowering genes 53
4. Discussion 56
4.1 Either LDs or vernalization are sufficient to initiate flowering in ZS11 56
4.2 Four *FT* homologues were identified in *B. napus* 57
4.3 Florigen function of BnFT homologues 59
4.4 The *B. napus FT* homologues show different photoperiod-responsive expression patterns to *A. thaliana FT* 60
4.5 An inverse relationship exists between promoter length and expression level 61
4.6 Parallel flowering regulatory pathways between *A. thaliana* and *B. napus* 62
5 Conclusion and Perspectives 64
6. References 65
7. Appendix 83
8. Abbreviations 90
Erklärung zur Dissertation 98
Delimitation of own contribution 99
Acknowledgements 100
Curriculum Vitae 101

Table of Content

1. Introduction

1.1 Introduction to *B. napus*

1.1.1 Introduction to the *Brassicaceae*

The Brassicaceae family contains over 3,700 species that possess a wide range of genetic and morphological variations (Cheng et al., 2014). The family is particularly important for agriculture, and it contains several economically important crops. In particular, some Brassica species have become dietary staples in numerous regions around the world and play a critical role in sustaining agricultural productivity (Jahangir et al., 2009; Maggioni et al., 2018).

Polyploidisation has played an important role in the evolution of the Brassicaceae (Lysak and Koch, 2011), and it has been hypothesised that nearly half of the Cruciferae taxa originated as recent polyploids (Franzke et al., 2011). All Cruciferae taxa have at least three palaeopolyploid events known as α, β, and γ whole-genome duplications (WGDs) (Bowers et al., 2003; Haudry et al., 2013). In addition, a later whole-genome triplication event in diploid Brassicas was identified through cytogenetic studies (Lysak et al., 2005; Ziolkowski et al., 2006), early comparative genetic mapping (Parkin et al., 2005), and whole-genome sequencing of Brassicaceae (Wang et al., 2011). Brassica species and *A. thaliana* diverged from a common ancestor of about 14.5–20.4 million years ago (Blanc et al., 2003; Bowers et al., 2003; Yang et al., 1999). The Brassica genus contains six cultivated members, as elucidated by the 'Triangle of U' framework, which was established through cytogenetic analysis and crossing experiments (Nagaharu, 1935). These members can be categorized into three diploid species: *Brassica rapa* (A genome), *Brassica nigra* (B genome), and *Brassica oleracea* (C genome). The *B. rapa* (A) and *B. oleracea* (C) genomes are more closely related to each other than to the *B. nigra* (B) genome. The *B. nigra* lineage was predicted to have diverged from the *B. rapa* and *B. oleracea* lineages approximately 7.9 MYA, and to have been followed by the separation of the A and C lineages about 3.7 MYA (Inaba & Nishio, 2002; Panjabi et al., 2008). Furthermore, hybridization among these three species caused the speciation of three allotetraploids: *Brassica juncea* (AABB), *Brassica napus* (AACC), and *Brassica carinata* (BBCC).

1.1.2 The origin and importance of *B. napus*

Brassica napus (AACC, 2n = 38), most commonly known as oilseed rape or canola, is one of the earliest allopolyploid oilcrops in temperate regions. It originated about 7,500 years ago through

natural hybridization between its diploid progenitors *B. rapa* (AA, 2n = 20) and *B. oleracea* (CC, 2n = 18) likely in the Mediterranean region (Chalhoub et al., 2014; Lu et al., 2019). No truly wild populations of *B. napus* have been documented, which is probably due to the morphologically diverse subspecies and long history of cultivation of its progenitors *B. rapa* and *B. oleracea* in Europe (Gómez-Campo & Prakash, 1999). As a result, the specific details surrounding the initial hybridization events that led to the formation of *B. napus*, including the nature of the hybridization, the direction of gene flow, and the geographic location of these events, remain uncertain (Allender & King, 2010). *B. napus* is a globally important oilseed crop, producing approximately 52 million tonnes of seed per year (2007–2008; http://www.worldoil.com/) and accounting for approximately 13–16% of the total vegetable oil output worldwide (https://www.fao.org/statistics/en/). It encompasses various growth forms, including tuberous forms such as swede or rutabaga, as well as leafy forms such as fodder rape and kale, which are used as animal fodder and human consumption, respectively.

Despite its shorter evolutionary history than that of its parental species, the global *B. napus* gene pool has undergone several post-domestication ecogeographic radiations (Zou et al., 2019), which has resulted in three main ecotype groups on the basis of their vernalization requirements; namely, spring, winter, or semi-winter crop cultivars. Winter rapeseed is mainly grown in Europe and requires a prolonged period of low temperatures (vernalization) to transition from vegetative to reproductive growth; semi-winter rapeseed is mainly cultivated in China in the Yangtze river valley and can initiate flowering after a shorter vernalization period; and spring rapeseed has a wide distribution in Northern Europe, Canada, and Australia, and can flower and reproduce without vernalization. Historical records indicate that winter *B. napus* was first cultivated in Europe and is considered the ancestral form of *B. napus* (Lu et al., 2019). After introduction to China, Australia, and North America in the twentieth century, it underwent adaptive changes driven by natural and artificial selection, and thrives in various geographical environments and climates. As a result, two additional ecotypes; namely, semi-winter oilseed rapes and spring-type oilseed rapes (Qian et al., 2006; 2007) emerged, which were specifically adapted to different vernalization times and temperatures.

1.2 *FLOWERING LOCUS T* (*FT*) plays a central role in the promotion of flowering in the model plant *A. thaliana*

1.2.1 Flowering time is important for plants

Flowering is critical in the development of higher plants. The floral transition from vegetative growth (the production of leaves) to reproductive growth (the production of flowers and seeds), is the major developmental switch in the plant life cycle. The precise timing of flower initiation is crucial for

subsequent seed development, and flowering must be completed during favourable growing conditions to ensure the reproductive success of wild plants and crop yields in agricultural settings (Amasino, 1996). Reproductive development is complex and involves a comprehensive response to external environmental stimuli (e. g., daylength, light quality and temperature) and endogenous factors such as senescence, hormones, and chromatin state (Amasino, 2010; He, Chen & Zeng, 2020). The multifaceted nature of these mechanisms provides plants with a sophisticated level of control and the ability to adapt phenotypically. Nevertheless, understanding the intricate network that governs the floral transition remains challenging.

1.2.2 FT, the *A. thaliana* florigen belongs to the PEBP family

A specific flowering stimulator was identified in chrysanthemum and named florigen, which was found to be synthesized in the leaves following photoperiod induction and subsequently transported to the shoot apical meristem (SAM) (Tsuji & Taoka, 2014; Kardailsky et al., 1999; Chailakhyan & Krikorian, 1975; Zeevaart, 1976). In *A. thaliana*, florigen was identified to be a product of the *FT* gene (Tsuji & Taoka, 2014, 2017; Kardailsky et al., 1999), whose mRNA accumulates in the phloem companion cells of leaf vascular tissue in response to inductive long-day (LD) signals, and the FT protein is subsequently transported to the SAM where it induces the floral transition (Corbesier et al., 2007; Jaeger & Wigge, 2007).

The FT protein belongs to the phosphatidylethanolamine-binding protein (PEBP) family, a class of evolutionarily conserved proteins that are widely conserved among plants, animals and microorganisms (Chautard et al., 2004; Rajkumar et al., 2016; Wickland & Hanzawa, 2015). The *A. thaliana* genome contains six PEBP-family genes that are involved in regulating floral transition (Chardon & Damerval, 2005; Hedman et al., 2009; Karlgren et al., 2011): *FT* (Kardailsky et al., 1999; Kim et al., 2013; Xu et al., 2012), *TWIN SISTER OF FT* (*TSF*) (Michaels et al., 2005; Yamaguchi et al., 2005; D'Aloia et al., 2011; Song et al., 2015), *MOTHER OF FT AND TFL1* (*MFT*) (Xi et al., 2010; Yoo et al., 2004), *TERMINAL FLOWER 1* (*TFL1*) (Kim et al., 2013), *BROTHER OF FT AND TFL1* (*BFT*) (Yoo et al., 2010), and *ARABIDOPSIS THALIANA CENTRORADIALIS HOMOLOG* (*ATC*) (Huang et al., 2012). Among these, *FT*, *TSF*, and *MFT* promote flowering, whereas *TFL1*, *ATC*, and *BFT* repress it (Huang et al., 2012; Kardailsky et al., 1999; Kobayashi et al., 1999; Yamaguchi et al., 2005).

Misexpression of *FT* leads to early flowering, independent of environmental or endogenous cues, whereas loss of *FT* function causes extremely late flowering under LD conditions, but has minimal

impact under short-day (SD) conditions (Kardailsky et al., 1999; Kobayashi et al., 1999; Koornneef et al., 1991)). The closest homologue of *FT* is *TSF*, and both encoded proteins share approximately 82% amino-acid sequence identity (Jang et al., 2009; Yamaguchi et al., 2005). Similar to *FT*, *TSF* responds rapidly to varying *CONSTANS* (CO) levels and is repressed by FLOWERING LOCUS C (FLC) and EARLY BOLTING IN SHORT DAYS (EBS) (Yamaguchi et al., 2005). *FT* and *TSF* show similar but distinct and non-overlapping expression patterns in the phloem, with *TSF* also being lowly expressed in the basal part of the SAM (Yamaguchi et al., 2005). Unlike *FT*, *TSF* only makes a minor contribution to flowering under LD conditions, probably due to its much weaker expression level compared with *FT*, but the partial redundancy of TSF protein is more obvious under SD (Jang et al., 2009; Yamaguchi et al., 2005). Specifically, the *tsf* mutation has only a minor effect on flowering time under LDs in the presence of an active *FT* gene, but *ft tsf* double mutants show a slightly later-flowering phenotype than *ft-10* single mutants (Kim et al., 2013, Yamaguchi et al., 2005). Moreover, TSF and FT proteins are both mobile; however, when expression is driven by the CaMV 35S promoter in the rootstock, the effect of TSF on floral induction in the grafted scions is weaker than that of FT, probably due to its lower mobility than FT (Jin et al., 2015).

FT-like genes are characterized by extensive gene duplication and subsequent diversification of *FT* functions, which occurred independently in modern angiosperm lineages (Pieper et al., 2021). The PEBP genes are present in various plant divisions, but FT-like genes are exclusively present in flowering plants (angiosperms) (Karlgren et al., 2011). This suggests that *FT* emerged with the evolution of angiosperms, consistent with its role in promoting flowering, which is a unique feature of flowering plants. The regulation of flowering time by FT-like genes and their resulting impact on the plant life cycle and seed production might have significantly contributed to the rapid diversification and terrestrial radiation of angiosperms (Pin & Nilsson, 2012).

1.2.3 Flowering pathways converge on the transcriptional regulation of *FT*

In *A. thaliana*, five main flowering pathways have been identified, namely, the autonomous, ageing, gibberellin (GA), photoperiod and vernalization pathways, which all converge on the transcriptional regulation of *FT* (Amasino, 2010; Andres & Coupland, 2012; Capovilla et al., 2015; Ponnu et al., 2011).

Mutants for genes in the autonomous pathway exhibit delayed flowering under both LD and SD conditions. However, this late-flowering phenotype can be reversed by vernalization (Koornneef, 1982), indicating that genes in this pathway function upstream of the floral repressor *FLC* (Michaels,

2001; Simpson & Dean, 2002). Further research identified that the autonomous pathway genes, including *FLOWERING CONTROL LOCUS A* (*FCA*), *FLOWERING LOCUS D* (*FLD*), *FLOWERING LOCUS K* (*FLK*), *FPA*, *FVE*, *FY*, *LUMINIDEPENDENS* (*LD*) and *RELATIVE* OF *EARLY FLOWERING 6* (*REF6*), encode proteins that inhibit *FLC* expression independent of photoperiod, which further de-represses *FT* transcription (Cheng et al., 2017; Simpson, 2004).

The ageing pathway ensures flowering even in the absence of floral signals and is regulated by microRNAs (miRNAs), which are small molecules usually between 18 and 24 nucleotides in length that silence mRNA rather than encode proteins (Spanudakis & Jackson, 2014; Teotia & Tang, 2015). Two miRNA families, miR156 and miR172, play opposing roles: miR156 acts as a floral repressor during the juvenile phase, whereas miR172 is a floral promoter that accumulates with plant age (Aukerman & Sakai, 2003; Wu et al., 2009; Wu & Poethig, 2006). miR156 represses SQUAMOUSA PROMOTER-BINDING PROTEIN-LIKE (SPL) genes, which are required to activate *FT* and meristem identity genes and miR172 negatively regulates APETALA2 (AP2)-like floral repressors, including *TARGET OF EAT1* (*TOE1*) and *TOE2* (Aukerman & Sakai, 2003; Wu & Poethig, 2006; Xu et al., 2016), which repress *FT* transcription.

The hormone pathway of flowering in plants includes various hormones, but primarily involves gibberellins (GAs) (Davis, 2009; Wilson et al., 1992). Mutants that disrupt GA biosynthesis (e.g., *ga1-3*) exhibit delayed flowering, which can be rescued by exogenous application of GA. Conversely, mutants that show constitutively active GA signalling, such as *spindly*, promote flowering. Additionally, exogenous GA application can accelerate flowering in wild-type plants exposed to SD conditions (Wilson et al., 1992; Jacobsen & Olszewski, 1993).

Vernalization refers to the acceleration of flowering in response to a prolonged period of cold exposure to temperatures between 1°C and 10°C, typically lasting between one to three months (Simpson & Dean, 2002). *FLC* encodes a MADS-domain TF that plays crucial roles in vernalization as a flowering repressor (Michaels, 2001; Sheldon et al., 1999). *FLC* suppresses flowering by repressing the transcription of *FT* and *AGAMOUS-LIKE20/SUPPRESSOR OF OVEREXPRESSION OF CONSTANS 1* (*SOC1*) during vegetative development or before winter (Kardailsky et al., 1999; Kim & Sung, 2013; Searle et al., 2006; Sheldon et al., 2000). Exposure to an effective vernalization period leads to the silencing of *FLC* expression, which is mediated via chromatin modifications and is therefore mitotically stable (Kim & Sung, 2013)

The photoperiod pathway allows plants to perceive and respond to changes in daylength, which serves as a crucial cue for flowering in many plant species, a phenomenon known as photoperiodism (Garner

& Allard, 1919). Plants have been classified into three major groups according to their responsiveness to photoperiod: SD plants (that flower after perceiving longer nights, usually in autumn), LD plants (that flower in response to shorter nights, typically in late spring and summer), and day-neutral plants (that flower independently of daylength) (Andrés & Coupland, 2012). The photoperiod is sensed in the leaves via the transcriptional activation of *FT* by CO (Kardailsky et al., 1999; Mizoguchi et al., 2005; Putterill et al., 1995; Sawa et al., 2007).

1.2.4 Induction of flowering by FT protein in the shoot apical meristem

After the activation of *FT* transcription in leaves in response to photoperiod, FT protein is then loaded from the companion cells into the neighbouring sieve elements through the regulation of *FT-INTERACTING PROTEIN 1* (*FTIP1*), *QUIRKY* (*QKY*), and *SYNTAXIN OF PLANTS121* (*SYP121*) (Corbesier et al., 2007; Liu et al., 2019; Yoo et al., 2013). Once FT is transported into the sieve element, it interacts with SODIUM POTASSIUM ROOT DEFECTIVE 1 (NaKR1), a heavy-metal-associated (HMA) domain-containing protein whose encoding gene is transcriptionally activated by CO under LD conditions, and the resulting protein complex is transported to the SAM through the phloem stream (Zhu et al., 2016). However, the long-distance transfer of *FT* protein can be hindered by its interaction with negatively-charged phosphatidylglycerol (PG) at low temperatures (Liu et al., 2020; Susila et al., 2021).

At the SAM, the FT protein forms a complex with the bZIP transcription factor FD, which directly activates the expression of floral meristem identity gene, *APETALA 1* (*AP1*) (Abe et al., 2005; Collani et al., 2019; Wigge et al., 2005). Moverover, this FT–FD complex also associates with a 14-3-3 molecular chaperone, thereby forming the florigen activation complex (FAC), which directly activates the expression of the gene encoding the MADS-domain transcription factor SOC1 (Collani et al., 2019; Taoka et al., 2011). SOC1 also interacts with another MADS-domain transcription factor, AGL24, and promotes the expression of the floral meristem identity gene *LEAFY* (*LFY*) (Lee et al., 2008; Liu et al., 2008a). The transcriptional activation of *LFY* and *AP1* triggers the initiation of flower development in the SAM, marking the transition to flowering. In addition, TFL1 interacts with FD and 14-3-3 proteins, and antagonises the function of FT by competing with FT for FD binding, and leads to the promotion of meristem indeterminacy and repression of flower formation (Goretti et al., 2020; Zhu et al., 2020).

1.3 The transcriptional regulation of *FT* in *A. thaliana*

The precise regulation of *FT* gene expression and subsequent flowering in *A. thaliana* involves the interaction and integration of environmental, endogenous, and hormonal signals.

1.3.1 The transcriptional activation of *FT* via the photoperiod-responsive pathway

A. thaliana is a facultative LD plant that initiates flowering under LD conditions via the photoperiod pathway and this involves four key regulatory genes: *FLAVIN-BINDING KELCH REPEAT F-BOX 1* (*FKF1*), *GIGANTEA* (*GI*), *CO*, and *FT* (Andrés & Coupland, 2012; Song et al., 2015). These genes are predominantly expressed in the vascular tissues of leaves and are regulated by both the internal circadian clock and external light signals that are also perceived in the leaves.

The *CO* gene encodes a transcription factor with a B-box zinc finger structure and a DNA-binding CCT (for CONSTANS, CONSTANS-LIKE, and TOC1) domain (Corbesier et al., 2007; Jaeger & Wigge, 2007; Mathieu et al., 2007; Wenkel et al., 2006), which activates *FT* expression at the appropriate time for floral induction by binding to its promoter (Goralogia et al., 2017; Imaizumi & Kay, 2006; Song et al., 2015). The transcription and posttranslational regulation of *CO* are dependent on the circadian clock and light, respectively (Samach et al., 2000; Suárez-López et al., 2001), Specifically, CYCLING DOF FACTORs (CDF*s*), which are clock-controlled plant-specific transcription factors, contribute to reducing the levels of *CO* expression by forming a complex with TOPLESS (TPL) transcriptional repressors during the morning (Fornara et al., 2009; Goralogia et al., 2017; Imaizumi et al., 2005). By contrast, FKF1 and GI are controlled by the circadian clock and show a peak of mRNA accumulation at about ZT12, and the subsequent formation of a FKF1–GI E3 ubiquitin ligase complex, targets CDF proteins for degradation via proteasome, thereby releasing the CDF-mediated inhibition of *CO* transcription (Fowler et al., 1999; Imaizumi et al., 2003; Imaizumi et al., 2005; Ratcliffe et al., 2003; Sawa et al., 2007). Therefore, the peak of CO transcription occurs at ZT12–ZT16 and reaches a plateau under both LD and SD conditions (Mizoguchi et al., 2005; Sawa et al., 2007, 2008).

The CO protein is regulated via various light signalling pathways. In the morning, the red-light photoreceptor phytochrome PHYB, and HIGH EXPRESSION OF OSMOTICALLY RESPONSIVE GENE 1 (HOS1), degrade CO protein, causing its low accumulation level (Valverde et al, 2004). In the afternoon, under LD conditions, transcripts of *CO* gradually accumulate when plants are exposed to light, leading to a coincidence between the peak of CO expression and the light phase, allowing stabilization of CO protein, which is mediated by PHYA and blue light photoreceptor

CRYPTOCHROME 2 (CRY2) (Valverde et al, 2004). Specially, phosphorylation is one of the most common protein modifications that affects the activity or stability of transcription factors involved in various developmental processes and signalling pathways. SHAGGY-like kinase 12 (SK12), a glycogen synthase kinase-3 (GSK3) member, represses flowering by phosphorylating CO (Chen et al., 2020). The phosphorylated form of the CO protein is preferentially degraded in the dark by the 26S proteasome through the activity of the E3 ubiquitin ligase complex, which consists of *CONSTITUTIVE PHOTOMORPHOGENIC 1* (*COP1*) and *SUPPRESSSOR OF PHYTOCHROME A-105* (*SPA*) (Hoecker et al., 1998, 1999; Jang et al., 2008; Laubinger et al., 2006; Liu et al., 2008b; Sarid-Krebs et al., 2015). CRY2 forms a complex with SPA1 and directly interacts with COP1, and therefore inhibits the degradation of CO protein mediated by the COP1–SPA complex (Wang et al., 2001; Yang et al., 2000; Zuo et al., 2011). By contrast, under SDs, *CO* transcription occurs only in the dark, when the protein does not accumulate (Valverde et al, 2004).

1.3.2 The repressive transcriptional regulation of *FT*

The MADS-domain transcription factors SHORT VEGETATIVE PHASE (SVP) and six FLC family members, which include FLC, FLOWERING LOCUS M (FLM)/MADS AFFECTING FLOWERING 1 (MAF1), and MAF2 to MAF5, all play a crucial role in the transcriptional regulation of *FT* and subsequent flowering process (Hartmann et al., 2000; Lee et al., 2007; Ratcliffe et al., 2001, 2003; Scortecci et al., 2001). The *FLC* gene is widely expressed in the SAM and leaves, and FLC represses the expression of *FT* prior to vernalization by directly binding to the CArG box within the first intron of *FT*, resulting in the repression of flowering (Lee et al., 2007; Li et al., 2008; Noh & Amasino, 2003; Searle et al., 2006). In addition, *SVP* regulates flowering time in response to ambient temperature changes and negatively regulates *FT* expression by binding directly to the CArG motifs in the intermediate *FT* promoter (Hartmann et al., 2000; Lee et al., 2007). Furthermore, FLC, FLM, MAF2, and MAF4 also interact with SVP, indicating the potential for the formation of large MADS-domain complexes that collectively repress *FT* expression (Gu et al., 2013; Lee et al., 2013).

The RAV (RELATED TO ABI3 AND VP1) transcription factors TEMPRANILLO 1 (TEM1) and TEM2 are involved in regulating the transition from the juvenile to the adult growth phase and exert their repressive effect on flowering by binding to the promoter region of the *FT* gene, resulting in the repression of *FT* expression (Castillejo & Pelaz, 2008; Sgamma et al., 2014). The group of AP2 genes known as the euAP2 family, which encode transcription factors, also play a role in repressing *FT* expression. This gene family includes *APETALA 2* (*AP2*), three *TARGET OF EAT* (*TOE*) genes (*TOE1*, *TOE2*, and *TOE3*), as well as *SCHLAFMUTZE* (*SMZ*) and its paralogue

SCHNARCHZAPFEN (*SNZ*), which are targeted for degradation by microRNA172 (miR172) (Mathieu et al., 2009). Specifically, SMZ inhibits *FT* expression by directly binding to the *FT* promoter region. The TOE1 protein binds to an AT-rich element in the *FT* promoter near the CO-binding site, and thereby represses *FT* expression during floral transition (Zhang et al., 2015a). Furthermore, ETHYLENE RESPONSE FACTOR1 (ERF1), a key component of the ethylene signal transduction pathway, directly binds to the *FT* promoter and inhibits its transcription (Chen et al., 2021).

1.3.3 Chromatin-mediated regulation of FT expression

The chromatin of the *FT* gene undergoes bivalent marking, including the Polycomb group (PcG)-mediated deposition of H3 lysine 27 tri-methylation (H3K27me3), which promotes an inaccessible chromatin state and repression of transcription; and Trithorax group (TrxG) protein-mediated deposition of H3 lysine 4 tri-methylation (H3K4me3)(Jiang et al., 2008). In plants and animals, PcG and TrxG proteins each form higher-order complexes that control gene expression: PcG proteins act as transcriptional repressors, whereas TrxG proteins promote transcription (Mozgova & Hennig, 2015; Sanchez et al., 2015). In *A. thaliana*, the repressive histone H3K27me3 mark is catalysed by the methyltransferases CURLY LEAF (CLF) and SWINGER (SWN), which are mutually exclusive core components of Polycomb Repressive Complex 2 (PRC2) (Goodrich et al., 1997; Jiang et al., 2008; Lopez-Vernaza et al., 2012; Luo et al., 2018; Shu et al., 2018). By contrast, the formation of NF–YB–YC–CO complexes antagonizes CLF binding and deposition of H3K27me3 at *FT* (Liu et al., 2018b; Luo et al., 2018). The B3-domain-containing transcription factor VIVIPAROUS1/ABSCISIC ACID INSENSITIVE3-LIKE1 (VAL1) and VAL2 proteins contribute to the recruitment of PRC components to *FT* chromatin before dusk, which is essential for mediating the deposition of H3K27me3 on *FT* chromatin (Jia et al., 2014; Jing et al., 2019a; Luo et al., 2018; Reidt et al., 2000; Yuan et al., 2021). The LIKE HETEROCHROMATIN PROTEIN 1 (LHP1) protein and histone H3 lysine-4 demethylase JMJ14 protein act as readers of H3K27me3 and interact with the plant-specific protein EMBRYONIC FLOWER1 (EMF1) to form a distinct Polycomb repressive complex 1 (PRC1)-like complex, which was named LHP1–EMF1c, and this complex can repress the expression of *FT* (Wang et al., 2014). Additionally, two other proteins, EBS and SHL, which contain BAH domains and serve as readers of H3K27me3, interact with EMF1 to form BAH–EMF1c complexes (Li et al., 2018; Yang et al., 2018). These PRC1-like EMF1c complexes, namely LHP1–EMF1c and BAH–EMF1c, bind to *FT* chromatin, read the H3K27me3 repression marks, and contribute to their maintenance.

On the other side, the chromatin remodeller PICKLE (PKL) recruits the TrxG protein ARABIDOPSIS HOMOLOG OF TRITHORAX 1 (ATX1), which is responsible for H3K4 methylation, to form a complex that increases H3K4me3 deposition in *FT* around dusk and thus prevents PcG-mediated silencing of *FT* (Alvarez-Venegas et al., 2003; Jing et al., 2019b). Furthermore, at dusk, the CO protein and PKL mutually enhance each other's binding to *FT* chromatin through physical association (Jing et al., 2019b). Additionally, at dusk in LDs, the readers of H3K4me3/H3K36me3, MORF-RELATED GENE 1 (MRG1) and MRG2, bind to *FT* chromatin and associate with the CO protein to further enrich it at *FT*, potentially establishing a positive feedback loop (Bu et al., 2014; Xu et al., 2014). However, it was reported that an increase in H3K4me3 or any other activating chromatin marks were barely detected in 35Spro:CO plants (Adrian et al., 2010). Therefore, it requires further proves to confirm the hypothesis that the physical interaction between CO and *FT* chromatin increases its H3K4 methylation.

Notably, although *FT* locus and the proximal promoter region are widely covered by the repressive H3K27me3 mark and LHP1 (Turck et al., 2007; Zhang et al., 2007); the distal enhancer, including the conserved block C that is crucial for CO responsiveness, represents a locally H3K27me3- and LHP1-poor region (Adrian et al., 2010). This result was further verified in a study which showed that in the vasculature, LD-induced accessible chromatin regions (ACRs) at more distal gene regions, a phenomenon that also applied to the FT gene (Tian et al., 2021). These results suggest the existence of a potential regulatory mechanism that maintains a constitutively distal accessible open chromatin region for regulatory factors.

1.3.4 Three conserved blocks within the flanking sequences of *FT* are required for its photoperiod-responsive transcriptional regulation

The transcription of *FT* in *A. thaliana* is precisely regulated, and is influenced by a network of active and repressive transcription factors, as already mentioned, as well as by the presence of regulatory elements both upstream and downstream of the *FT* coding sequence. In particular, a 5.7-kb region located upstream of the Transcription Start Site (TSS) of *FT* has been demonstrated to be essential for initiating *FT* expression under LD conditions (Liu et al., 2014a). This region encompasses two core regulatory elements known as Block A and Block C, which are conserved among various Brassicaceae species (Adrian et al., 2010). Block A corresponds to the proximal *FT* promoter and is located at the TSS (Adrian et al., 2010). As the CO protein accumulates towards dusk in LDs, it binds with a histone fold domain (HFD) dimer composed of NF–YB2/YB3 and NF–YC3/YC4/YC9, to form a trimeric NF–CO complex (Cao et al., 2014; Gnesutta et al., 2017; Wenkel et al., 2006). Within

the NF–CO complex, the CCT domain of CO recognizes the CCACA motifs contained in the CO-responsive element (CORE) present in Block A in the proximal *FT* promoter region (Gnesutta et al., 2017; Tiwari et al., 2010), which were also identified in another study and were named P1 and P2 (Adrian et al., 2010). Furthermore, the HFD dimer of NFYB2/NFYB3 and NF–YC3/YC4/YC9 also interacts with the DNA-binding subunit, NF–YA, to form a trimeric NF–Y complex, which recognizes a CCAAT motif located in the distal *FT* promoter region, referred to as Block C, positioned approximately 5.3 kb upstream of the TSS (Adrian et al., 2010; Cao et al., 2014; Siriwardana et al., 2016a). It was speculated that NF–Y complexes not only prevent deposition of H3K27me3 on the *FT* promoter, but are also important for the formation of the looping structure, a physical interaction that occurs between the distal region and the proximal promoter region of *FT* at around dusk in LD conditions (Cao et al., 2014; Liu et al., 2018b). Specifically, the formation of a loop on the *FT* promoter induces the reconfiguration of its chromosomal conformation and a reduction in the enrichment of PcG factors, including PRC2 and EMF1c, on the *FT* chromatin (Liu et al., 2018b; Luo et al., 2018), which leads to the de-repression of *FT* in the leaf veins at dusk. It was initially proposed that the interaction between CO and NF–Y complex is the reason for the looping structure (Cao et al., 2014); however, NF–YA and CO were demonstrated to interact with the same domain of the NF–YB/YC complex through similar interfaces (Lv et al., 2021), suggesting that it is unlikely that both NF–YA and CO simultaneously bind to the same NF–YB/YC complex. This leaves the detailed mechanism by which NF–Y complexes bring Block C in proximity to Block A to be clarified. Furthermore, a reduction in the distance between the distal enhancer and the proximal promoter of *FT* results in a much higher level of *FT* expression in inductive conditions (Liu et al., 2014a). This either indicates that a minimal distance between the regulatory elements is required to fully repress the promoter in non-inductive conditions, or that binding sites for repressive transcription factors are located between Block C and Block A, or a mixture of both.

In addition to the presence of Block A and Block C, Block E is located 1 kb downstream of the *FT* gene body and is also conserved among members of the Brassicaceae (Zicola et al., 2019).). Block E contains a G-box (CACGTG), which is located within the binding peak of *PHYTOCHROME INTERACTING FACTOR 4* (*PIF4*) (Pedmale et al., 2016). Furthermore, Block E functions as a transcriptional enhancer additively with Block C, such that in combination with the proximal *FT* promoter, they control the expression of *FT* in response to photoperiod in the leaf phloem (Zicola et al., 2019). An NF–Y-binding site is also present within Block E, which leads to the assumption that Block E participates in *FT* transcriptional regulation by also forming a DNA loop in an NF–Y-dependent manner.

1.4 Beyond flowering-time regulation

1.4.1 *FT* is a conserved activator of flowering in diverse plant species

Numerous experiments have shown that misexpression of FT-like genes perturbs flowering time in a broad range of plant species, suggesting that their encoded proteins act as mobile flowering signals (Pin & Nilsson, 2012; Wigge, 2011).

In rice (*Oryza sativa* L.), a facultative SD plant, two *FT* homologs have been identified, namely, *Heading-date3a* (*Hd3a*) and *RICE FLOWERING LOCUS T 1* (*RFT1*), both of which are expressed in leaves (Komiya et al., 2008, 2009; Tamaki et al., 2007). *Hd3a* is responsive to SDs and its overexpression causes early heading in rice and early flowering in transgenic *A. thaliana* (Kojima et al., 2002; Tamaki et al., 2007). By contrast, although *RFT1* has a similar temporal and spatial expression pattern to that of *Hd3a*, it is expressed at a lower level than *Hd3a* and promotes flowering under non-inductive LD conditions (Komiya et al., 2008; Komiya et al., 2009). Accordingly, *Hd3a* and *RFT1* have been proposed to be the SD- and LD-specific florigens, respectively, in rice (Tsuji et al., 2011). Five pairs of *FT* homologous genes have been identified in soybean (*Glycine max*), a SD plant, among which *GmFT2a* and *GmFT5a* show diurnal expression patterns and are highly upregulated in expression under SD conditions, whereas under LD conditions their expression is downregulated and without a diurnal pattern (Kong et al., 2010). Furthermore, *GmFT2a* and *GmFT5a* are floral activators, and their overexpression promotes early flowering under SD conditions in both soybean and *A. thaliana* (Cai et al., 2018; Kong et al., 2010). By contrast, *GmFT1a* and *GmFT4* are both floral repressors and their overexpression delays flowering and maturation in soybean, and flowering time in transgenic *A. thaliana* (Liu et al., 2018a; Zhai et al., 2014). It has been proposed that a balance of functionally antagonistic *GmFT4* and *GmFT2a*/*GmFT*5a gene functions determines the flowering time of soybean (Liu et al., 2018a). Two FT-like paralogues, *SELF PRUNING 3D* (*SP3D*) and *SELF-PRUNING 6A* (*SP6A*), were identified in potato (*Solanum tuberosum*), a day-neutral plant (Navarro et al., 2011). *StSP3D* is mainly expressed in leaves in response to LDs, and mediates floral transition, as demonstrated by the late-flowering phenotype of *StSP3D* RNAi lines (Navarro et al., 2011). However, although overexpression of *StSP6A*, which is also expressed in the leaves, rescued the late-flowering phenotype of *A. thaliana, StSP6A* RNAi potato plants flower normally (Navarro et al., 2011). *SINGLE FLOWER TRUSS* (*SFT*), an *FT* orthologue in tomato (*Solanum lycopersicum*), a day-neutral plant, is expressed in the leaves and SFT acts as a florigen signal, whose overexpression results in early flowering and the *sft* mutant shows delayed flowering, which could be rescued by graft-transmissible SFT signals (Lifschitz et al., 2006). Ectopic expression of *FT* homologues from upland cotton (*Gossypium hirsutum*), a photoperiod-sensitive perennial plant, accelerated the floral transition in transgenic *A. thaliana* plants under both SD and LD conditions (Zhang et al., 2016).

Similarly, mutants for *PsFTa1* in pea (*Pisum sativum*) and mutants for *MtFTa1* in barrel clover (*Medicago truncatula*), respectively, showed strongly delayed flowering (Hecht et.al., 2011).

In summary, these findings suggest that FT orthologues represent a conserved and long-distance transportable flowering signal in diverse photoperiodic flowering regimes (LDs, SDs and day neutral) in a wide range of flowering plant species, including eudicots and monocots (Pin & Nilsson, 2012).

1.4.2 *FT* executes multiple functions in addition to promoting flowering

The regulatory roles of *FT* in addition to promoting flowering are multifaceted. In *A. thaliana*, *FT* also plays a pivotal role in impeding reversion to the vegetative phase, as evidenced by the reversion of *ft* mutants from reproductive to vegetative growth (Liu et al., 2014b). Additionally, *FT* has been postulated to contribute to transgenerational memory, whereby maternal *A. thaliana* influences the germination of progeny seeds (Chen et al., 2014). This phenomenon involves *FT* expression in fruit tissues, with the exposure of maternal plants to varying temperatures influencing *FT* expression in siliques. Consequently, *FT* regulates seed dormancy by suppressing proanthocyanidin biosynthesis in fruits and modulating the tannin content of the seed coat (Chen et al., 2014). This intricate interplay underscores the ability of the plant to interpret temperature signals through *FT*, thereby orchestrating adaptive adjustments in growth and development to successfully regulate distinct phases of their life cycles.

The functional diversification beyond that of florigen and the promotion of flowering has also occurred for *FT* homologues in other species than *A. thaliana*. For example, in soybean, *GmFT2a* and *GmFT5a*, which both promote floral transition, also terminate post-flowering stem growth, with *GmFT5a* having a stronger effect than *FT2a* (Takeshima et al., 2019). When multiple *FT* homologues are present in a single species, functional diversification might have occurred among different *FT* copies. Specifically, in potato, in contrast to the exclusive expression of *StSP3D* in leaves, *StSP6A* is highly expressed in leaves and stolons under SD conditions (Navarro et al., 2011). Correspondingly, *StSP6A* overexpression lines can tuberize under non-inductive LD conditions, and *StSP6A*-silenced lines exhibit strongly delayed tuber formation in inductive SD conditions, suggesting that *StSP6A* plays a crucial role in promoting tuberization (Navarro et al., 2011). Furthermore, *FT1* and *FT2* from poplar (*Populus* spp.) are homologues of *FT* and *TSF*, respectively, and overexpression of *FT1* and *FT2* promotes early flowering in poplar (Böhlenius et al., 2006; Hsu et al., 2006, 2011). *FT1* is expressed in winter and initiates the transition of vegetative meristems to the reproductive phase, whereas *FT2* controls vegetative growth, including growth cessation, bud set, and the onset of dormancy during the growth season (Hsu et al., 2011). The differences in the temporal expression and function between *FT1* and *FT2* suggest that perennial poplar plants have evolved adaptive growth traits following genome duplication (Hsu et al., 2011).

1.5 Current flowering research in *B. napus*

1.5.1 Identification of *FT* homologues and their functional characterization in *B. napus*

In recent decades, several genes and loci that regulate flowering time in *B. napus* have been identified. Two strategies have been applied to clone flowering-time genes. The first is homology cloning, which relies on the conservation of gene sequences between *A. thaliana* and Brassica species. The second strategy involves the use of diverse *B. napus* populations to delineate quantitative trait loci (QTLs) associated with flowering (Chen et al., 2022)

Six *BnFT* genes were identified in Tapidor, a European winter cultivar of *B. napus*, using BAC library screening. Among these genes, a single copy was located on chromosomes A02 and C02 and were named *BnFT.A2* and *BnFT.C2*, respectively, and two copies were located on chromosomes A07, named *BnFT.A7a/b*, and two copies on chromosome C06, named *BnFT.C6a/b* (Wang et al., 2009). These genes share high coding sequence (CDS) similarity of 92%–99% with each other and 85%–87% identity with *A. thaliana FT*. Among the six paralogues, *BnFT.A2*, *BnFT.C6a/b* were demonstrated to be associated with two major QTL clusters for flowering time (Wang et al., 2009). Notably, *BnFT.C2* was silenced, and one speculation is that this is due to the insertion of a DNA transposable element (TE) and a miniature inverted-repeat transposable element (MITE) within the upstream region, which also leads to major differences between the orthologous A and C genome sequences (Wang et al., 2012). By contrast, the remaining five paralogues were present in *B. napus*, *B. rapa*, and *B. oleracea* (Wang et al., 2009). *BnFT.A2* and *BnFT.C2* were found to lack the CArG box that is located within the first intron of *FT* and has been shown in *A. thaliana* to be the binding site for FLC, the regulator of vernalization (Searle et al., 2006). Correspondingly, *BnFT.A2* was transcribed in all leaf samples across various developmental stages in both *B. rapa* and *B. napus*, whereas *BnFT.A7/C6* paralogues were specifically silenced in winter-type *B. napus* but were abundantly expressed in spring-type cultivars in the absence of vernalization, which is consistent with the presence of a CArG box in their first intron (Wang et al., 2012). Furthermore, Block A and Block C that are important for the activation of *FT* by CO in *A. thaliana*, were found to be conserved within the upstream region of *BnFT.A2* and its progenitor diploids (Wang et al., 2012).

In addition, EMS mutants of *BnFT.C6b* exhibited delayed flowering compared with the control group, whereas the flowering time of mutants of *BnFT.C6a* was similar to that of the non-mutated parent winter-type inbred line Express 617 (Guo et al., 2014). Furthermore, loss-of-function mutants of *BnFT.A2* in Westar and *BnFT.A2* RNAi lines in Tapidor had smaller leaves and a lower net

photosynthetic rate, as well as a considerable delay in flowering time compared with control plants, which further demonstrated that *BnFT.A2* promotes flowering time in *B. napus* (Jin et al., 2022).

A 288 base-pair (bp) deletion within the second intron of *BnFT.A02* (BnaA02g12130D) was identified in three inbred lines—namely, Adriana, JN, and Galileo (Vollrath et al., 2021). Conversely, the remaining four lines, including the common parent Lorenz, had no deletions within this gene region, which was identical to the reference genome Darmor-bzh v4.1 (Chalhoub et al., 2014). The 288-bp fragment encompasses the putative binding sites for the CIRCADIAN CLOCK-ASSOCIATED 1 (CCA1), LHY and several members of the REVEILLE family of transcription factors, which implies a notable correlation between this DNA region and flowering-time regulation (Vollrath et al., 2021). Correspondingly, *BnFT.A2* is the only copy among the six identified homologues that was clearly associated with a flowering-time QTL (Vollrath et al., 2021). Notably, another study revealed the presence of a 288-bp MITE insertion within the second intron of *BnFT.A2* in semi-winter type ZS11 and winter-type Darmor-bzh, Tapidor (Jin et al., 2022). The apparent contradiction between the deletion and insertion findings between these two studies can be attributed to the use of different reference genomes. Furthermore, two insertions within the promoter region of *BnFT.A2* were identified: a 3,971-bp CACTA insertion within semi-winter-type ZS11 and a 1,079-bp Helitron insertion within Ningyou7 and Westar, compared with winter-type Darmor-bzh and Tapidor (Jin et al., 2022). Although the different *BnFT.A2* alleles displayed comparable tissue-specific expression patterns, their transcriptional profiles among different cultivars exhibited distinct patterns. In particular, most of the winter-type rapeseed accessions that possessed neither of the two insertions corresponded with the observed low *BnFT* transcription level, whereas 87.4% of the spring types possessing the 1,079-bp insertion were observed to have high transcription level and early flowering (Jin et al., 2022). It was therefore assumed that different haplotypes closely correspond with flowering time and ecotype variation across various accessions (Jin et al., 2022).

These observations imply that a single *BnFT* copy can adopt diverse haplotypes, and thereby perform distinct functional roles across various rapeseed accessions, underscoring the complexity of its regulatory mechanisms and the huge possibilities of its range of functions.

1.5.2 The genome characteristics of *B. napus*

Comparative mapping analysis has revealed the existence of three segmental homologous regions between the *A. thaliana* and Brassica genomes, which retain a substantial degree of collinearity and have undergone triplication within diploid species of Brassica (Lagercrantz, 1998; Lysake et al., 2005; Parkin et al., 2005; Ziolkowski et al., 2006). Within the *B. napus* genome (2n = 38, AACC), which is

derived from hybridization, the genomes of *B. rapa* and *B. oleracea* remain predominantly conserved and intact (Lagercrantz, 1998; Lukens et al., 2003; Lysak et al., 2005; Nagaharu, 1935; Parkin et al., 2005; Rana et al., 2004). However, genome triplication and duplication has resulted in the genome of *B. napus* being complex (Lagercrantz & Lydiate, 1996), and characterized by the presence of multiple gene homologues, which has reduced the selective pressure on individual gene copies and has allowed for mutations with limited phenotypic effects. Over time, these mutations can accumulate, leading to the acquisition of novel functions (neo-functionalisation), the loss of original functions (sub-functionalisation), or complete non-functionality, both in natural and artificial contexts (Conant & Wolfe, 2008). In addition, Brassica species have undergone significant chromosomal rearrangements attributed to polyploidization, which has caused not only the genes encoding specific transcription factors to be present in multiple copies, but also their targets and regulators, leading to a significant increase in the number of regulatory links within gene regulatory networks (Osborn, 2003; Parkin et al., 1995; Pires et al., 2004). All these events complicate the understanding of specific gene functions, gene regulatory networks and phenotypic variation. Therefore, although a significant amount of knowledge regarding flowering time in Brassica species has been derived from research conducted in *A. thaliana*, it is difficult to directly transfer findings from *A. thaliana* to *B. napus* (Conant & Wolfe, 2008). To address these complexities, it becomes essential to identify divergence among multi-copy homologues and to determine the function of each gene copy, i.e., whether they perform similar functions as the orthologous gene or have undergone neo-, sub- or non-functionalisation (Woodhouse, 2021).

1.6 Aims of this study

The gene regulatory networks that regulate flowering have been well studied in the model plant *A. thaliana*, and reveal six interdependent pathways that converge on the transcriptional regulation of *FT*, a key activator of the flowering process.

In contrast to *A. thaliana*, *B. napus* is an allotetraploid species characterized by a recent genome duplication and a paleontological genome triplication and recombination, which has given rise to the complex scenario in which many genes exist in multiple copies that have potentially undergone neo-/sub-/non-functionalization during evolution. As a result, the regulatory networks that govern flowering in *B. napus* are complex and less well understood than those in *A. thaliana*. Moreover, our understanding of *FT* homologues and their transcriptional regulation in *B. napus* remains limited.

Therefore, the primary aim of this study is to identify and functionally characterize *FT* homologues in *B. napus*, and to reveal their transcription regulation. The secondary aim is to characterize the flowering regulatory network in *B. napus* and to compare it with that in *A. thaliana*.

2. Materials and Methods

2.1 Plant material and growth conditions

All *A. thaliana* mutants were in the Columbia (Col-0) background and Col-0 was used as wild type for all experiments. Mutant *ft-10* (GK-290E08), an *FT* loss-of-function allele caused by T-DNA insertion in the first intron of *FT* (Rosso et al., 2003; Yoo, 2005) was used as the background for transgenic complementation experiments. The *B. napus* semi-winter cultivar ZS11 and spring cultivar Westar were used for experiments and *Nicotiana benthamiana* was used for infiltration with *Agrobacterium tumefaciens*.

All plant materials were cultivated in the greenhouse, growth chamber, or vernalization room of the Max Planck Institute for Plant Breeding Research. *A. thaliana* plants were cultivated in a temperature-controlled greenhouse in LD photoperiods (20–24°C, 16 h light/8 h dark). *B. napus* plants were grown in the greenhouse (20–24°C), or in growth chambers (CLF Plant Climatics, AR-95L3X, 60% light intensity (12570 LUX), 75% relative humidity) under LDs (16 h light/8 h dark) or SD (8 h light /16 h dark) conditions as indicated. For vernalization treatments, plants were placed in a vernalization room (4°C, SD). For *B. napus*, bolting time was recorded when the main shoot of seedlings had elongated to about 2 cm. *N. benthamiana* was cultivated in the greenhouse under LD conditions.

2.2 Genomic sequence collection and phylogenetic analysis

The genomic sequences of *FT*, *TSF*, *TFL1*, *BFT* and *MFT* from *A. thaliana* were obtained from the TAIR database (https://www.arabidopsis.org/). The genomic sequences of the *FT* and *TSF* homologues in *A. lyrate* and *Schrenkiella parvula* were obtained from NCBI (https://www.ncbi.nlm.nih.gov/) and Phytozome (https://phytozome-next.jgi.doe.gov/), respectively. The genomic sequences of *BnFT* candidates in ZS11 and Westar cultivars were obtained from BnPIR (Song et al., 2020) (http://cbi.hzau.edu.cn/) and BnIR (Yang et al., 2023) (https://yanglab.hzau.edu.cn/BnIR). The genomic sequences of *FT* homologues and candidate homologues in *B. rapa* and *B. oleracea* were obtained from BRAD (http://brassicadb.cn/#/GeneSequence/) and EnsemblPlants (https://plants.ensembl.org/index.html), respectively.

The FT (AT1G65480) protein sequence was used as a tblastn query against the *B. napus* pan-genome information resource (Song et al., 2020) (BnPIR; http://cbi.hzau.edu.cn/bnapus) and the reference

genomes of *B. rapa* (http://brassicadb.cn/#/GeneSequence/) and *B. oleracea* (https://plants.ensembl.org/index.html), with the screening criteria of E-value ≤ 1.0E-20, coverage ≥ 95%, and identity ≥ 80%. Lastal blast (scoring matrix) was performed with the FT (AT1G65480) protein sequence used as a tblastn query against the same *B. napus*, *B. rapa* and *B. oleracea* genomes with the criteria of identity ⩾ 80%.

Protein alignments were performed with ClustalW and a neighbour-joining (NJ) tree with 1,000 bootstraps was constructed using Mega11. The tree was rooted using TFL, BFT and MFT as the outgroups. Finally, a 60% majority-rule consensus tree showing posterior probability for each node was constructed. Genes of the encoded proteins used for analysis are listed in Table 1 and Appendix Table 1.

2.3 Online webtool analysis

The gene synteny alignments of *FT* and *TSF* homologues in *S. parvula, B. rapa, B. oleracea, and B. napus* were performed using "CoGe" (https://genomevolution.org/coge/SynFind.pl), which includes genome information for the spring cultivar Westar and winter cultivar Darmor (Lyons & Freeling, 2008). Genomic sequences, including upstream and downstream sequences extending to the next flanking gene, were submitted to the mVISTA webtool (https://genome.lbl.gov/vista/mvista/submit.shtml). Genes used for analysis are listed in Table 1 and Appendix Table 1.

2.4 Gene expression analysis

2.4.1 RNA extraction and reverse transcription

For all samples harvested for expression analyses, three biological replicates were performed to ensure reliable results and statistical significance. Total RNA was extracted using the RNeasy Mini Kit (Qiagen, Cat. no. 74104) following the manufacturer's instructions. For each sample, 4 µg total RNA was treated with DNA-free™ Kit (Invitrogen, REF AM1906), and cDNA synthesis was performed with the Superscript™ IV reverse transcriptase kit (Invitrogen, REF18090050) following the manufacturer's instructions. qRT-PCR was conducted using the Bio-Rad CFX384™ system (Bio-Rad) for three technical replicates for each biological replicate.

2.4.2 Reverse transcription-quantitative polymerase chain reaction (RT-qPCR)

The expression levels of *BnFT.A2*, *BnFT.C2*, *BnFT.A7*, *BnFT.C6*, *BnNFT.A7*, *BnCFT.C4*, *BnCO.A10*, *BnCO.C9* and *BnENTH* were quantified with primer pairs BnFT.A2-qF/R, BnFT.C2-qF/R, BnFT.A7-qF/R, BnFT.C6-qF/R, BnNFT.A7-qF/R, BnCFT.C4-qF/R, BnCO.A10-qF/R, BnCO.C9-qF/R, and BnENTH-qF/R, respectively. The RT-qPCR primer sequences are listed in Appendix Table 2. Gene expression levels were determined using the $2^{-\Delta\Delta CT}$ method. The *BnENTH* gene was used as an internal reference gene. Standard curves for each pair of primers were obtained by PCR using gradient-diluted ZS11 genome DNA as the template, and amplification efficiencies were calculated accordingly. The expression of each gene using ZS11 genomic DNA as a template was set to 1 and used as a common reference to normalize the gene expression data.

2.5 Isolation of DNA and purification of PCR products

The NucleoSpin® Plasmid Kit (Macherey-Nagel, Düren, Germany) was used to isolate plasmid DNA from *Escherichia coli* following the manufacturer's recommendations. The DNeasy® Plant Mini Kit (Cat.No. 69104) was used to isolate genomic DNA from *A. thaliana* and *B. napus* following the manufacturer's recommendations.

DNA fragment amplification was performed using polymerase chain reaction (PCR) with an Eppendorf Mastercycler nexus gradient eco machine. The appropriate polymerase was selected based on the intended use of amplification. The amplification of long fragments or coding sequences for vector construction was carried out using either PrimeSTAR GXL DNA Polymerase (Takara, Cat# R050A) or Q5® High-Fidelity DNA Polymerase from New England Biolabs (NEB, Frankfurt, Germany). Reagents were added following the manufacturer's instructions. The NucleoSpin® Gel and PCR Clean-up Kit (Macherey-Nagel, Düren, Germany) was used to purify PCR products.

2.6 Plasmid construction

2.6.1 Plasmid for *ft-10* complementation

For *ft-10* complementation assays, the vector C+Ap::FTcDNA-pGreen and transgenic *C+Ap::FTcDNA*/*ft-10* plants were previously described (Liu, et al., 2014). Full-length coding sequences of *BnFT.A2*, *BnFT.C2*, *BnFT.A7*, *BnFT.C6*, *BnNFT.A7*, and *BnCFT.C4* were amplified from ZS11 leaf cDNA using primer pairs BnFT.A2C2-pFT-F/BnFT.A2-pFT-R, BnFT.A2C2-pFT-F/BnFT.C2-pFT-R, BnFT.A7C6-pFT-F/BnFT.A7-pFT-R, BnFT.A7C6-pFT-F/BnFT.C6-pFT-R,

BnNFT.A7-pFT-F/R and BnCFT.C4-pFT-F/R, respectively. Amplicons were introduced into C+Ap::FTcDNA-pGreen (Liu, et al., 2014) via *Hin*dIII and *Sac*I restriction enzyme sites to replace the original *FT* CDS using NEBuilder® HiFi DNA Assembly Master Mix (NEB, Frankfurt, Germany).

Additionally, the full-length coding sequences of *BnFT.A7* and *BnFT.C6*, and those encoding a 2HA tag at the N-terminal ends, were amplified by two rounds of PCR. The first round used primer pairs BnFT.A7C6-pFD-F/BnFT.A7-pFD-R and BnFT.A7C6-pFD-F/BnFT.C6-pFD-R, respectively, with ZS11 cDNA as a template. The second round used primer pairs pFD-2HA-F/BnFT.A7-pFD-R and pFD-2HA-F/BnFT.C6-pFD-R, respectively, and the first-round PCR products as templates. Similarly, the mutant version of *BnFT.A7* and *BnFT.C6*, namely, *BnFT.A7*m and *BnFT.C6*m, including sequences encoding a 2HA tag at the N-terminal ends, were amplified from vectors C+Ap::BnFT.A7-pGreen and C+Ap::BnFT.C6-pGreen described above, using primer pairs BnFT.A7C6-pFD-F/BnFT.C6-pFD-R and BnFT.A7C6-pFD-F/BnFT.A7-pFD-R, respectively, for the first round of PCR. Primer pairs pFD-2HA-F/BnFT.C6-pFD-R and pFD-2HA-F/BnFT.A7-pFD-R, respectively, were used for the second round of PCR, and the first-round PCR products as templates. The full-length coding sequence of *FT*, including sequences encoding a 2HA tag at the N-terminal ends, was amplified from Col-0 leaf cDNA using primer pairs FT-pFD-F/R, pFD-2HA-F/FT-pFD-R for the first and second rounds of PCR, respectively. The corresponding PCR products were inserted into FDp::FDter-pER8 using *Xho*I restriction enzyme sites and the NEBuilder® HiFi DNA Assembly Master Mix (NEB, Frankfurt, Germany) kit . The sequences of the inserts of the generated vectors were verified using sanger sequencing and the vectors were transformed into *ft-10* by floral dipping (Clough & Bent, 1998).

2.6.2 Plasmid for tobacco infiltration

For transient luciferase (LUC) reporter assays, the vectors 35Sp::LUC-pGreen and 35Sp::H2B-pGreen were used as positive and negative controls, respectively. *Renilla-luciferase* (*RLUC*) was used as infiltration reference gene. For reporter vectors, the 35Sp:: RLUC cassette was firstly inserted into BlockAp::LUC-pGreen via *Eco*RI restriction enzyme sites using Gibson assembly. The fidelity of the insert sequence of the vector BlockAp::LUC-35Sp::RLUC-pGreen was verified by Sanger sequencing. Different promoter lengths of *FT*, *BnFT.A2*, *BnFT.C2*, *BnFT.A7*, *BnFT.C6* were amplified from ZS11 gDNA using primer pairs listed in Appendix Table 2, and were introduced into the generated vector BlockAp::LUC-35Sp::RLUC-pGreen via *Sca*I and *Nco*I restriction enzyme sites to replace the Block A promoter using Gibson assembly. The sequences of the inserts of the

corresponding generated vectors were verified by Sanger sequencing. For effector vectors, the cassettes 35Sp::CO, 35Sp::BnCO.A10 and 35Sp::BnCO.C9 were introduced into the vector BlockAp::LUC-pGreen via restriction enzyme sites *Sca*I and *Sac*I using Gibson assembly, to replace Block Ap::LUC.

All destination plasmids were introduced into *A. tumefaciens* strain GV3101 with pSoup helper plasmid. Amplification primers and 2HA tag sequences are indicated in Appendix Table 2. Plasmids used in this study are indicated in Appendix Table 3.

2.7 Gibson assembly and *Agrobacterium*-mediated transformation

The *E coli* strain DH5α was used for plasmid amplification. The *A. tumefaciens* strain GV3101 carrying the helper plasmid pSoup for amplifying the pGreen destination vector was used for transformation of *A. thaliana* and transient infiltration of tobacco.

Gibson assembly was performed using NEBuilder® HiFi DNA Assembly Master Mix (NEB, Frankfurt, Germany) according to the manufacturer's instructions. A molar ratio of 2–3 times the amount of each insert to 50–100 ng of backbone vector was used. In the case of 4–6 fragment assemblies, the molar ratio of insert to vector was 1:1. The samples were incubated in a thermocycler at 50°C for 15 min for 2 or 3 fragment assemblies and for 60 min for 4–6 fragment assemblies. After incubation, the samples were stored either on ice or at -20°C for subsequent transformations.

For *E. coli* transformation, competent cells from the -80°C freezer were placed on ice to thaw slowly. No more than 10 μL plasmid DNA or the Gibson assembly ligation product was added to 50 μL competent cells and the cells were incubated on ice for 30 min. The reaction tubes were then subjected to heat shock at 42°C for 45 s, followed by cooling on ice for 2 min. Lysogeny Broth (LB) liquid medium (500 μL) without antibiotics was added to the tube and the mixture was then incubated for 45 min at 37°C with shaking at 200 rpm. Finally, the 300 μL of the cells were plated onto a solid LB plate (LB solid medium) with the appropriate antibiotic for selection and the plate was incubated overnight at 37°C. Positive colonies were detected by colony PCR and DNA extracted from these colonies by miniprepping was submitted for Sanger sequencing with appropriate primers to confirm the fidelity of the cloning. For plasmids used for *ft-10* complementation experiments with the backbones of C+Ap::FTcDNA-pGreen and FDp::FDter-pER8, the antibiotics were phosphinotricin (PPT) and hygromicin B (hyg), respectively. For plasmids used for tobacco infiltration with the backbone of BlockAp::LUC-pGreen, the antibiotic was kanamycin (kan).

For *A. tumefaciens* transformation, competent cells of *A. tumefaciens* strain GV3101-pSoup were removed from the -80℃ freezer and placed on ice to thaw slowly and were then gently mixed with 1 μL of target plasmid. The mixture was transferred to a pre-chilled 1-mm electroporation cuvette. The cuvette was placed into a MicroPulser Electr operator (Bio-Rad) and subjected to 1440 volts for one pulse. Then, 1 mL LB medium without antibiotics was added to the cuvette to suspend the cells. The cell suspension was then transferred to a 2-mL microcentrifuge tube and incubated at 28℃ with continuous shaking for 3 h. Finally, about 100 μL of the cell suspension was spread onto LB agar plates containing the appropriate antibiotics. The plates were incubated at 28℃ in an incubator overnight. The resulting single colonies were subjected to colony PCR to identify positive clones, which were then miniprepped and the DNA was submitted for Sanger sequencing to confirm the fidelity of the cloning. The transformed bacteria were mixed with 50% glycerinum in a ratio of 1:1 for storage, and tubes containing the mixture were frozen in liquid nitrogen and stored at -80℃ for further use. For plasmids with the backbone of C+Ap::FTcDNA-pGreen, the antibiotics were rifampicin (rif), gentamicin (gent), tetracyclin (tet) and PPT. For plasmids with the backbone of FDp::FDter-pER8, the antibiotics were rif, gent, tet and hyg. For plasmids with the backbone of 35Sp::LUC-pGreen, the antibiotics were rif, gent, kan and carbenicillin (carb). For plasmids with the backbones of 35Sp::H2B-pGreen and BlockAp::LUC-pGreen, the antibiotics were rif, gent, tet and kan. For plasmid P19, the antibiotics were rif and kan.

The compositions of LB liquid culture medium and LB solid plates are indicated in Appendix Table 4. The concentrations of antibiotics are indicated in Appendix Table 5.

2.8 Transgenic plant generation and selection

A. tumefaciens-mediated transfer of T-DNA to plants was performed by floral dipping following established protocols (Clough & Bent, 1998). The *ft-10* mutant (GK-290E08) was used as the receptor for the transgenes (Rosso et al., 2003; Yoo, 2005).

Transformants carrying the vector backbone C+Ap::FTcDNA-pGreen were sown on soil and grown in the greenhouse. To select stably transformed plants, T1 seedlings with two true leaves were sprayed with 0.1% glufosinate (BASTA®, BAYER) 2–3 times in one week. The T2 seeds from each T1 plant were selected on germination medium (GM) containing PPT on the basis of a 3:1 segregation. Homozygous lines were identified by selection of T3 seedlings on GM medium containing PPT. The composition of the GM culture medium is indicated in Appendix Table 4.

Seeds of transformants carrying the vector backbone FDp::FDter-pER8 were surface sterilized and sown on GM plates supplemented with hyg. The plates were placed in a growth chamber for approximately 10 days until resistant T1 seedlings had produced two true leaves, and the seedlings were then transplanted onto soil and transferred to the greenhouse. The T2 seeds from each T1 plant were selected on GM medium containing hyg on the basis of a 3:1 segregation. Homozygous lines were identified by selection of T3 seedlings on GM medium containing hyg.

For surface sterilization, approximately 300 µL *A. thaliana* seeds was placed into a spin column in a 2-mL collection tube, 650 mL 70% ethanol was added and the seeds were incubated for 5 min, centrifuged briefly in a bench-top 5427 R centrifuge (Eppendorf) at 11,000 *g* for 1 min. Then, 650 mL 100% ethanol was added to the tube and the seeds were again incubated for 3 min and centrifuged at 11,000 *g* for 1 min. The flow-through was discarded after each centrifugation. To sterilise seeds of *B. napus*, approximately 300 µL of seeds was placed into a spin column in a 2-mL collection tube, 650 mL 70% ethanol was added and the seeds were incubated for 7 min and centrifuged at 11 000 *g* for 1 min. Then, 650 mL 100% ethanol was added and after incubation for 5 min, the tube was centrifuged at 11,000 *g* for 1 min. The flow-through was discarded after each centrifugation

2.9 Tobacco infiltration

2.9.1 Infiltration

The cell suspension of *A. tumefaciens* GV3101-pSoup strains carrying the relevant plasmids of interest was mixed according to the experimental design and then infiltrated into the underside of the *N. benthamiana* leaves as described (Sparkes et al., 2006). There were several adjustments: 10 mM MES (final concentrations) and 40 µM acetosyringone (final concentrations) were added to the *Agrobacterium* culture, which was then incubated overnight at 28°C. The culture was then centrifuged at 4,000 *g* for 15 min and the supernatant was replaced with the infiltration medium. After that, the *Agrobacterium* culture was then placed at room temperature for at least 3 h before being used for infiltration.

2.9.2 Luciferase signal quantification

At 48 h after infiltration, infiltrated *N. benthamiana* leaves were excised and sprayed with triple-diluted Luciferase Assay Reagent (Promega E1500). Fluorescence signal images were taken at least 10 min later with the ChemiDoc Imaging System (Bio-Rad). If signals were observed, the infiltrated leaf spots were sampled with a punch and transferred into 1.5-mL Eppendorf tubes containing

magnetic beads (the diameter of 0.32 cm). The samples were snap-frozen in liquid nitrogen and were stored at -80°C for subsequent signal quantification.

The frozen samples from -80°C were ground with the TissueLyser II machine (QIAGEN) for 1 min at 30 Hz. Then, 150 µL of 1× lysis reagent (Promega E1500) was added to the sample, which was mixed well and centrifuged at full speed with a bench-top 5427 R centrifuge (Eppendorf) for 1 min. A 60-µL portion of the supernatant was then transferred to a 96-well plate. An equivalent volume (60 µL) of Dual-Glo® Luciferase Reagent (Promega E2920) was added to each well and mixed with the sample. After at least 10 min, the firefly luminescence was measured using a multimode reader TriStar² LB 942 (BERTHOLD). The same volume of 60 µL oDual-Glo® Stop & Glo® Reagent (Promega E2920) was added to each well and mixed with the sample. At least 10 min later, the RLUC luminescence was quantified using the same luminescence reader.

2.10 Transcriptome analysis

Plants of ZS11 were cultivated for four weeks in separate LD or SD growth chambers, were vernalized for 4 weeks, and were then transferred back to the respective LD or SD chambers. Leaf 6 samples were harvested the day before plants were transferred to the vernalization room and leaf 8 samples were harvested the day when plants were transferred back to the original LD or SD chambers and after one week of adaptive growth. Sampling was performed every 4 h for 24 h and RNA was extracted as described. Each sample was collected in three independent replicates and sent to BGI (Hongkong, China) for library construction and sequencing using a NovaSeq 6000 System (Illumina). Low-quality RNA sequences and adaptors were removed using Trim Galore (Martin, 2011). The remaining clean reads were then mapped to the *B. napus* ZS11 reference genome version Bna202009 (Song et al., 2020) using STAR, version 2.7.0e (Dobin et al., 2013). Gene expression was quantified using Feature Counts (Liao et al., 2014). Differentially expressed genes (DEGs) were identified using the DESeq2 (Love et al., 2014) packages in R (version 4.2.1). The cut-off criteria for significant DEGs were an absolute value of $\log_2$(fold-change) ≥1 and a *p*-value < 0.05. Genes shown in the heatmap are listed in Appendix Table 6.

3. Results

3.1 Documentation of *B. napus* growth and development in different environmental conditions

In this study, the semi-winter accession ZS11 was selected to document the growth and development of *B. napus* in response to vernalization and photoperiod. ZS11 plants were subjected to five different conditions: growth in LD without vernalization (LD) or with vernalization for 4 weeks after 4 weeks cultivation (LD+V), growth in SD without vernalization (SD) or with vernalization for 4 weeks after cultivation for 4 weeks (SD1+V) or 6 weeks (SD2+V) (Fig. 1A). Two vernalization regimes in SD were designed to compare the response to vernalization between plants grown for the same time (LD+V vs. SD1+V) and until a comparable growth stage (LD+V vs. SD2 +V) before vernalization. Throughout the growth period, photographs captured critical time points: growth stages before vernalization, at the end of vernalization, and after cultivation for one (SD2+V), three (SD1+V, LD+V), five (SD2+V) and seven (SD1+V, LD+V) weeks in warm ambient temperature after vernalization. Non-vernalized plants were assessed at a comparable growth time in warm ambient temperature (Fig. 1A, B).

Developmental stages were assessed by counting the number of expanded leaves and visible flowers on the main shoot over time (Fig. 1C). Before and immediately after vernalization, all plants were in the vegetative growth stage as evaluated by the absence of visible floral buds. Notably, LD+V and SD2+V were at a similar growth stage after vernalization (10 leaves), with little change during vernalization, indicating very limited leaf outgrowth during the cold phase. Similarly, SD1+V and SD displayed only 8 leaves before and immediately after vernalization (Fig. 1B, Fig. 1C).

The three cohorts of plants with vernalization demonstrated distinct growth characteristics across three stages. Prior to vernalization, all groups displayed linear growth, with a faster growth rate of 3 leaves/week under LD conditions compared with 1.8 leaves/week under SD conditions (Fig. 1C). Following the plateau phase with minimal additional leaves being produced during vernalization, the SD1+V and SD2+V groups displayed parallel growth curves, with a similar developmental rate of leaf production of 3.5 leaves/week, which was clearly slower than the 7 leaves/week observed in the LD+V group (Fig. 1C). Thus, despite differences between LD and SD, all three groups presented a higher growth rate after vernalization compared with before vernalization. In the absence of vernalization, LD plants maintained a growth rate of 3 leaves/week until week 11, when the rate increased to 5 leaves/week (Fig. 1C). The SD cohort showed a constant growth rate of 1.8

leaves/week until week 12, after which time a non-linear increase from 3.2 leaves/week was observed between week 12 and 15, and of 5.5 leaves/week after week 15 (Fig. 1C).

Comparison of the growth of vernalized and non-vernalized plants after a comparable number of days in warm ambient temperature revealed that vernalization was sufficient to induce flowering (10 warm weeks for SD1+V, 11 warm weeks for SD2+V), a process that was greatly accelerated by LD photoperiod (7 warm weeks for LD+V). Before the formation of the first flower, SD1+V and SD2+V plants had formed 25 and 24 leaves, respectively, whereas the LD+V cohort formed flowers after 25 leaves, which is the same as SD1+V cohort. By contrast, LD alone induced flowering only after 16 weeks growth in warm ambient temperature, corresponding to the formation of 56 leaves before flower formation, whereas SD-grown plants did not flower without vernalization until the end of the experiment at 17 weeks (Fig. 1C). It should be noted that for SD1+V, SD2+V and LD+V, growth for the first week after vernalization at warm ambient temperature occurred in growth chambers, whereas growth for the subsequent weeks occurred in a greenhouse environment, which maintained LD or SD conditions. The SD2+V group experienced 6 and 5 weeks of warm temperature growth at prior- and post-vernalization stages, respectively, whereas the SD1+V group experienced 4 and 7 weeks of warm-temperature growth at prior- and post-vernalization stages, respectively. Therefore, the slight delayed flowering of SD2+V compared to SD1+V might be attributable to both a difference in post-vernalization cultivation and/or differences in the growth stage prior to vernalization.

Bolting (stem elongation) in the plant indicates the transition from vegetative growth to reproductive growth and flower formation. Early bolting limits vegetative growth and can therefore severely decrease yield (Fu et al., 2020). Although bolting is very obvious in rosette-forming plants such as *A. thaliana*, it corresponds to a more gradual increase in internode length in *B. napus* and can be difficult to score (Fig. 1C and B). SD1+V and SD2+V cohorts initiated bolting ca. 2 weeks after vernalization after producing a comparable number of leaves (12 and 13, respectively), and LD+V plants bolted 5 days after vernalization, with the same 13 leaves as SD2+V (Fig. 1C). By contrast, non-vernalized LD and SD plants showed visible internode elongation after an equal number of leaves had formed (24 leaves), corresponding to growth of 9 and 12 weeks, respectively.

Finally, it is worth noting that after 11 weeks, plants in the LD cohort had produced 18 leaves with a firm texture, dark green coloration, and a white waxy surface; whereas 12 leaves had been produced by plants in the SD cohort and these maintained a relatively fresh and bright-green appearance (Fig. 1B. iv', v').

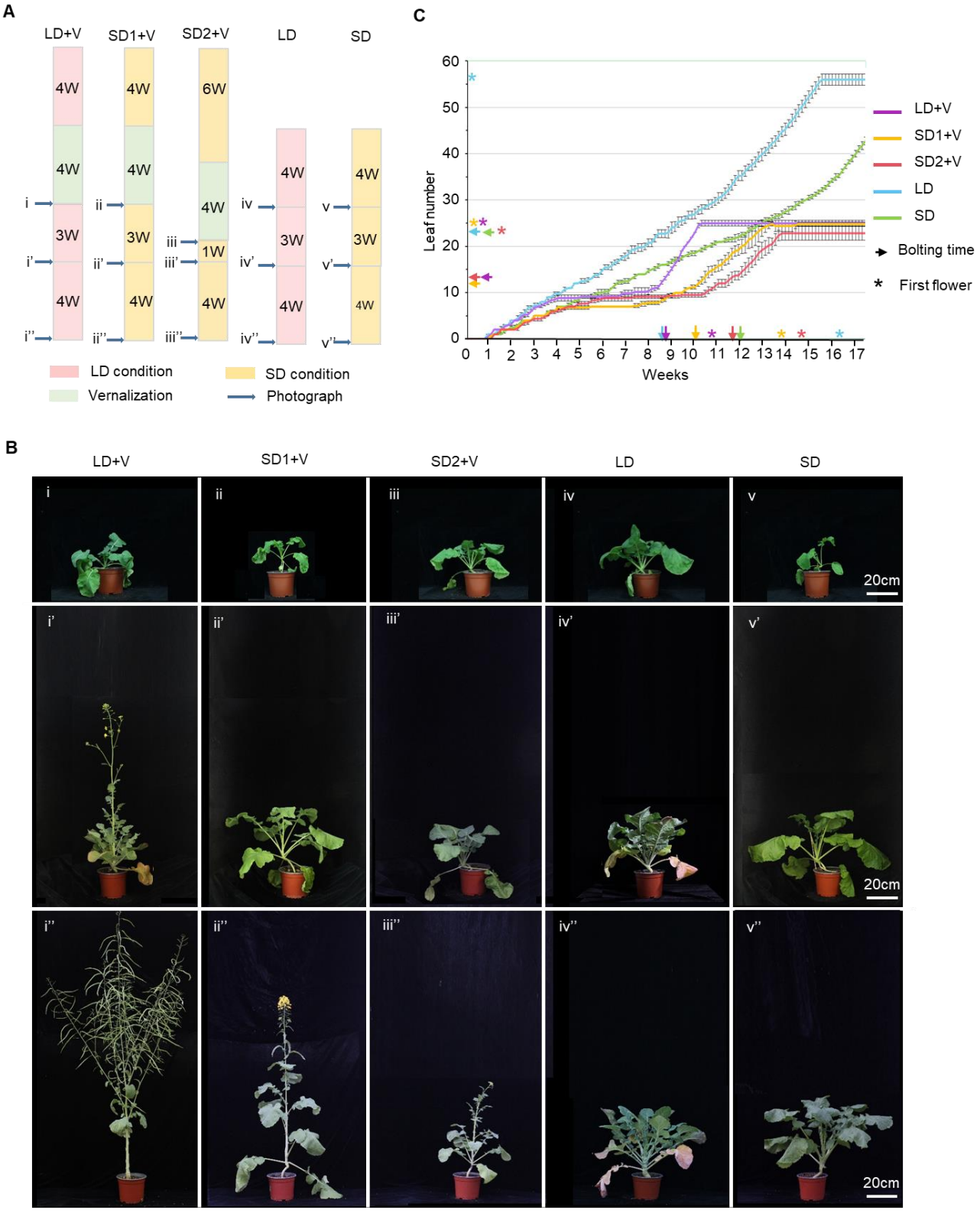

Figure 1. The development of ZS11 plants under different combinations of photoperiod and vernalization treatments

(A) Schematic diagram to illustrate the different growth conditions and treatments of ZS11 plants. “LD + V”, “SD1 + V”, “SD2 + V”, “LD” and “SD” correspond to i, ii, iii, iv and v, respectively. Pink, yellow and green boxes

represent LD, SD and vernalization treatments, respectively. For detailed information refer to methods. Blue arrows represent time points when plants were photographed, corresponding to lowercase i, ii, iii, iv, v; i', ii', iii', iv', v'; and i'', ii'', iii'', iv'', v'', respectively. Numbers in each box represent the time period of the condition, and "W" represents week.

(B) Representative images of ZS11 at different developmental stages. LD+V: plants cultured for 4 weeks under LDs after sowing and 4 weeks vernalization (i), and then 3 weeks growth in LDs (i'), or 7 weeks growth in LDs (i''). SD1+V: plants cultured for 4 weeks under SD after sowing and 4 weeks vernalization (ii), and then 3 weeks of growth (ii'), or 7 weeks of growth in SDs (ii''). SD2+V: plants cultured for 6 weeks under SDs after sowing (until the similar growth state of plants cultured 4 weeks LD after sowing was reached) and 4 weeks vernalization (ii), and then 1 week of growth under SDs (ii'), or 5 weeks of growth under SDs (ii''). LD: plants grown for 4 weeks (iii), 7 weeks (iii'), or 11 weeks (iii'') in LDs after sowing. SD: ZS11 plants grown for 4 weeks (iv), 7 weeks (iv'), or 11 weeks (iv'') in SDs after sowing.

(C) Timing of developmental stages in ZS11. "LD + V", "SD1 + V", "SD2 + V", "LD" and "SD" refer to i, ii, iii, iv, v series shown in (A) and (B). Results are the mean ± standard deviation for n ≥ 5 plants. The arrow and five-pointed star with different colours represent the bolting time point and time of first flower emergence, respectively.

In summary, among all the plant groups studied, only the SD plants failed to initiate flowering by the end of the experiment (4 months after sowing), whereas vernalization promoted earlier flowering than LD photoperiod alone, and both pathways resulted in a synergistic effect on flowering time (Fig. 1C). This observation suggests that ZS11, which is classified as a semi-winter type of *B. napus*, is able to initiate flowering when exposed to either vernalization or exposure to continuous LD conditions, underscoring its versatile responsiveness to environmental cues for flowering induction. Since the SD group of plants finally flowered after 7 months of growth in continuous SDs, the presence of a possible internal ageing or autonomous pathway that contributes to reproductive growth is suggested.

3.2 Four *BnFT* genes, two *BnNFT* genes and one *BnCFT* gene exist in *B. napus*

3.2.1 Identification of *BnFT* homologues

A previous study using BAC library screening identified six *FT*-related genes in Tapidor, a European winter cultivar of *B. napus* (Wang et al., 2009). To identify *FT* homologues in *B. napus*, a tblastn search against a current high-quality assembly of *B. napus* semi-winter cultivar ZS11, spring cultivar Westar, *B. rapa* and *B. oleracea* was performed using FT protein as the query sequence to the BnPIR database (http://brassicadb.org; (Song et al., 2020)). Under the criteria of E-value ≤ 1.0E-20, coverage ≥ 99%, identity ≥ 80%, six, three, and three *FT*-related genes were identified in *B. napus*, *B. rapa* and *B. oleracea*, respectively (Table 1). In addition, lastal blast (scoring matrix) with the criteria of identity ≥ 80% identified two extra genes that were located on chromosome C02 and C06 in *B. napus*

and *B. oleracea* (Table 1). Furthermore, the scipio webtool was used to query the genomic sequence for the presence of *FT*-encoding reading frames (https://www.webscipio.org/search). The analysis confirmed that the first six identified homologues obtained by tblastn search are complete FT-like genes and revealed that two extra genes obtained by lastal blast are probably encoded by pseudo-genes due to presence of frameshifts in the predicted coding sequence and the presence of non-canonical introns (data not shown).

Table 1. *FT* homologues screened by blast and synteny analysis

	B. napus			
Gene name	Westar	ZS11	*B. oleracea*	*B. rapa*
FT. A2	*BnaA02T0157300WE*	*BnaA02T0156900ZS*		*Bra022475*
FT.C2	*BnaC02T0193500WE*	*BnaC02T0200600ZS*	*Bo2g051350*	
FT. A7	*BnaA07T0277700WE*	*BnaA07T0282700ZS*		*Bra004117*
FT.C6	*BnaC06T0346000WE*	*BnaC06T0323800ZS*	*Bo6g099320*	
CFT.C4	*BnaC04T0175500WE*	*BnaC04T0181400ZS*	*Bo4g061100*	
NFT.A7	*BnaA07T0361000WE*	*BnaA07T0365100ZS*		*BraA07g040390*
*NFT.C2**	*BnaC02T0290900WE*	*BnaC02T0302200ZS*	*BolC02g033320.2J*	
*NFT.C6**	*BnaC06T0446200WE*	*BnaC06T0428800ZS*	*BolC06g048270.2J*	

*non-functional

To analyse the syntenic relationship of *B. napus FT* homologous genes, FT-like proteins of *A. thaliana*, *B. napus* ZS11 cultivar were blasted against all proteins encoded by these genomes, and the genomes of *B. oleracea*, *B. rapa* and *S. paruvula*, which represents a diploid genome more related to the *Brassica* genus than *A. thaliana* (Dassanayake et al., 2011). The resulting blast hits were used to identify synthetic blocks using the mcscan pipeline (Tang et al., 2008). The analysis confirmed the previous study that identified four *FT* syntenic genes located on chromosomes A02, C02, A07 and C06 (Wang et al., 2009) (Fig. 2A). Analysis performed with the *TSF* (*AT4G20370*) gene showed that a *TSF* orthologue was present in *S. parvula* but was absent in the corresponding syntenic block in *B. napus* (Fig. 2B). On the other hand, *S. parvula* and *B. napus* featured an FT-like gene at a novel syntenic position on chromosome A07, for which no correspondence was found in *A. thaliana* (Fig. 2C). This gene was named *NEW SISTER OF FT AND TSF* (*NFT*). *BnNFT.A7*, which encodes a functional protein, is syntenic to the two pseudo-genes identified with the lastal blast method in *B. napus* and *B.olerace*, and these were named *BnNFT.C2/C6 and BoNFT.C2/C6* respectively (Fig. 2C) Surprisingly, a sixth functional *FT* homologue located on chromosome C04 was located at a position that is unique to *B. napus* and the C-genome parent, *B. oleracea*, but absent from *S. parvula* and *A. thaliana* (Fig. 2D). I propose the name *C-GENOME SISTER OF FT AND TSF* (*CFT*) for this gene.

Genome-wide alignment between the *A. thaliana* (TAIR10) and *B. napus* spring cultivar Westar genomes (CoGe webtool, https://genomevolution.org/coge/SynFind.pl; (Lyons & Freeling, 2008)) further revealed that four fragments within chromosome A02/C02/A07/C06 of *B. napus* were syntenic to an approximately 6-Mb fragment in *A. thaliana* Chr.01 where *FT* is located (Fig. 2E). Notably, *BnFT.A7*/*BnNFT.A7* and *BnFT.C6*/*BnNFT.C6* are located near a region showing a large inverted duplication on chromosomes A07/C06 that has been previously reported (Parkin et al., 2005). The inversion formed a distinctive "V" shape in the scatterplot; however, juxtaposition with the *FT* and *NFT* syntenic segments showed that the *FT* gene was situated at the margin of the original syntenic fragment, narrowly avoiding the duplication (Fig. 2E).

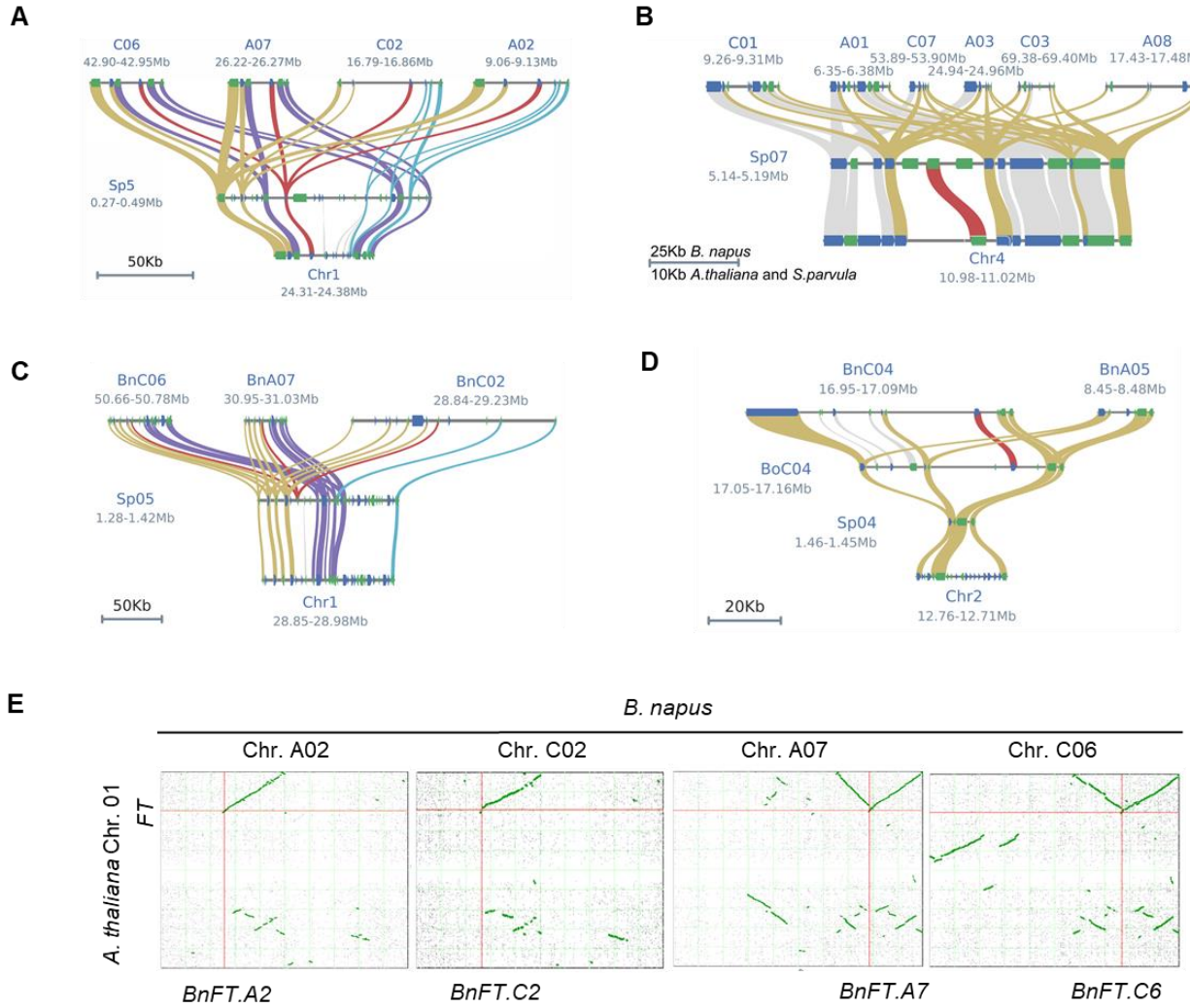

Figure 2. Synteny analysis of *FT, TSF, NFT, CFT* homologues in *A. thaliana, B. napus, B. oleracea* and *S. parvula* genomic backgrounds.

(A) Synteny analysis of *FT* in *S. parvula* and *B. napus* genomic backgrounds identified one and four syntenic genes, respectively.

(B) Synteny analysis of *TSF* in *S. parvula* background identified one syntenic gene, whereas against *B. napus* genomic background identified six syntenic regions but no syntenic genes.
(C) Three novel positions of FT-like gene on Chr. A07/C02/C06 in *B. napus* syntenic to the same region in *S. parvula*, which have no correspondence in *A. thaliana* genome.
(**D**) A unique copy of an FT-like gene exists on Chr. C04 in *B. napus* and the C-genome parent *B. oleracea*, but is absent in the *S. parvula* and *A. thaliana* genomes.
(**E**) Dotplot of genome-wide alignments between *A. thaliana* Chr. 01 and *B. napus* Chr. A02, C02, A07 and C06. Distinctive "V" shapes in the scatterplot were identified on Chr. A07 and C06, but not on Chr. A02/C02. The pink line represents the position of *FT* and its orthologous genes in the *A. thaliana* and *B. napus* genomes.
Red lines (A–B) represent the target genes and their syntenic regions among *A. thaliana*, *S. parvula*, *B. napus* and *B. oleracea* genomes. Yellow lines mark genes with conserved synteny among *A. thaliana*, *S. parvula*, *B. napus* and *B. oleracea* genomes. Purple and blue lines represent genes with synteny among *A. thaliana*, *S. parvula* and *B. napus* Chr.A07/C06, and Chr. A02/C02, respectively.

3.2.2 Phylogenetic analysis of *BnFT* candidates

To investigate the phylogenetic relationships among the candidate BnFT proteins, a neighbour-joining phylogenetic tree was constructed using protein sequences encoded by *FT*, *TSF*, *TFL1*, *BFT*, *MFT*, *AlFT*, *AlTSF*, *Sp.FT*, *Sp.TSF* and *Sp.NFT* (Appendix Table 1)*;* as well as those encoded by *FT* homologues from *B. napus*, *B. rapa*, and *B. oleracea* identified by sequence blast and synteny analysis (Table 1). The frame shifts in the two non-functional genes *BnNFT.C2* and *BnNFT.C6* were corrected (https://www.webscipio.org/search) and the corresponding proteins were included in the phylogenetic analysis. TFL1, BFT and MFT were added as outgroups.
The resultant tree distinctly delineated four parts. At the base of the tree, the first group included the TFL1, BFT and MFT proteins in *A. thaliana*, which served as outgroups and formed a sister clade to all others (Fig. 3, blue box); FT from *A. thaliana* and *A. lyrata* were located on an independent branch (Fig. 1, green box); TSF from *A. thaliana*, *A. lyrata* and *S. parvula* clustered with CTFs and NTFs from *Brassica* species and *S. parvula* to form a third branch (Fig.1, grey box), and the fourth branch contained FT homologues from *Brassica* species and *S. parvula* (Fig. 3, pink box).
The “grey group” included SpTSF, located in parallel with a sub-branch composed of TSF and AlTSF and a third independent sub-branch containing all CTFs and NTFs, which were further divided into two parallel groups: SpNFT, and NFTs and CFTs from *B. napus* and its genome donor species, *B. oleracea*. Thus, based on the similarity of their encoded proteins, NTF genes may have arisen as paralogues of *TSF*, whereas *CTFs* are probably paralogues of NTF genes.
The “pink group”, which includes the four *FT* orthologs of *B. napus* was divided into two sub-branches, which showed a closer relationship to proteins encoded by paralogues located on Chr.

A02/C02 and Chr. A07/C06, respectively (Fig. 2A; Fig. 3), indicating that the genomes that contributed to the genome triplication of the *Brassica* genus were more diverged than the subsequent A and C lineage within the genus.

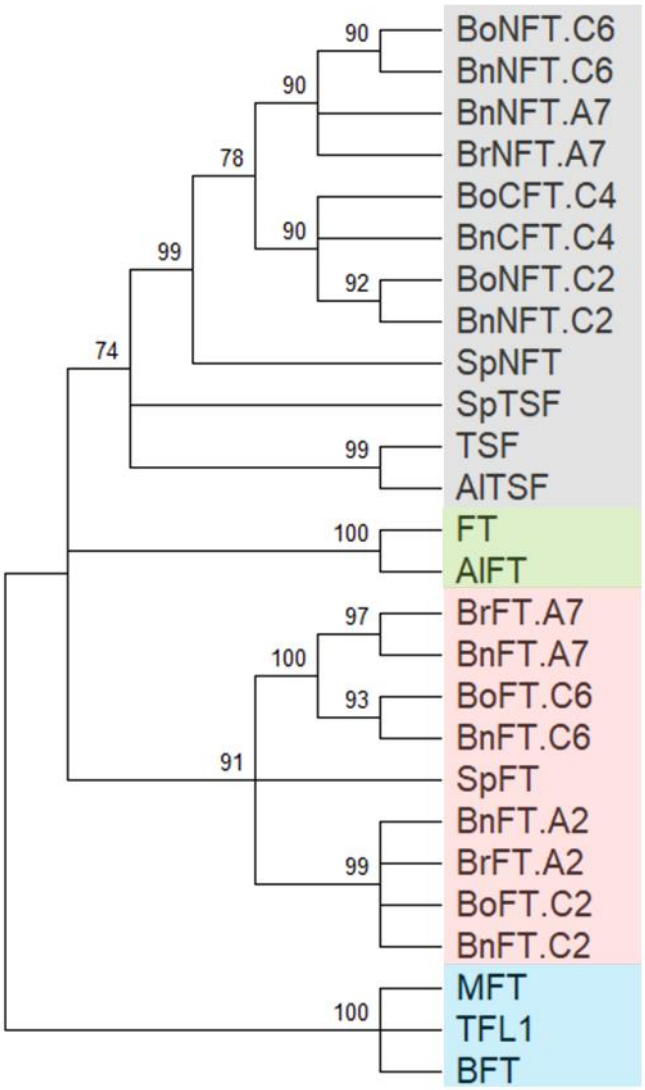

Figure 3. **Phylogenetic analysis of *FT, TSF, NFT* and *CFT* homologues.**

Full-length protein sequences of FT, TSF and FT homologues obtained by blast and synteny analysis against *B. napus*, *B. rapa*, *B. oleracea* and *S. parvula* genomes were used to create the neighbour-joining (NJ) consensus tree using MEGA-11 with 1,000 bootstraps. TFL1, BFT, MFT were set as an outgroup, and FT and TSF orthologues in *A. thaliana* and *A. lyrata* were added for reference. The tree was divided into four independent branches, which are labelled with different colours.

In summary, on the basis of a combination of blast results, synteny and phylogenetic relationship analysis, the following homologues were identified: four *FT* homologues (*BnFT.A2*/C2/A7/C6); three

NFT copies, (*BnNFT.A7/C2/C6*), two of which are probably encoded by pseudo-genes; and one *BnCFT.C4* gene, which is unique to *B. napus* and the C-genome parent, *B. oleracea*, but absent from *S. parvula* and *A. thaliana*.

3.3 Preparation for expression data analysis

3.3.1 Sequence alignment of *FT* and BnFT-like genes

To gain deeper insights into the characteristics of gene sequences and their interrelationships, a sequence alignment analysis of the coding sequences (CDS) and 5' UTR sequence was performed using *FT*, four *BnFT* homologues and *BnNFT.A7* and *BnCFT.C4* from ZS11 (Fig. 4). A high overall CDS sequence similarity of 90.69% and a lower 3' UTR sequence similarity of 53.7% were identified (Fig. 4A, B)

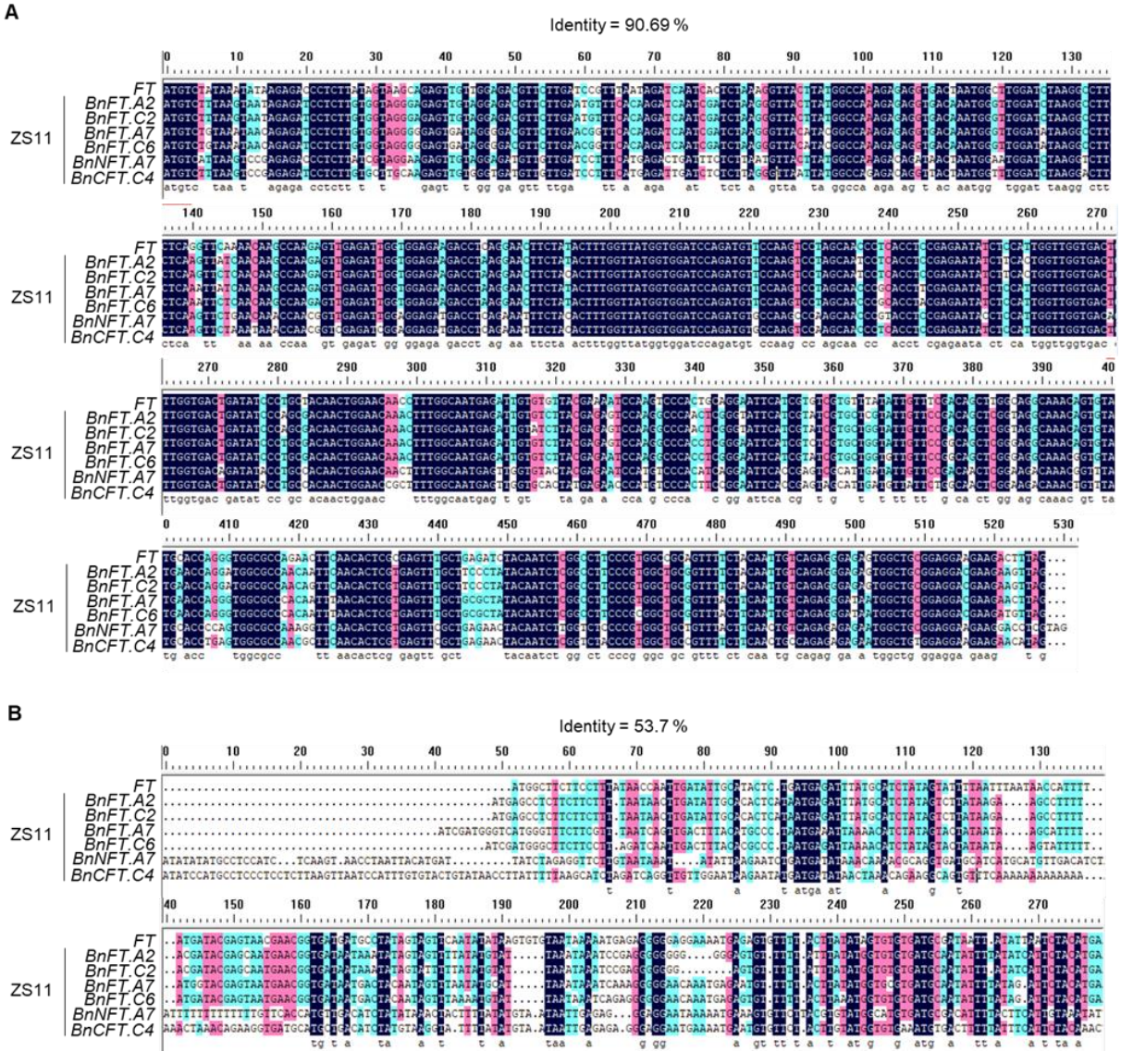

Figure 4. Coding sequence and 3' UTR sequence alignment between *FT*, *BnFT*, *BnNFT*, and *BnCFT*.

Full-length CDS (A) and 3' UTR sequence (B) of *FT*, *BnFT*, *BnNFT* and *BnCFT* were aligned using the DNAMAN software. *BnFT*, *BnNFT* and *BnCFT* were from the ZS11 cultivar.

3.3.2 qPCR primer design

To ensure a comprehensive representation of expression data for various *BnFT*, *BnNFT* and *BnCFT* copies, it was necessary to develop copy-specific qPCR primers. Due to the high CDS similarity, RT-qPCR forward primers were designed to the last exon and reverse primers were designed to the 3' UTR, where more SNPs were present to distinguish various BnFT-like transcripts (Fig. 5A). Primers were used for PCR amplification with *B. napus* genomic DNA as a template and the corresponding amplicons were confirmed using Sanger sequencing (data not shown).

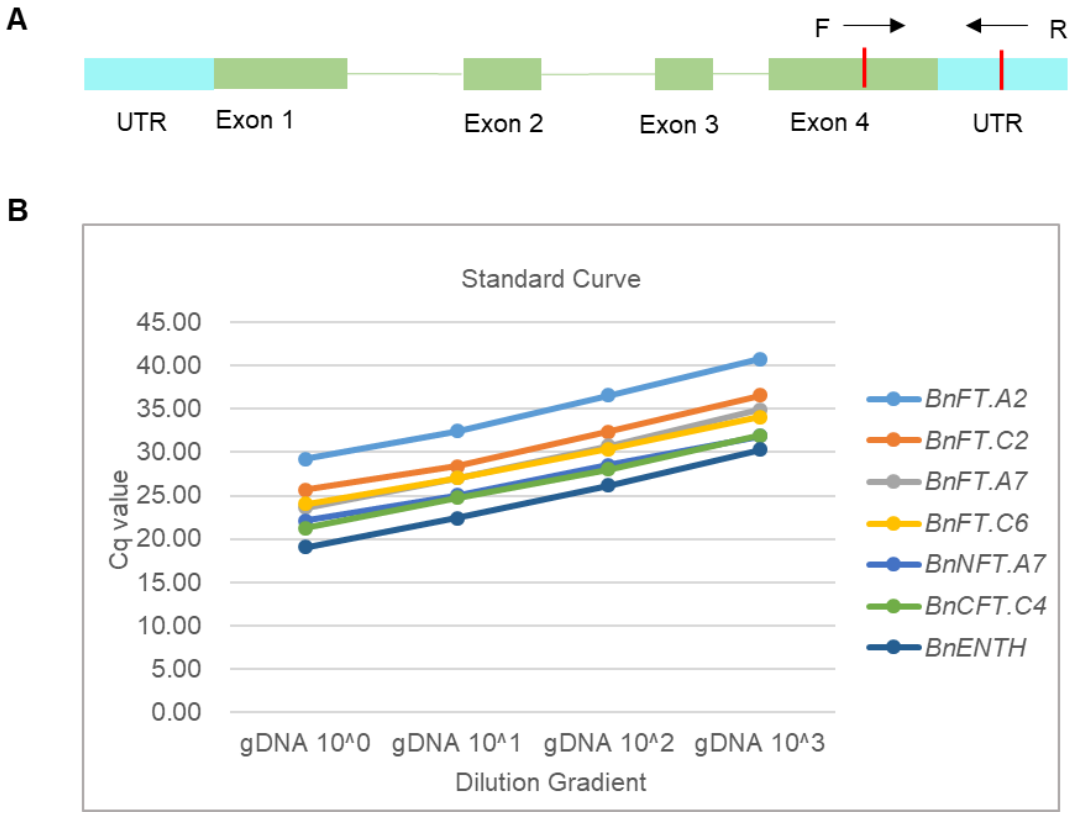

Figure 5. Copy-specific qPCR primers for *BnFTs*, *BnNFT* and *BnCFT*.

(A) Schematic diagram to show the position of the qPCR primers.

(B) Standard PCR amplification curve for qPCR primers with gradient-diluted ZS11 genomic DNA as template.

To calculate the amplification efficiency of primer pairs, the standard PCR amplification curves for different primer pairs were drawn using Cq values at different gDNA concentrations, using gradient-

diluted ZS11 gDNA as the template. In addition, by deriving the formula for linear regression, the slope for each pair of primers was obtained, which was used to calculate the amplification efficiency. The slopes for *BnFT.A2*, *BnFT.C2*, *BnFT.A7*, *BnFT.C6*, *BnNFT.A7*, *BnCFT.C4* and the reference *BnENTH* were determined to be 3.57, 3.68, 3.52, 3.44, 3.14, 3.24, and 3.77, respectively (Fig. 5B). Furthermore, using the expression of each gene in ZS11 genomic DNA as the baseline with a value of 1, a comprehensive comparison of expression levels among *BnFT*, *BnNFT* and *BnCFT* genes could be conducted.

3.4 Tissue-specific expression data

3.4.1 The paraclade leaf exhibits consistently higher gene expression than other tissues

To analyse tissue-specific gene expression, Westar and ZS11 were cultivated in the greenhouse under LD conditions for 4 weeks, were vernalized for 4 weeks and were then transferred back to the greenhouse under LDs. Throughout development, plant tissues were harvested at Zeitgeber time 12 (ZT12) with three biological replicates. Root material and leaf 6 were sampled prior to vernalization, leaf 8, paraclade leaves, floral buds, flowers and siliques were sampled after vernalization. Leaf 6 and leaf 8 represent the sixth and eighth leaves formed during development. The paraclade leaves are those formed latest and are located closest to the flower.

The expression of *BnFT.A2* was considerably higher in paraclade leaves than other tissues in both Westar and ZS11 (Fig. 6A). In both cultivars, the expression levels of *BnFT.A7* and *BnFT.C6* were comparable in leaf 8 and the paraclade leaf, and the expression of these genes in these tissues surpassed that in all other tissue types (Fig. 6C, D). For *BnFT.C2*, *BnNFT.A7* and *BnCFT.C4*, an elevated expression level was observed in the paraclade leaf (Fig. 6B, E, F). By contrast, the lowest expression levels for all genes were observed in the roots, whereas expression levels in flower bud, flower and silique ranged from low to high, and expression was consistently highest in paraclade leaf.

In addition, *BnFT* homologues except for *BnFT.C2* are more highly expressed than *BnNFT*.A7 and *BnCFT.C4*. Specifically, *BnFT.A2* in paraclade leaves, exhibited the highest expression of 13 and 22 in Westar and ZS11, respectively (Fig. 6A). *BnFT.A7* and *BnFT.C6* exhibited a relative higher expression level of 7 and 9, 3 and 7.5 in Westar and ZS11, respectively (Fig. 6C, D). Notably, the expression of *BnFT.C2*, *BnNFT.A7* and *BnCFT.C4* were low, with maximum relative values below 0.2, 0.15, and 0.03, respectively (Fig. 6B, E, F).

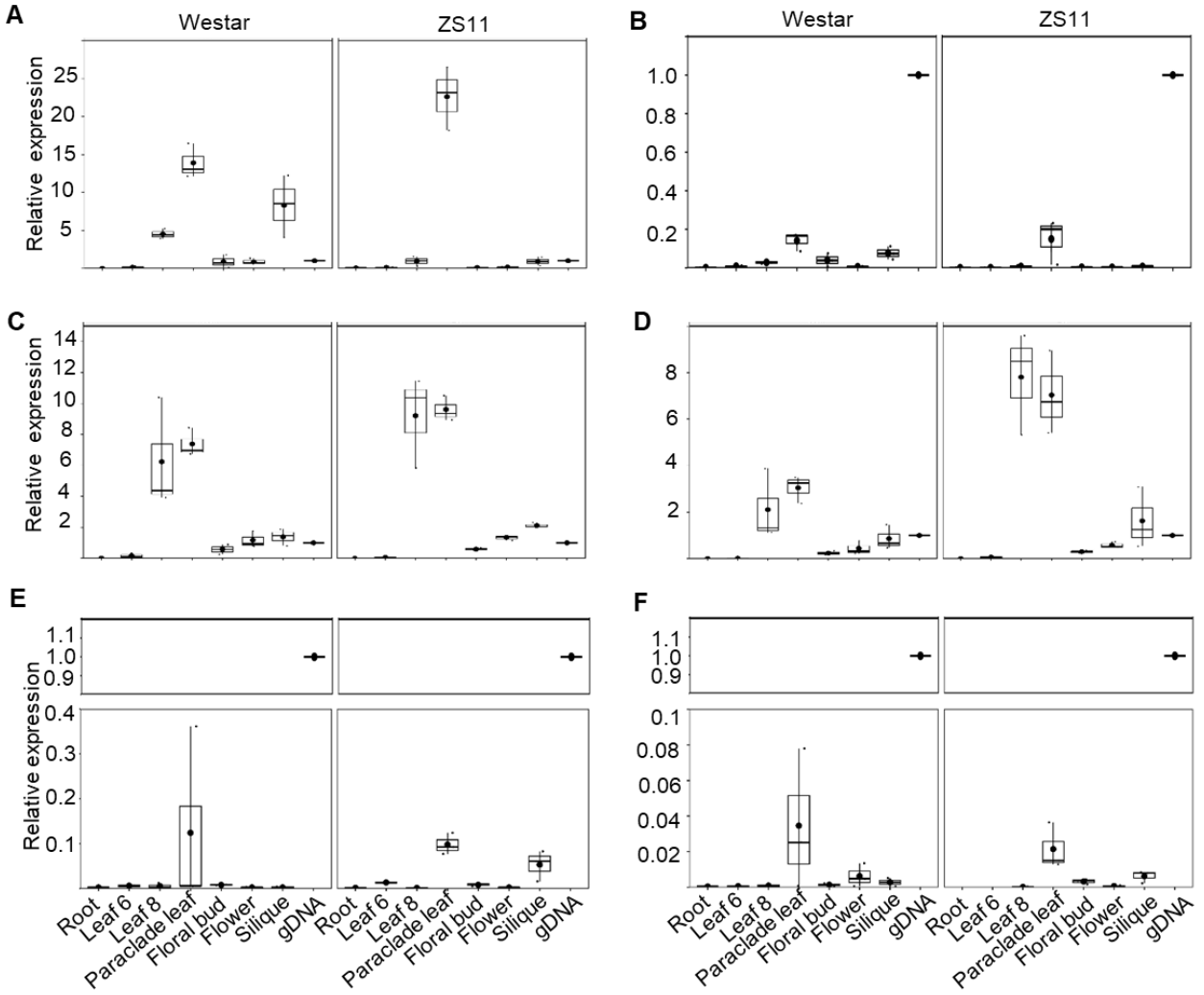

Figure 6. The tissue-specific expression of *BnFT, BnNFT and BnCFT* in Westar and ZS11 cultivars.

Relative expression of *BnFT.A2* (A)**,** *BnFT.C2* (B)**,** *BnFT.A7* (C), *BnFT.C6* (D), *BnNFT.A7* (E) and *BnCFT.C4* (F) in roots, leaf 6, leaf 8, paraclade leaves, floral buds, flowers and siliques in *B. napus* spring cultivar Westar and semi-winter cultivar ZS11. All samples were harvested at ZT12 under LD; the fold change of ZS11 genomic DNA was set as 1, and *BnENTH* was used as an internal reference; boxes represent the quartiles of three biological repeats, and dots represents their means.

3.4.2 Similar tissue-specific expression patterns in Westar and ZS11

The above expression analysis reveals a similar tissue-specific expression of *BnFT.C2*, *BnFT.A7*, *BnFT.C6* and *BnCFT.C4* in Westar and ZS11 cultivars, with the highest expression levels occurring in the paraclade leaf and leaf 8 (Fig. 6B, C, D, F). Slight differences in expression were observed

between *BnFT.A2* and *BnNFT.A7*. Specifically, siliques of the Westar cultivar expressed *BnFT.A2* more highly than all other tissues except for the paraclade leaf, which was not the case for ZS11 (Fig. 6A). This suggests that *BnFT.A2* potentially plays a role in silique development in the Westar cultivar. A similar scenario was observed for the higher expression of *BnNFT.A7* in siliques of ZS11 than in siliques of Westar (Fig. 6E). However, given the extremely low levels of expression, this difference might not be biologically relevant.

3.5 Protein function validation

3.5.1 High protein similarity among FT, BnFTs, BnNFT and BnCFT

The amino-acid sequence of FT, the four BnFT proteins, BnNFT, and BnCFT were aligned to understand the potential conservation of their functions. A high sequence similarity of 89.94% was identified, with the greatest conservation observed for the central region than both end regions (Fig. 7). In addition, BnNFT.A7 and BnCFT.C4 shared a lower protein similarity with FT and the four BnFT homologues, which was expected from the phylogenetic tree.

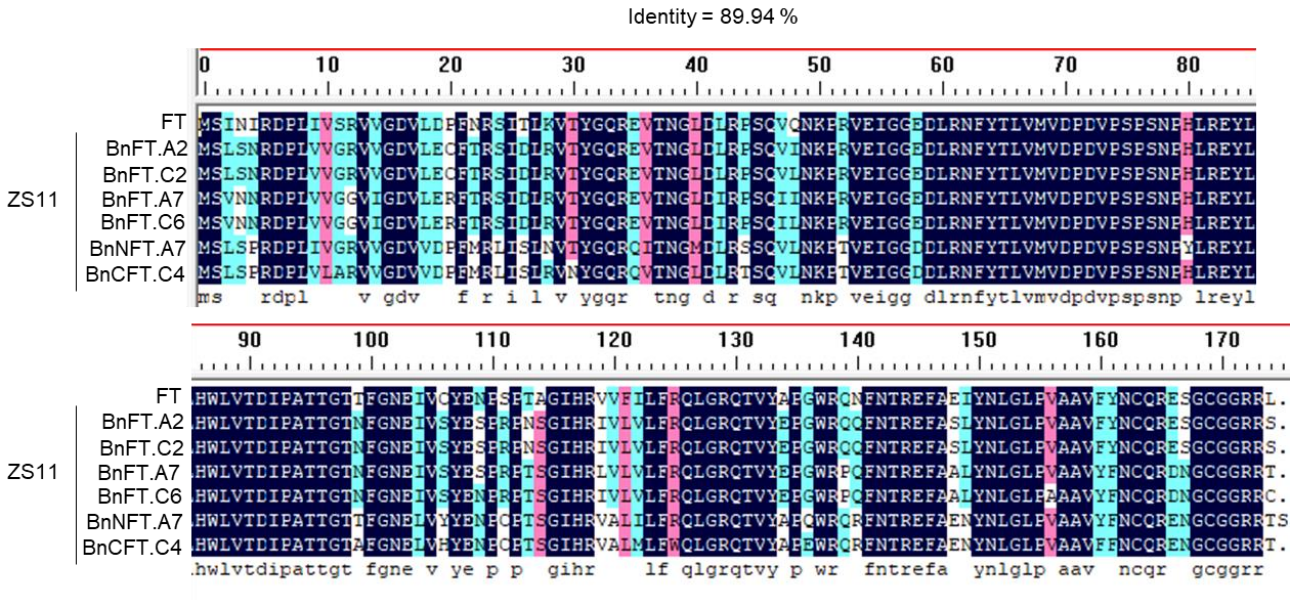

Figure 7. Amino-acid sequence alignment for FT, BnFT, BnNFT and BnCFT proteins.

Full-length protein sequences of FT, BnFT, BnNFT and BnCFT were used for alignment with the DNAMAN software. BnFT, BnNFT and BnCFT were from the ZS11 cultivar.

3.5.2 Mutation of the last amino-acid of BnFT.A7and BnFT.C6 affects their complementation ability

To elucidate the conservation of florigenic functions of the six *B. napus* genes, a cross-species complementation experiment was performed by transforming *ft-10* mutants with plasmids using Block (C+A) from the *FT* promoter region to drive the expression of *FT* homologues coding sequences from ZS11 (Fig. 8A). This promoter was previously shown to express transgenes in phloem companion cells under LD photoperiods, similar to endogenous *FT* (Liu et al., 2014a). The flowering time of the T3 generation was assessed by counting the total number of rosette and cauline leaves. For each *FT* homologues, the flowering time of two independent lines was recorded and analysed.

The results revealed that all six *B. napus* genes partially complemented the late-flowering phenotype of *ft-10*, but not to the same level as the control line expressing *FT* (Fig. 8B). In addition, the genes formed two distinct complementation groups: *BnFT.A2*/*A7*/*C2* complemented *ft-10* with 2 to 7 more leaves than the *FT* control line (median between 17–22 leaves versus 15 leaves, respectively) (Fig. 8B). Conversely, *BnFT.C6*, *BnNFT.A7* and *BnCFT.C4* exhibited markedly weaker complementation, with a median total leaf number ranging from 28 to 37, which was more similar to the late-flowering phenotype of the *ft-10* mutant (median of 38 leaves) (Fig. 8B).

Notably, one of the four *FT* orthologues in *B. napus*, *BnFT.C6*, demonstrated clearly weaker florigen function than the other three *BnFT* genes (Fig. 8B). Several reasons might explain the poor complementation of *ft-10* by heterologous proteins, and these include reduced protein stability in the heterologous system, impaired interaction with the transcription factor FD in the SAM, or reduced transport due to poor interaction with the phloem factors FTIP1, QKY and SYP121 that facilitate FT uploading from the phloem companion cells to the sieve elements, or with NaKR1 that facilitates FT uploading from the sieve elements to the SAM region (Liu et al., 2012).

To further investigate protein functionality, the syntenic pair BnFT.A7 and BnFT.C6 were selected, because these proteins share the highest protein similarity (only five amino-acid differences) but show differences in their ability to complement *ft-10*. It was reported that the C-terminal seven amino-acid residues are important for the movement of FT (Kim et al., 2016). Among these C-terminal seven amino-acid residues, BnFT.A7 and BnFT.C6 differ by only the final N-terminal amino acid, which is T175 or C175, respectively. Targeted mutations were introduced into the final amino-acid position of both proteins, leading to the creation of modified versions termed BnFT.A7m and BnFT.C6m, in which the last C-terminal amino acids were switched from T to C and C to T, respectively (Fig. 8C). As expected, T1 plants transformed with *BnFT.A7* showed a non-significant delay in flowering

compared with *ft-10 FT* transformed control lines (Fig. 8D). By contrast, *BnFT.C6* transformed T1 plants were clearly later flowering than *BnFT.A7* and the *FT* control (Fig. 8D). *BnFT.A7m* and *BnFT.C6m* complementation lines flowered at a similar time to *BnFT.C6* lines, with a median leaf number of 21 to 22 (Fig. 8D). Thus, for BnFT.A7, the substitution of the last amino acid from T to C reduced the ability of the BnFT.A7 protein to complement *ft-10*, whereas for BnFT.C6, the substitution from C to T did not affect its ability to complement *ft-10*.

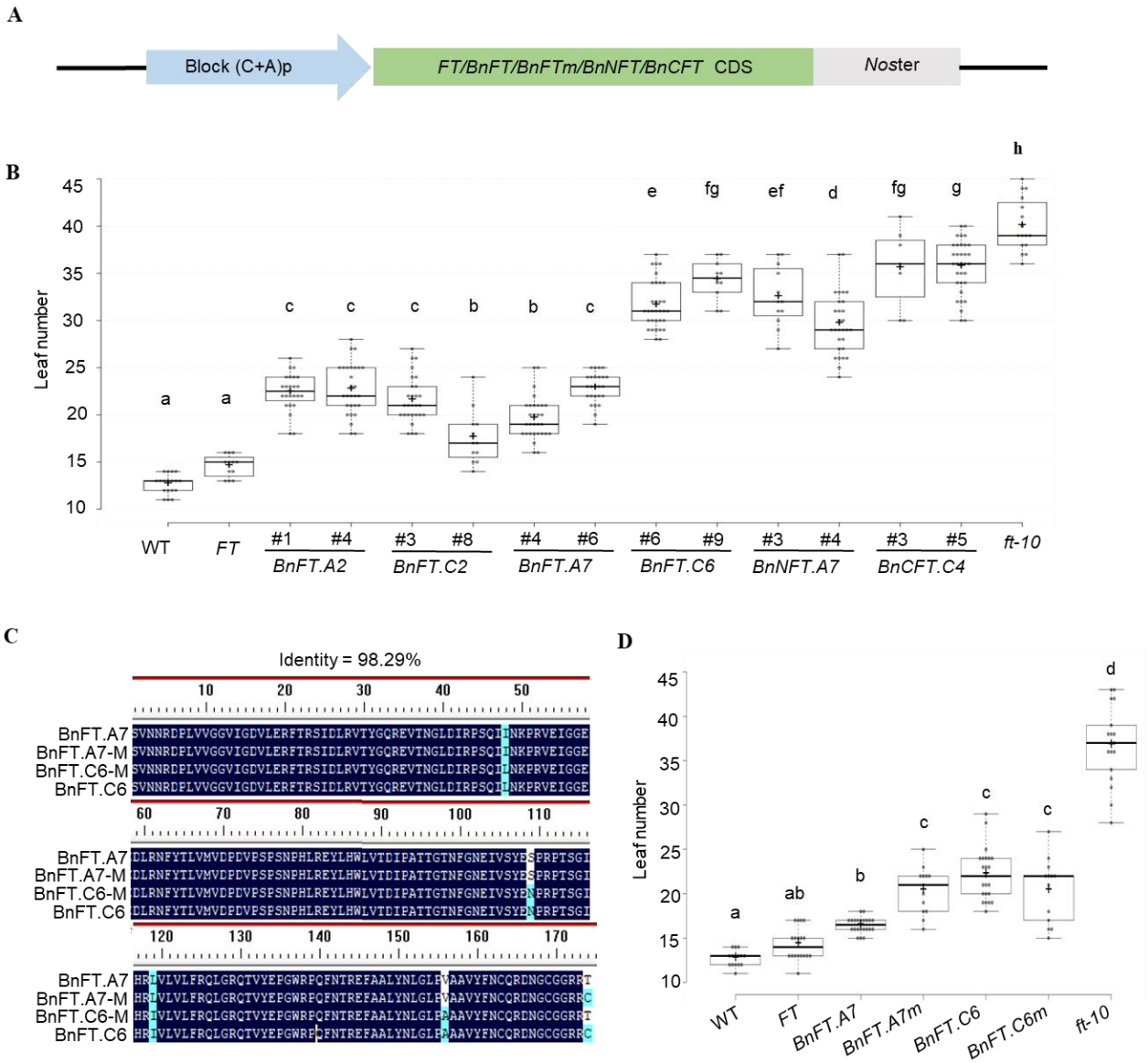

Figure 8. complementation of *ft-10* by *BnFT, BnNFT* and *BnCFT* under control of the Block (C+A) promoter.

(A) Schematic illustration of the constructs used to complement *ft-10*. A synthetic promoter of approximately 1 kb, including Block A and Block C of *FT*, was used to drive expression of *FT*, *BnFT, BnNFT and BnCFT* cDNA from cultivar ZS11 in *ft-10* plants.

(B) Flowering time of *ft-10* T3 plants transformed with *FT*, *BnFT.A2/C2/A7/C6*, *BnNFT.A7* and *BnCFT.C4* within constructs depicted in (A). Plants were grown in the greenhouse in LDs at 20–24°C. The number of plants used for analysis was greater or equal to 7.

(C) Protein alignment of BnFT.A7, BnFT.A7m, BnFT.C6 and BnFT.C6m.

(D) Flowering time of *ft-10* T1 plants transformed with *BnFT.A7/C6* and *BnA7m/C6m*, within constructs depicted in (A). Plants were grown in the greenhouse in LDs at 20–24°C. The number of plants used for analysis was greater or equal to 13.

For flowering-time data in (B) and (D), WT, *ft-10* and *FT* cDNA complementation lines were grown as controls. Total leaf number (including both cauline and rosette leaves) was recorded after bolting. Centre lines show the medians; box limits indicate the 25th and 75th percentiles. Different symbols from a to h above the plots indicate significant differences ($P < 0.05$, two-way analysis of variance (ANOVA) with Tukey's multiple comparison test).

3.5.3 The low complementation abilities of *BnFT.C6*, *BnNFT.A7* and *BnCFT.C4* were increased by expressing them from the *FD* promoter

To test whether poor complementation of *ft-10* was more likely connected with protein movement or to impaired protein function at the SAM, the *FD* promoter was used to drive the expression of *BnFT*, *BnNFT* and *BnCFT* (Fig. 9A). This promoter drives the expression of genes in the SAM, thereby bypassing movement of the encoded proteins through the vasculature (Abe et al., 2005).

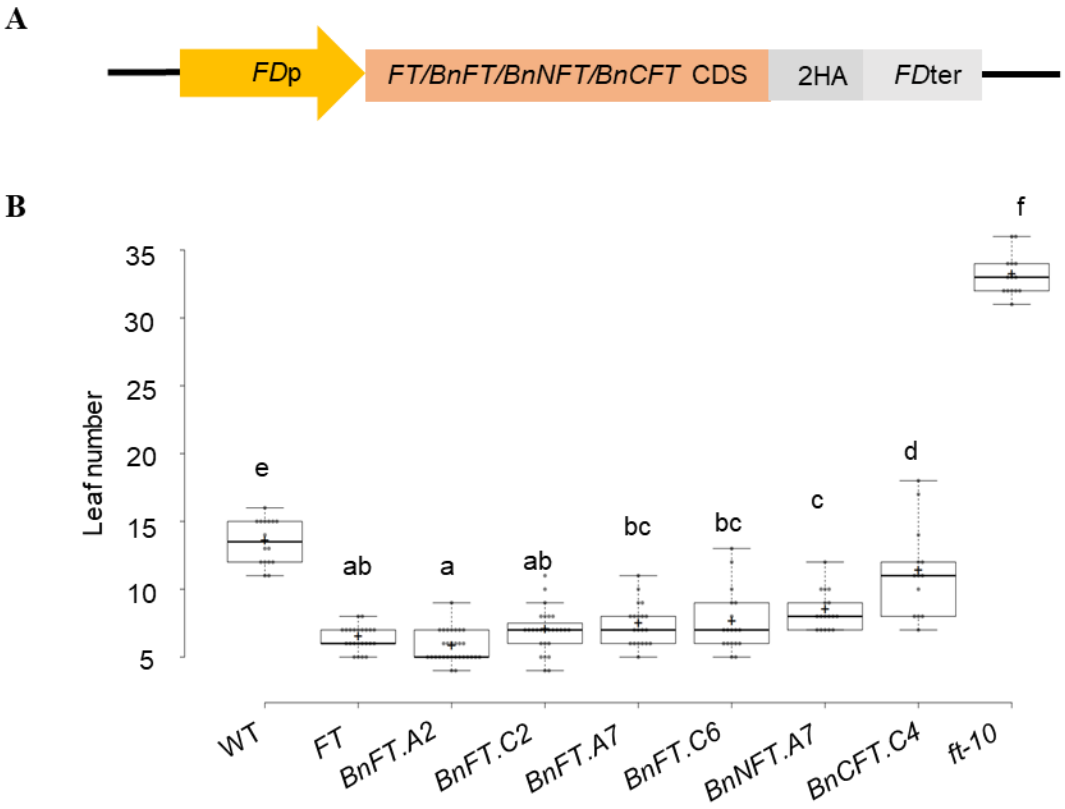

Figure 9. Complementation of *ft-10* by expression of *FT*, *BnFT, BnNFT* and *BnCFT* under control of the *FD* promoter.

(A) Schematic illustration of the constructs used in the *ft-10* complementation analysis. The *FD* promoter was used to drive *FT, BnFT, BnNFT and BnCFT* cDNA from cultivar ZS11 in the SAM.

(B) Flowering time of T1 *ft-10* plants transformed with *FT*, *BnFT.A2/C2/A7/C6*, *BnNFT.A7* and *BnCFT.C4* with constructs as depicted in (A). Plants were grown in the greenhouse in LDs at 20–24 °C. The number of T1 plants used for analysis was greater or equal to 13.

For the flowering time data in (B), WT, *ft-10* and *FT* cDNA complementation lines were grown as controls. Total leaf number after bolting (including both cauline and rosette leaves) was recorded. Centre lines show the medians; the box limits indicate the 25th and 75th percentiles. Different symbols from a to h above the plots indicate significant differences ($P < 0.05$, two-way analysis of variance (ANOVA) with Tukey's multiple comparison test).

When *ft-10* plants were complemented by *BnFT.C6* driven by the *FD* promoter, the flowering time of T1 plants was not significantly different to that of *BnFT.A2/C2/A7* and *FT* transformed controls, with a median leaf count of approximately 6 to 7. Thus, when expressed directly in the SAM, *BnFT.C6* exhibited a similar protein function to the other three *BnFT* homologues. In addition, the flowering time of plants transformed with all the different constructs was significantly earlier than that of WT plants, whose median leaf number was 14 (Fig. 9B). These experiments suggest that interaction of BnFT proteins with FD is conserved throughout speciation, whereas protein transport might be the primary determinant of the observed differences in complementation efficiency. A similar scenario might also apply to *BnNFT.A7*, because the flowering time of the corresponding transformants was not significantly different to that of *BnFT.A7*/*C6*. By contrast, expression of *BnCFT.C4* under the control of the *FD* promoter led to significantly later flowering than all other complementation lines, indicating that the protein carries amino-acid changes that impair its functions at the SAM, such as the interaction with FD (Fig. 9B).

3.6 Photoperiod-responsive expression analysis

3.6.1 Three *BnFT* homologues show vernalization- and photoperiod-responsive expression

FT expression occurs only in LD photoperiods and is dependent on the presence of the direct activator CO in *A. thaliana* leaves. For the semi-winter cultivar ZS11, four weeks of vernalization is required to decrease the expression of the floral repressor *BnFLC* genes, and thus to de-repress the expression of *BnFTs* and initiate normal flowering. To quantify the expression of *B. napus* FT-related genes in response to photoperiod and vernalization, ZS11 was cultivated for six weeks in separate LD and SD

growth chambers, after which they were vernalized for 4 weeks, and were then transferred back to LD or SD chambers, respectively. Leaf 6 was sampled the day before plants were transferred to the vernalization room and leaf 8 samples were harvested the day when plants were transferred back to the original LD or SD chambers and after one week of adaptive growth. Sampling was performed every 4 h for a 24-h period. RT-qPCR for *BnFT*, *BnNFT* and *BnCFT* homologues was performed with the same primers used for the tissue-specific expression analysis (Appendix Table 2). A blast search using the BnPIR website (http://cbi.hzau.edu.cn/bnapus/) identified two *CO* homologues in ZS11, consistent with a previous study, and these were named *BnCO.A10* and *BnCO.C9* (Appendix Table 6) (Jin et al., 2021). Gene-specific primers for RT-qPCR analysis of *BnCO* gene expression were designed accordingly (Appendix Table 2).

BnFT.A2, *BnFT.A7*, and *BnFT.C6* showed a similar expression pattern: markedly higher expression levels under vernalization in LDs than in the other three growth conditions, forming an upward parabolic pattern with the lowest expression value at ZT8, and expression not decreasing during darkness, which is different to the temporal expression profile of *FT* in *A. thaliana* (Fig. 10A, C, D). *BnFT.C6* was expressed approximately 7-fold and 1.6-fold more highly than *BnFT.A2* and *BnFT.A7*, respectively. The expression of *BnFT.C2* was variable and was low, at approximately 1/200 the level of that of *BnFT.C6*. This observation is similar to that in a previous study that attributed the expression silence of *BnFT.C2* to the presence of large transposable element insertions within the promoter region (Fig. 10B; Wang et al., 2012). The expression of *BnNFT.A7* was significant higher under the growth condition of LDs prior to vernalization, and showed a downward parabolic shape with the peak reaching 0.9 at ZT8, whereas remarkably low expression levels were observed in the remaining three conditions (Fig. 10E). The expression of *BnCFT.C4* was consistently low across all conditions, with the highest value being below 0.05 (Fig. 10F).

In summary, the three *FT* homologues *BnFT.A2/A7/C6* respond to both photoperiod and vernalization and are considerably more highly expressed than *BnFT.C2*, *BnNFT.A7* and *BnCFT.C4.*

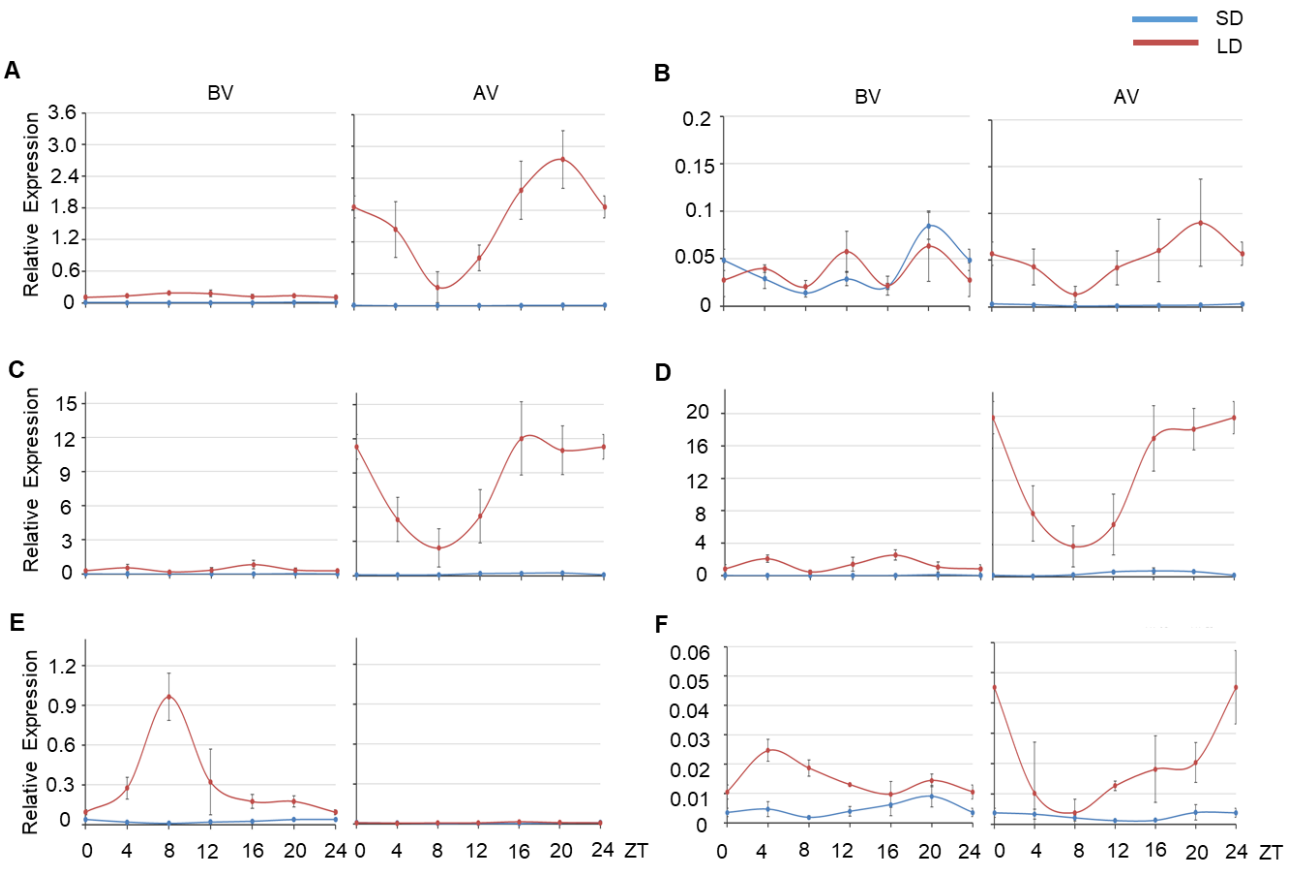

Figure 10. Diurnal expression of *BnFT*, *BnNFT* and *BnCFT* in ZS11 plants under different growth conditions.

Diurnal expression of *BnFT.A2* (A), *BnFT.C2* (B), *BnFT.A7* (C), *BnFT.C6* (D), *BnNFT.A7* (E) and *BnCFT.C4* (F) before and after vernalization in SD and LD photoperiods. Leaf material was sampled every 4 h from ZS11 plants grown in LD- and SD-chambers. Time is plotted in reference to when the light was switched on, and is expressed as Zeitgeber. Leaf 6 and leaf 8 were sampled before (BV) and after vernalization (AV), respectively. Expression levels were analysed by gene-specific qRT-PCR using three independent biological replicates and genomic DNA as common reference points. *BnENTH* was used as an internal reference. Data are means ± standard deviation.

3.6.2 *BnCOs* exhibit a similar expression to *CO* in LDs

For each of the *BnCO* copies, notably similar expression patterns were observed for prior- and post-vernalization phases, although expression level before vernalization was slightly lower than that after vernalization (Fig. 11). *BnCO.A10* exhibited a comparable temporal expression pattern in LD and SD conditions, but the expression level was consistently higher under LDs than in SDs, with the lowest and highest expression occurring in LDs at ZT4 and ZT24, to give a distinct upward "U" shape (Fig. 11A). Similarly, the expression of *BnCO.C9* was similar in LDs to that of *BnCO.A10*, whereas its expression pattern in SDs differed significantly, forming a downward "U" shape with the peak and trough at ZT16 and ZT4, respectively (Fig. 11B). Notably, the expression of *BnCO*.C9 in LDs and

SDs diverged primarily at two time points, ZT20 and ZT24, where expression in LDs was markedly higher than in SDs (Fig. 11B). Moreover, the expression of *BnCO.C9* was consistently higher than that of *BnCO.A10*. Prior and post vernalization, the peak expression values for *BnCO*.C9 in LDs were 1.9 and 3.2, respectively, whereas for *BnCO.A10*, these values were 0.4 and 0.8, respectively.

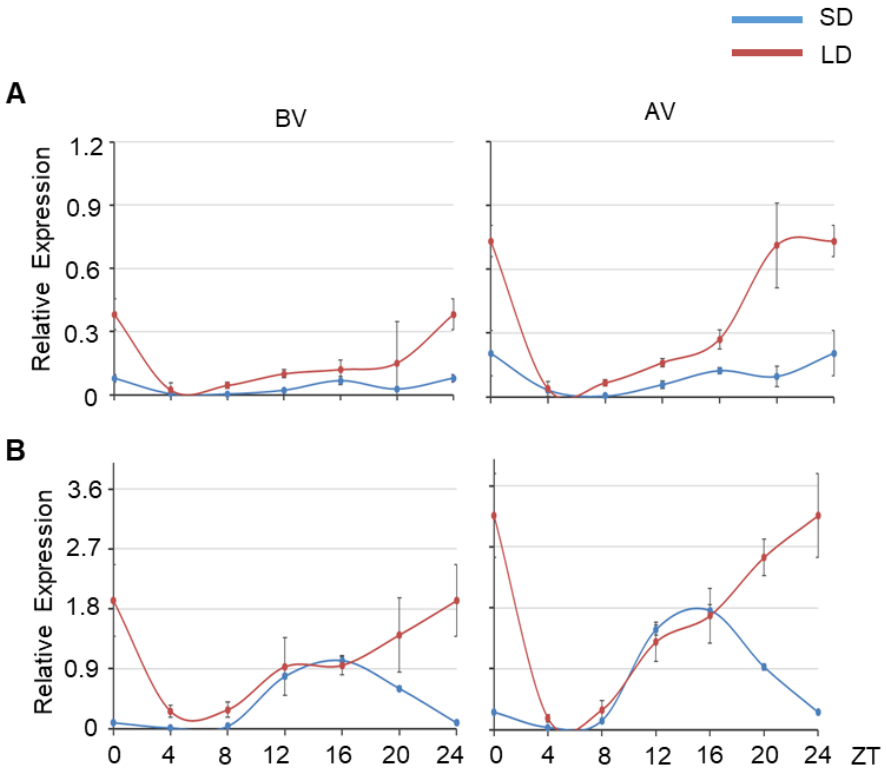

Figure 11. Diurnal expression of *BnCOs* in ZS11 plants under different growth conditions.

Diurnal expression of *BnCO.A10* (A), *BnCO.C9* (B) before and after vernalization in SD and LD photoperiods. Leaf material was sampled every 4 h from ZS11 plants grown in LD- and SD-chambers. Time is plotted in reference to when the light was switched on, and are expressed as Zeitgeber. Leaf 6 and leaf 8 were sampled before (BV) and after vernalization (AV), respectively. Expression levels were analysed by gene-specific qRT-PCR using three independent biological replicates and genomic DNA as common reference point. *BnENTH* was used as an internal reference. Data are means ± standard deviation.

3.7 Conservation of *cis*-regulatory regions at FT-related genes in *B. napus*

3.7.1 Four *BnFT* homologues all show conservation of Block C, Block A and Block E

The photoperiod-responsive expression of *FT* depends on its interaction with CO, which is facilitated by three conserved sequence blocks called Block A, Block C and Block E located within the flanking sequences (Adrian et al., 2010; Cao et al., 2014; Siriwardana et al., 2016b; Tiwari et al., 2010).

Results

Because the FT-related genes in *B. napus* showed different photoperiod-responsive expression patterns to *FT*, it was relevant to analyse whether the three blocks were conserved in *BnFT*, *BnNFT* and *BnCFT* genes. Genomic sequence alignment was performed with mVISTA using sequences of FT-related genes, including all up- and downstream sequences extending to the next flanking coding region (https://genome.lbl.gov/vista/mvista/submit.shtml). The analysis also included *FT* and *TSF* homologues from *A. thaliana*, *A. lyrata*, *S. parvula*; *NFT*, *CFT* homologues from *B. napus*, *B. rapa* and *B. oleracea*, and the *A. thaliana FT*' genomic sequence was used as the reference.

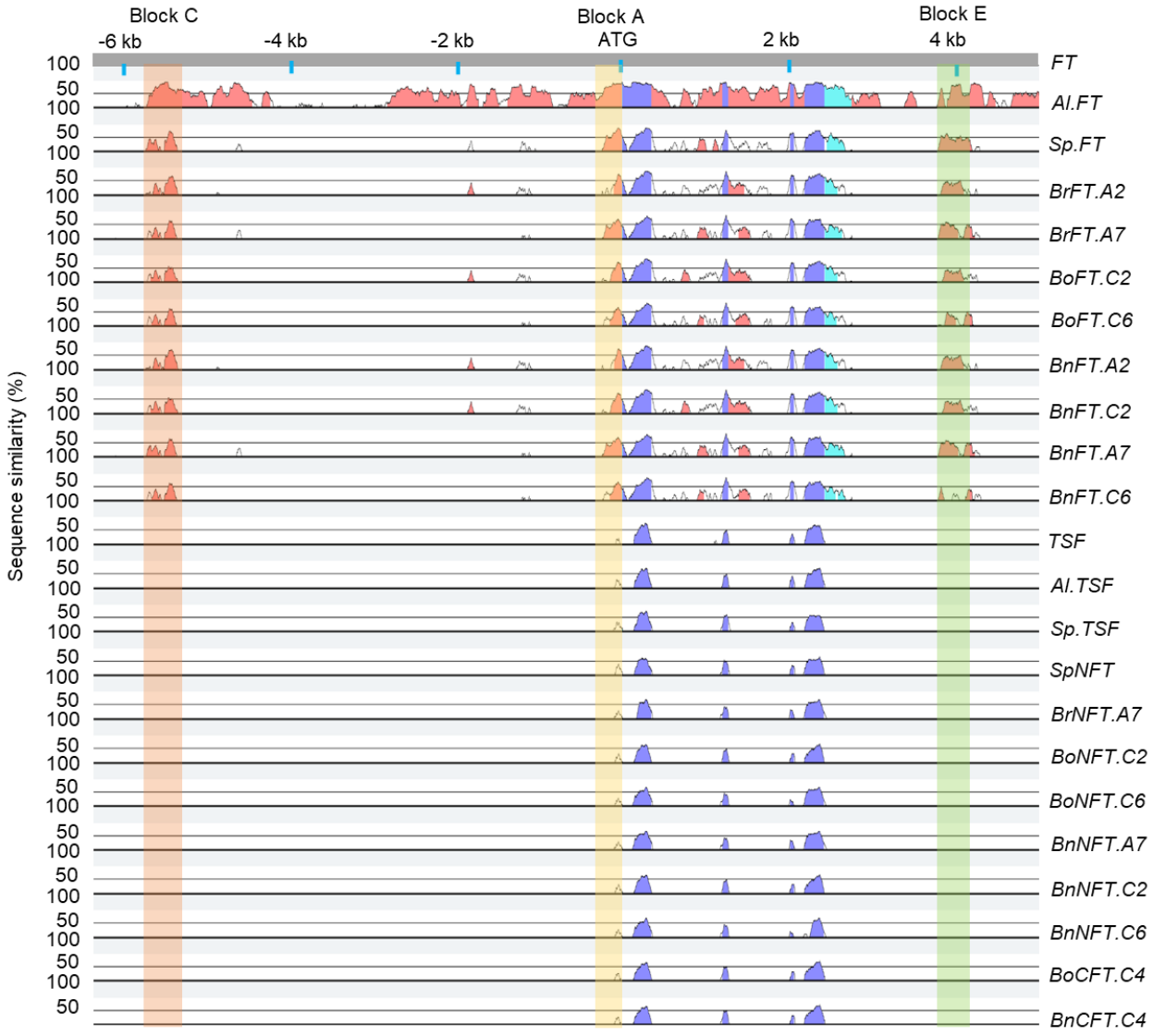

Figure 12. Genome structure alignment analysis

Pairwise alignment of genomic sequences of *FT*, *TSF*, *NFT*, *CFT* homologues from different species to the *FT* genomic sequence using mVISTA. The graphical output shows base-pair identity in sliding 100-bp windows in a range of 50% to 100%. The pink regions are "Conserved Non-Coding Sequences" ("CNS"), the dark blue regions

are exons, and the light-blue regions are UTRs. Orange, yellow and green boxes indicate the location of conserved Block C, Block A, and Block E, respectively.

A high level of conservation was observed between *FT* in *A. thaliana* and *A. lyrata*, as indicated by prominent and widely distributed peak blocks across their complete sequence (Fig. 12). This observation is expected given the close evolutionary relationship between these two species. A limited degree of conservation was observed between *FT* and its orthologues in *S. parvula* and the *Brassica* genus. This includes the highly preserved gene body, as well as conserved Block A, Block C, and Block E in the flanking sequence. By contrast, *TSF*, *NFT*, *CFT* and their homologues showed no conservation of Block C and Block E, only low conservation of Block A and gene bodies with a truncated exon 1 (Fig. 12).

3.7.2 Flowering-time motifs are generally conserved among *FT* and *BnFT* homologues

Specific *cis*-motifs within Block A, C and E play crucial roles in flowering-time regulation pathways (Fig. 13A). To identify the presence of these motifs in *BnFT* homologues, the sequences of Block A, Block C and Block E within *FT*, *BnFT.A2/C2/A7/C6*, *TSF*, *BnNFT* and *BnCFT* were aligned.

The motifs that were generally conserved among *FT* and all four *FT* homologues were: CORE and CCAAT-box motifs within Block C, CORE motif within Block A, and PBE-box and CCAAT-box within Block E (Fig. 13B). Moreover, partial conservation between *FT* and two of the four *BnFT* homologues was also observed. For example, within Block A, a trio of two CORE and a CORE-strict motif, as well as an E-box, was present exclusively in *FT* and *BnFT.A2/C2*. Similarly, the partially overlapping E-box and CCAAT-box within Block E was present in *FT* and *BnFT.A7*/*C6*. Furthermore, among the four *BnFTs*, conservation of motif distribution between the pairs *BnFT.A2*/*C2* and *BnFT.A7*/*C6* was observed. Particularly noteworthy is the identical motif distribution within Block A and nearly identical motif distribution within Block C, with the appearance of an extra E-box, between *BnFT.A2* and *BnFT.C2* (Fig. 13B). Similarly, *BnFT.A7* and *BnFT.C6* share an identical motif distribution within Block A and nearly identical motif distribution within Block C and Block E (Fig. 13B). Notably, two CCAAT-boxes are present within Block A from *BnFT.A7* and *BnFT.C6*, which are the binding sites of the NF-YA/B/C complex (Gnesutta et al., 2017). The binding of NF-YC antagonizes the association of CLF with chromatin and the CLF-dependent deposition of H3K27me3 on the *FT* promoter, thus relieving the repression of *FT* transcription (Liu et al., 2018b). Therefore, the additional CCAAT-box might be the reason for the higher expression of *BnFT.A7* and *BnFT.C6* compared with *BnFT.A2* in leaf 8 (Fig. 10A, C, D).

By contrast, *TSF*, *BnNFT* and *BnCFT* only partially share Block A with much shorter length and lower similarity with *FT* homologues (Fig. 12, Fig. 13B). Furthermore, only an E-box is present within Block A from *BnNFT.C2* and *BnCFT.C4* (Fig. 13B).

A

Motif name	Sequence	Binding site of	Function
CORE	TGTGG /TGTGA	CONSTANS	Activator of *FT* expression in LD
CORE-strict	TGTG(N2-3)ATG	CONSTANS	Activator of *FT* expression in LD
CCAAT-box	CCAAT	NF-YA/B/C	Involving in activation of *FT* expression indirectly
G-box	CACGTG	PIFs	Activator of *FT* expression
PBE-box	CATGTG/CACATG	PIFs	Activator of *FT* expression
E-box	CANNTG	CIB1(PIFs)	Enhance *FT* expression in response to blue light
CArG box 1/2	CTATTTTTGG/CCAAAAATAAG	SVP/FLC	Mediate *SVP*/*FLC*-dependent repression of *FT*/*SOC1*
TBS-like	CCTCGAC/AACCTAA	TOE1	Mediate *TOE1*-dependent negative regulation of *FT*

B

Figure 13. Analysis of *cis*-elements within conserved Block A, Block C and Block E

(A) Core flowering-related *cis*-elements in *A. thaliana*

(B) Schematic diagram showing the distribution of motifs within conserved blocks in *FT*, *TSF*, *BnFT*, *BnNFT* and *BnCFT*. The *cis*-elements are marked in different colours. Block C, Block A and Block E are represented by white strips, whose length is proportional to their actual length in base pairs.

In summary, the overall conservation of *cis*-element distribution between *FT* and *BnFT* homologues suggests that the transcriptional regulation of these genes is conserved between *B. napus* and *A. thaliana*; however, the differences in *cis*-element distribution indicate potential evolutionary divergence for certain TF interactions.

3.7.3 An inverse relationship exists between Block distances and the expression level of *BnFT* genes

To explore the relationship between Block distances and gene expression levels, the post-vernalization expression profiles of four *BnFT* genes under LDs were extracted and compared with each other (Fig. 14A). Meanwhile, analysis using mVISTA analysis exhibit parallel alignment of conserved Block C, Block A and Block E across different species. It is important to note that the promoter lengths of the different genes vary considerably. Therefore, the three conserved blocks from four *BnFT* homologues were drew on their respective promoter sequence proportionally to their actual distribution (Fig. 14B).

The results indicated that there is a clear inverse correlation between the expression levels of the four *BnFT* genes and the distance between Block C and Block E. Notably, *BnFT.C6* showed the highest expression level and the shortest Block distance of 6 kb (Fig. 14). Moreover, *BnFT.A7* and *BnFT.A2*, with block distances of 16 kb and 17.6 kb, respectively, showed intermediate expression levels, and *BnFT.C2* displayed the lowest expression level and possessed the greatest distance of 27 kb between *cis*-regulatory regions (Fig. 14).

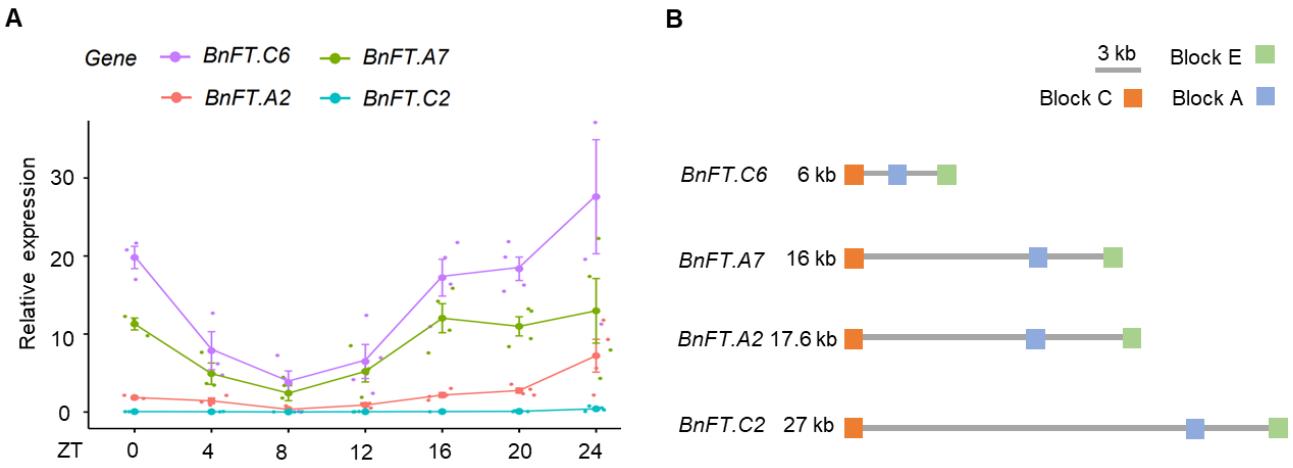

Figure 14. Expression of *BnFT* homologues level is inversely proportional to distance between the sequence blocks.

(A) Diurnal pattern of expression of four *BnFT* homologues in LD.

(B) Schematic diagram showing the blocks and distances of four *BnFT* homologues. The boxes in orange, blue and green represent Block C, Block A and Block E, respectively. Numbers on the left side of the schematic indicate the exact distance between Block C and Block E.

3.7.4 An inverse relationship between the distances between *cis*-regulatory sequence blocks and expression level was confirmed in tobacco infiltration assay

To test the relationship between promoter length and gene expression level, tobacco infiltration was performed. *N. benthamiana* plants were cultivated in the greenhouse under LD conditions at 20°C - 24°C. After the production of 6-8 true leaves, the 4th -6th leaves were infiltrated. Two days after infiltration, leaf samples were harvested for quantification of LUC signals with a multimode reader.

It was hypothesised that the silencing of *BoFT.C2* was caused by the insertions of a DNA transposon (6 kb) and a retrotransposon (5.2 kb) within the upstream Block A and Block B, respectively (Wang et al., 2012). Using mVISTA analysis, these two insertions were observed also exist within *BnFT.C2* from ZS11 plants, but not within *BnFT.A2/A7/C6* (data not shown). In this study, for *BnFT.C2*, which possesses the greatest distance between Block C and Block A, two truncated promoter variants were constructed by removing different portions of the middle region between Block C and Block A, and were used to drive the expression of *LUC* gene (Fig. 15A, B). Both of the two truncated promoter versions did not contain the retrotransposon, whereas the 5.3-kb and 1.8-kb promoter kept 4.1 kb and 1 kb of the transposon sequences, respectively (Fig. 15B).

As shown in the results, two negative control groups exhibited extremely low (LUC/RLUC) *100 signals which were close to 0. Furthermore, the resulting promoter fragments of 5.3 kb and 1.8 kb resulted in significantly different (LUC/RLUC) *100 signal values: the 1.8 kb promoter gave a much higher signal than the 5.3-kb promoter when combined with both BnCO.A10 and BnCO.C9 (Fig. 15C). Specifically, in the 5.3 kb group, in which most of the intermediate region including the retrotransposon and 1.9 kb of the DNA transposon was deleted, clear (LUC/RLUC) *100 signal was observed (35-45) compared with the negative control group (close to 0). For plants infiltrated with the 1.8 kb construct, when a longer fragment between Block C and Block A that included 5 kb of the DNA transposon was deleted, the (LUC/RLUC) *100 signal increased significantly to 70-75 compared with that of the smaller partial deleted 5.3 kb group. These results strongly support the hypothesis that these two long insertions in the upstream region are the basis for the silencing of *BnFT.C2*.

By contrast, no significant differences in (LUC/RLUC) *100 signal were observed between these two promoter versions in the presence of CO from *A. thaliana*. Notably, in each of these two groups with different length of *BnFT.C2* promoter, the signals were always stronger when combined with BnCOs than with CO, suggesting that the *B. napus* CO proteins activate *BnFT.C2* more strongly than CO from *A. thaliana*.

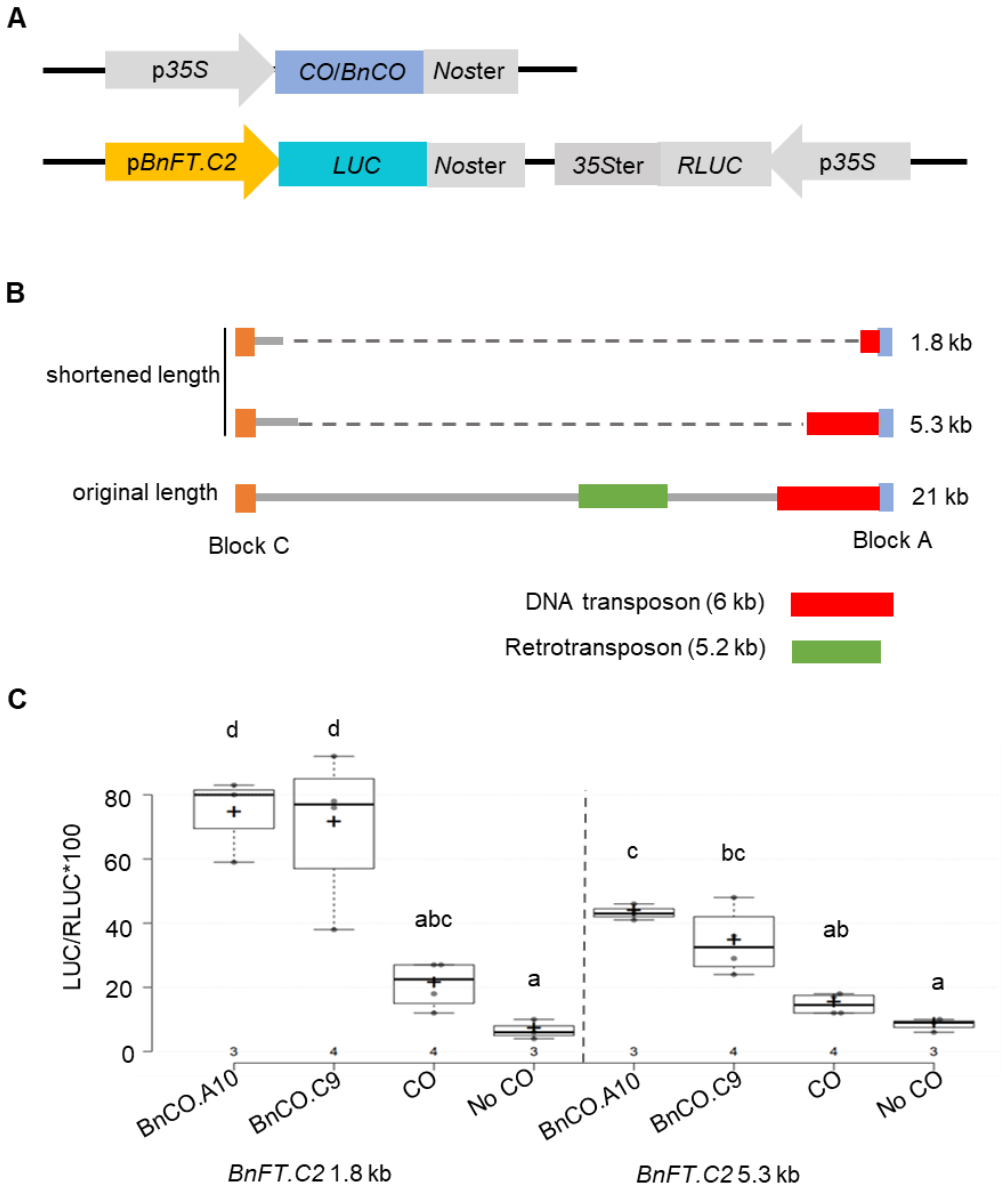

Figure 15. Block distances affect *BnFT.C2* expression levels

(A) Schematic illustration of the constructs used for tobacco infiltration. The upper construct represents the effector construct that includes the CDS of CO, *BnCO.A10* and *BnCO*.C9, all driven by the CaMV 35S promoter. The lower construct represents the reporter construct, featuring Renilla Luc driven by the CaMV 35S promoter and LUC driven by the *BnFT.C2* different promoter lengths.

(B) Different lengths for various promoter types from *BnFT.C2*. The dashed lines represent the deleted region in the middle of the promoter. The solid grey lines denote the regions retained for vector construction. The red and green boxes represent the DNA transposon and retrotransposon, respectively.

(C) Tobacco infiltration results for two types of *BnFT.C2* promoters. The first four boxes and last four boxes represent combinations of *CO*/*BnCO* and *BnFT.C2* promoters with lengths of 1.8 kb and 5.3 kb; respectively. The

symbols from ‘a’ to ‘d’ above the plots indicate significant differences ($P < 0.05$) determined using a two-way analysis of variance (ANOVA) with Tukey’s multiple comparisons test.

3.8 Transcriptome analysis

3.8.1 Principal component analysis

For a more general view on the diurnal expression patterns of the flowering gene regulatory network of *FT* homologues in *B. napus*, leaf 6 was sampled before vernalization and leaf 8 was sampled after vernalization during a 24-h time-course from plants grown in SD and LD photoperiods and were then submitted for RNA-seq analysis. Detailed plant growth treatments and sampling dates refer to photoperiod-responsive expression analysis. Principal component analysis (PCA) of the data showed that the three biological replicates for each sample group clustered together, indicating that variability was higher among experimental conditions than among replicates (Fig. 16). Notably, samples collected at the different ZT form a circular pattern of clustering, aligning with the diurnal rhythm (Fig. 16).

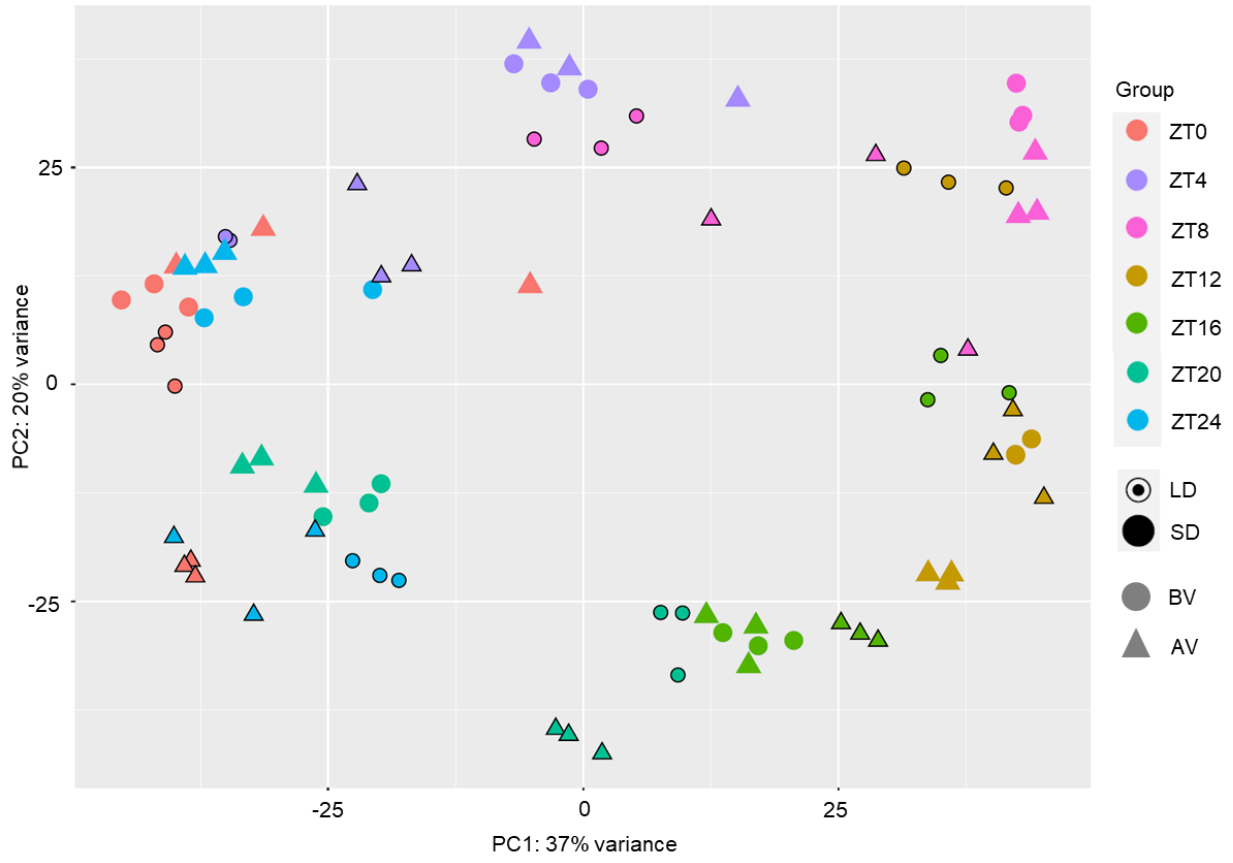

Figure 16. Principal component analysis of transcriptome sequencing.

Different colours represent samples harvested at different ZT. Circles and triangles represent samples collected before and after vernalization, respectively. Symbols with and without the frame represent samples grown under LD or SD conditions, respectively. BV = Before vernalization; AV = After vernalization.

3.8.2 Combinational expression analysis of key flowering genes

To obtain an overview of the gene regulatory network in *B. napus*, the expression values of candidate genes (Appendix Table 6) were extracted from the RNA-seq data and were compared in a heatmap. For enhanced clarity, values were scaled within the range of 0 to 1 and genes that showed similar expression patterns were clustered by hierarchical clustering, which facilitated the identification of genes that respond in a similar manner to diurnal and photoperiodic cues.

3.8.3.1 *BnADO2*, *BnGI*, *BnSVP* and *BnCDF1* responds to photoperiod, whereas *BnFLC* responds to vernalization

Blast with *FKF1* in *B. napus* genome identified six *ADAGIO PROTEIN 2* (*ADO2*) genes that have no synteny relationship with *FKF1* (also known as *ADO3).* Two *FKF1* homologues (*BnaADO2.C7*, *BnaADO2.A7*), two *GI* homologues (*BnGI.C5*, *BnGI.A9*), and two *SHORT VEGETATIVEPHASE* (*SVP*) homologues (*BnSVP.C8*, *BnSVP.A9*) exhibited pronounced responsiveness to photoperiod both before and after vernalization (Fig. 17). Specifically, they showed a notable increase in expression from ZT4 to ZT16 under LD conditions, an upregulation from ZT4 to ZT8 under SD conditions and significantly lower expression at ZT20 and ZT24. By contrast, four *CDF1* homologues (*BnCDF1.C2*, *BnCDF1.A2*, *BnCDF1.C3*, *BnCDF1.A6*) also showed photoperiod responsiveness, but showed an opposite expression pattern: a notable decrease in expression from ZT8 to ZT20 under LD conditions, and a decrease in expression from ZT8 to ZT16 under SD conditions. Six *FLC* homologues (*BnFLC.C2*, *BnFLC.A10*, *BnFLC.A3A*, *BnFLC.A2*, *BnFLC.C3*, *BnFLC.A3*) displayed striking vernalization-responsive expression patterns: Prior to vernalization, these genes exhibited consistently high expression throughout the day under both LD and SD conditions; however, this high expression drastically decreased following vernalization (Fig. 17).

3.8.3.2 *BnFTs*, *BnNFT*, *BnCFT*, *BnCOs*, *BnFDs* and *BnSOC1s* respond to both photoperiod and vernalization

Some genes responded to both photoperiod and vernalization: as expected from the RT-qPCR data, three *FT* homologues (*BnFT.A2*, *BnFT.A7*, *BnFT.C6*) were predominantly expressed in samples from plants grown in LD after vernalization. By contrast, *BnFT.C2* and *BnCFT.C4*, with the extremely low expression level, showed obvious vernalization and photoperiod-dependency expression in the RNA-seq but not in the RT-qPCR data set, which might be caused by the normalization process in RNA-

seq data analysis that amplified the expression differences among different conditions. In addition, *BnNFT.A7* was also predominantly expressed in LD samples after vernalization according to the RNA-seq data, whereas the RT-qPCR data showed it was most highly expressed in the plants grown in LD prior to vernalization (Fig. 10E, Fig. 17). This inconsistency might be due to the relatively low expression of *BnNFT.A7*. In addition to six *FT* homologues, *t*wo *CO* homologues (*BnCO.A10*, *BnCO.C9*), two *FD* homologues (*BnFD.C7*, *BnFD*.A3) and five *SOC1* homologues *(BnSOC1.C3*, *BnSOC1.A4*, *BnSOC1.A3*, *BnSOC1.C4*, *BnSOC1.A5*) showed different patterns of expression in SDs and LDs and before and after vernalization. These genes were significantly more highly expressed under LD conditions after vernalization treatment compared with expression in the other three conditions, suggesting that they probably play pivotal roles in either the intricate regulation of flowering, or in the ageing pathway (Fig. 17).

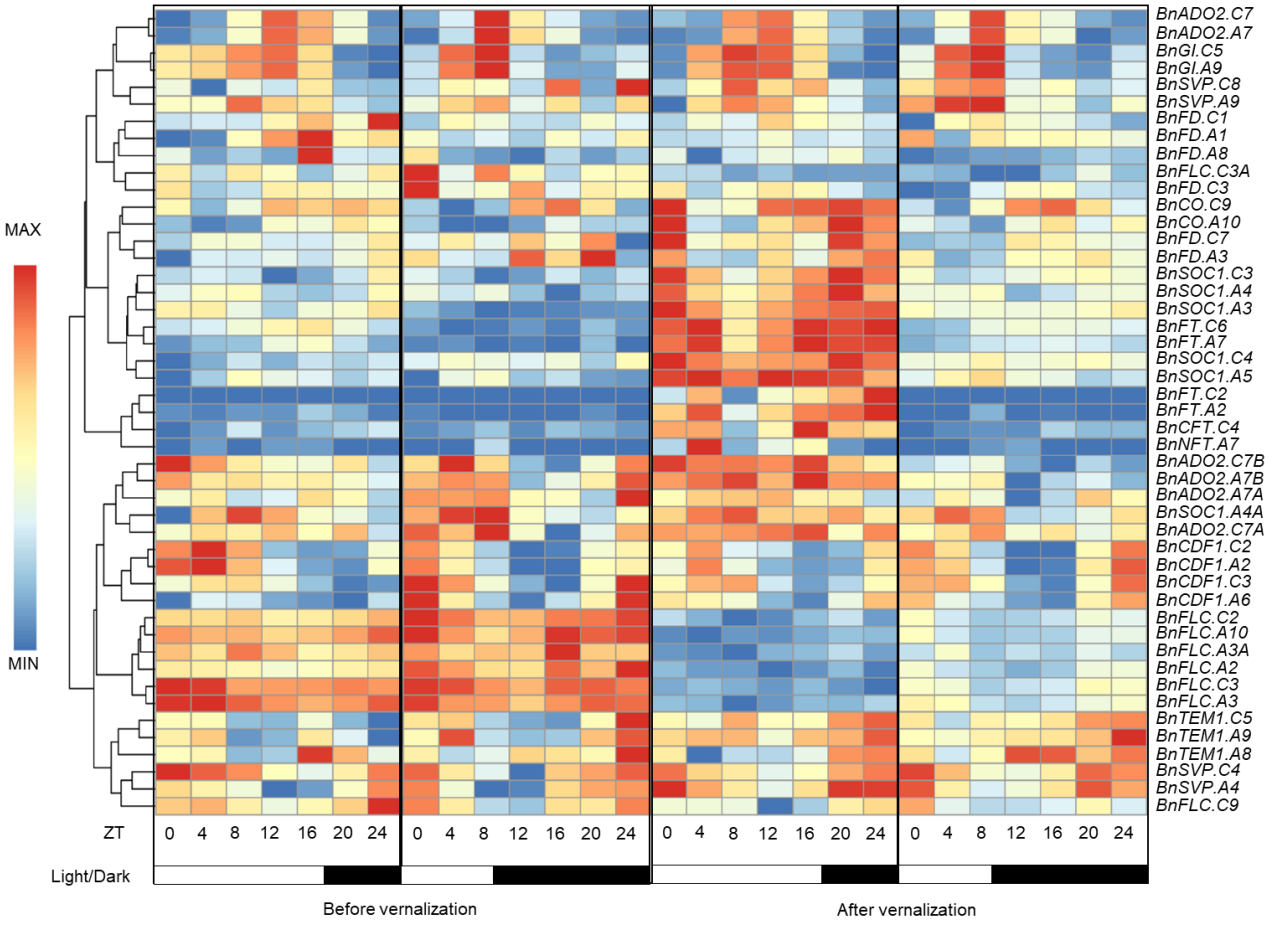

Figure 17. Heatmap of main flowering genes

The original FPKM values were adjusted to $\log_2$(FPKM) values. TBtools used the euclidean distance method and the complete linkage method to cluster rows and columns (Chen et al., 2020). Gene expression values range from red (high expression) to blue (low expression). The mean values of three biological replicates were scaled from 0 to

1 for each gene. The ZT time point is depicted at the bottom of the heatmap; white and black boxes indicate light and dark periods, respectively.

3.8.3.3 Variable expression patterns in multi-copy genes of *B. napus*

Intriguingly, the analysis also revealed that multi-copy genes in *B. napus* exhibited distinct expression patterns. For example, two *BnADO2* genes (*BnADO2.C7* and *BnADO2.A7*) positioned at the top of the heatmap displayed prominent photoperiod responsiveness as depicted above, whereas the other four copies (*BnADO2.C7A*, *BnADO2.C7B*, *Bn ADO2.A7A*, *BnADO2.A7B*), which were located in the middle of the heatmap, exhibited a different expression pattern in LDs got slightly higher expression after vernalization than before vernalization whereas in SDs they showed the opposite pattern (Fig. 17). Similarly, six *BnFLC* copies clustered together and demonstrated pronounced vernalization responsiveness, whereas the other two copies that were not part of this cluster (*BnFLC.C3A*, *BnFLC.C9*) displayed only a slight vernalization response. These differential expression patterns among different gene copies offer valuable insights into potential functional dominance or divergence. This variability underscores the complex regulatory mechanisms that govern the flowering process in *B. napus*.

4. Discussion

4.1 Either LDs or vernalization are sufficient to initiate flowering in ZS11

Plants of ZS11 grown under various light and vernalization conditions showed distinct flowering responses. In the LD+V group, similar with previous study, vernalization effectively alleviated the repression of *BnFT* most probably by repressing *BnFLCs* (Fig. 10, 18; Chen et al., 2018). Meanwhile, LDs probably ensured the accumulation of CO protein, which further activated thee expression of the *BnFT* genes. As a result of these dual activation conditions, LD+V plants flowered earliest among all groups (Fig. 1).

Analogously, SD+V plants also initiated flowering, although this was slightly later than LD+V plants. Nevertheless, under SD+V conditions, expression of the *BnFT* genes was notably low (Fig. 10). This observation suggests that the induction of flowering in ZS11 after vernalization under SD conditions is not under the direct regulation of *BnFT* genes. In *A. thaliana*, the GA pathway plays a crucial role in the floral transition under SD conditions (Wilson et al., 1992), and this might be the reason for why *A. thaliana* eventually flowers under SD conditions without *FT* induction (Cao et al., 2021; Song et al., 2015). Considering the similar flowering regulatory network between *B. napus* and *A. thaliana*, the GA pathway in *B. napus* might also promote flowering as an alternative to the photoperiod pathway mediated by *BnCO* and *BnFT* proteins.

Plants grown under LDs without vernalization flowered considerably later than plants in the two vernalization treatments described above (Fig. 1). LDs probably activate the transcription of *BnFT* genes via BnCO proteins (Fig. 10, 11). However, the repressive state of *BnFTs* mediated by BnFLCs might not be alleviated due to the absence of vernalization (Fig. 10, 18). It can be hypothesized that the autonomous pathway might contribute to the flowering outcomes of LD plants, in light of a study in *A. thaliana* that showed that autonomous pathway genes, including *FCA*, *FPA*, *FVE*, *FLD*, *FLK*, *FLOWERING LOCUS Y* (*FY*), *LD* and *REF6*, encode proteins that inhibit *FLC* expression and promote flowering independently of photoperiod (Baurle & Dean, 2008; Chen et al., 2005; Lee & Amasino, 2013; Lim et al., 2004; Liu et al., 2007; Michaels & Amasino, 2001; Reeves & Coupland, 2001; Rouse et al., 2002; Simpson, 2004). Homologues of these autonomous genes probably exist in *B. napus* and play similar functions in repressing *BnFLC* and promoting flowering.

In summary, the GA and autonomous pathways might play a crucial role in promoting flowering when plants are grown under unfavourable conditions. However, it is not possible for these pathways

to completely substitute for the photoperiod and vernalization pathways in *B. napus*, because SD+V and LD plants flowered clearly later than LD+V plants. Additionally, *B. napus* plants did not flower in SDs during the course of the experiment, suggesting that at least one out of the two LD and vernalisation pathways, should be experienced to initiate flowering of ZS11 (Fig. 1).

4.2 Four *FT* homologues were identified in *B. napus*

In this study, six functional *FT* homologues were identified through blast search utilizing the *FT* protein as a query against the *B. napus* genome, among which four *FT* orthologs, namely *BnFT.A2*/C02/A07/C06, and two first named gene, namely *BnNFT.A7* and *BnCFT.C4*, were identified in both Westar and ZS11 cultivars, in conjunction with synteny analysis, phylogenetic relationship analysis, and protein function validation. However, it is noteworthy that six *BnFT* paralogous genes were identified in the *B. napus* winter cultivar Tapidor through BAC library screening (Wang et al., 2009). Among these paralogues, two copies were identified on chromosomes A07/C06, occupying adjacent positions at the same locus, and were designated *BnA7.FT.a*/*BnA7.FT.b* and *BnC6.FT.a*/*BnC6.FT.b*, respectively. In our study, two out of the six functionally *FT* homologues were located on Chromosome A7 (*BnFT.A7*, *BnNFT.A7*) and one was located on Chromosome C6 (*BnFT.C6*). Protein sequence alignment between *BnA7.FT.a*/*BnA7.FT.b* from Tapidor, and *BnFT.A7*, *BnNFT.A7* from ZS11and Westar revealed that BnA7.FT.a, BnA7.FT.b, and BnFT.A7 share higher sequence identity with each other (98.71%) than with *BnNFT.A7* (91.57%), which suggests that neither *BnA7.FT.a* nor *BnA7.FT.b* corresponds to *BnNFT.A7* (data not shown). Additionally, BnA7.FT.a shares the same protein sequence with BnFT.A7 from both ZS11and Westar, whereas BnA7.FT.b has 9 amino-acid differences (data not shown). Therefore, I propose that *BnA7.FT.a* corresponds to *BnFT.A7* identified in this study. However, BnC6.FT.a and BnC6.FT.b share protein sequence identities with BnFT.C6 from ZS11and Westar of 97.90% and 99.24%, respectively (data not shown). Considering a previously study that indicated that BnC6.FT.b mutants were late flowering, whereas BnC6FTa mutants flowered at the same time as the non-mutated parent (Guo et al., 2014); and our cross-complementation results revealed that the expression of *BnFT.C6* directly in the SAM had a similar protein function to that of *FT* in *A. thaliana*, I propose that *BnFT.C6* identified in this study corresponds to *BnC6.FT.b* and probably possesses a similar florigen function in *B. napus* to *FT* in *A. thaliana*.

A sequencing study elucidated the triplication event within the *B. rapa* genome relative to *A. thaliana*, identified orthologous blocks in the *B. rapa* genome, and uncovered a marked variation in gene loss (fractionation) across the triplicated blocks, which divided the blocks into three categories: the "least

fractionated" (LF), the "medium fractionated" (MF1), and the "most fractionated" (MF2) sub-genome, respectively (Wang et al., 2011). The *FT* gene in *A. thaliana* is situated on the ancestral Block E of chr.01, which corresponds to three duplicated E blocks in the *B. rapa* genome (Wang et al., 2011). Comparative genome analysis of *B. rapa* and *A. thaliana* (Cheng et al., 2012), coupled with an examination of ancestral genome block distributions in the *B. rapa* genome (Cheng et al., 2013), revealed a specific configuration on chromosome A07 in which two E blocks that belong to the LF and MF2 sub-genomes are linked end-to-end (Wang et al., 2011). However, an investigation of the region around *FT* in *B. rapa* disclosed the loss of the syntenic copy within MF2, and therefore only one *FT* orthologue remained on chromosome A07 in both *B. rapa*, and subsequently *B. napus*, which was consistent with our results (Zhang et al., 2015b).

BnNFT.A7 and *BnCFT.C4* were identified to be not *FT* orthologues in *B. napus* because of their different synteny and phylogeny relationship, transcription regulation structure and complementation functions compared to the four BnFT homologs. These two genes named according to their chromosomal localization, and more importantly, their specific synteny relationships across several species. *BnNFT.A7* belongs to a novel syntenic region in *B. napus* and *S. parvula*, while has no correspondence in *A. thaliana* (Fig. 2D). Additionally, two extra *B. napus* genes were identified to map to the same syntenic gene in *S. parvula* as *BnNFT.A7* (Fig. 2D). However, these two copies are predicted to be pseudogenes due to the presence of a frameshift, which caused the high sequence identify but lower sequence coverage with *FT* than the other six functional genes. Therefore, when searching for *FT* homologues using tblastn, a method that employs both identity and coverage, these two pseudogenes were not identified. *A. thaliana*, *B. napus* and *S. parvula* all belong to Brassicaceae family, among which *A. thaliana* belongs to clade A, whereas *B. napus* and *S. parvula* belong to *Clade B* (Huang et al., 2016). We propose two hypotheses to explain the origin and evolution of *FT*, *TSF*, *NFT* and *CFT* homologues. The first hypothesis is that *FT*, *TSF* and *NFT* homologues existed in the common ancestor of clade A and clade B of the Brassicaceae family, which include *A. thaliana*, *S. parvula* and the *Brassica* genus. During evolution, *A. thaliana* inherited *FT* and *TSF* but lost *NFT*. Meanwhile, *S. parvula* inherited all these three genes, whereas *TSF* genes were lost in *Brassica* species. An alternative hypothesis is that *FT* and *TSF* homologues existed in the common ancestor of *A. thaliana*, *S. parvula*, and *B. napus*, and were inherited successfully by *A. thaliana* in clade A. *NFT* homologues appeared in the common ancestor of clade B, and were inherited together with *FT* and *TSF* homologues by *S. parvula*. The divergence of the *Brassica* genus caused the loss of *TSF* homologues, but *FT* and *NFT* homologues were retained from the clade B common ancestor. *BnCFT.C4* was found to be a unique gene that is only present in *Brassica* species (Fig. 2E). Considering their close phylogenetic relationship, it is possible that *BnCFT.C4* is an *NFT* homologue

in *B. napus* (Fig. 3), and the absence of synteny with any of the other genes might be caused by the complicated chromosome recombination events in *B. napus*.

4.3 Florigen function of BnFT homologues

To be noted, our results of BnFTs protein functions were obtained through cross-complementation experiments, which means that there are many aspects affect the final results. When driven by C+A promoter, four *BnFT* homologues all complemented less than *FT*, which might be the result of either overall weaker protein stability of BnFT proteins than FT, or weaker interactions between BnFTs and *A. thaliana* transcription factors, which could further be divided into two parts: factors related to protein transport in the phloem, or factors related to the flowering pathway in the SAM. When driven by the *FD* promoter, which circumvents the need for protein transport and have direct expression in SAM, BnFT homologues demonstrated the same strong florigen functions as FT, suggesting the similar protein properties between BnFTs and FT in terms of their molecular interactions with downstream genes, and the conserved functions of homologous proteins in the flowering regulatory pathways. However, the reasons for the weaker complementation results of *BnFTs* when they were driven by the C+A promoter remain unclear and might reflect a limitation of cross-complementation assays.

One of the four *FT* orthologues in *B. napus*, *BnFT.C6*, resulted in a significantly weaker complementation phenotype than the other three *BnFT* homologues when driven by the C+A promoter (Fig. 8A), but this was not the case when its expression was driven by the *FD* promoter. Protein transport and stability might explain this observation and potentially, BnFT.C6 is degraded during transport. It was reported that FT degradation *in vivo* is mediated by protease-dependent cleavage, which probably occurs at the E167 and S168 residues (Kim et al., 2016). BnFT.A7 and BnFT.C6 share the same D167 and N168 residues and should be similarly affected by protein cleavage, indicating that protein cleavage is not the major reason for the different florigen functions of BnFT.A7 and BnFT.C6. In addition, the C-terminal seven amino-acid residues were revealed to be important for the movement of FT (Kim et al., 2016). Among these C-terminal seven amino-acid residues, BnFT.A7 and BnFT.C6 only differ in a single amino acid, with the last residue being either T175 or C175, respectively. Cysteine (C) and threonine (T) are both uncharged, polar, hydrophilic amino acids, but cysteine (C) in particular, can form covalent bonds with other molecules, including disulphide bonds, which are important components in determining the three-dimensional structure of many proteins. Complementation experiments were performed with BnFT.A7m and BnFT.C6m, which possess substitutions of the last amino acid from T175 to C175, and C175 to T175, respectively.

The results revealed that although they possessed the same C-terminal seven amino-acid residues, BnFT.A7 and BnFT.C6m did not show similar florigen function (Fig. 8D), suggesting that the C-terminal seven amino-acid residues do not constitute the only factor that affects the movement of BnFT proteins and their function ─ perhaps the remaining four amino-acid differences between BnFT.A7 and BnFT.C6 also play a crucial role. The amino-acid substitutions significantly decreased the ability of BnFT.A7 to complement the *ft-10* mutant, suggesting that this amino acid is important for the florigenic function of BnFT.A7 (Fig. 8D).

In summary, considering a previous study which revealed that *BnFT.A2* and *BnFT.C6b* were associated with two major QTL clusters for flowering time in Tapidor (Wang et al., 2009), it is difficult to conclude whether BnFT.C6 is also a "weaker" allele than the other *BnFT* genes in ZS11.

4.4 The *B. napus FT* homologues show different photoperiod-responsive expression patterns to *A. thaliana FT*

In *A. thaliana*, diurnal *FT* mRNA accumulation follows a downward parabola with the peak occurring at ZT16 in LDs (Fig. 19A) (Turck, Fornara, & Coupland, 2008). In this thesis under LD and post-vernalization conditions, *BnFT* homologues, with the exception of *BnFT.C2*—whose expression was markedly attenuated which probably due to an insertion in its promoter region—manifested a consistent expression pattern characterized by an upward parabolic curve, with the trough and peak of expression occurring at ZT8 and ZT16, respectively (Fig. 10A, C, D; Fig. 19A). The different expression patterns between *FT* and its homologues in *B. napus* were mainly observed at ZT20 and ZT24 — two time points that showed a sustained high expression level in the dark for *BnFT* genes. In *A. thaliana*, the reduction in *FT* mRNA levels after ZT16 is attributed to the degradation of the CO protein during the dark phase (Jang et al., 2008; Valverde et al., 2004). The phosphorylated form of CO is preferentially degraded in the dark by the 26S proteasome through the activity of the E3 ubiquitin ligase complex COP1–SPA (Hoecker et al., 1999; Hoecker et al., 1998; Jang et al., 2008; Laubinger et al., 2006; Liu et al., 2008b; Sarid-Krebs et al., 2015). Under the precondition of continuous accumulation of *BnCO* mRNA, the sustained accumulation of BnCO proteins might be the reason for the sustained high expression of *BnFT* transcripts in the dark. Consequently, this raises the possibility of either an atypical phosphorylation of the BnCO protein or the diminished presence of upstream COP1 and SPA proteins. Alternatively, if BnCO is rapidly degraded in the dark, similar to CO in *A. thaliana*, then the high level of *BnFT* mRNA would suggest the presence of distinctive regulatory pathways involving other pivotal genes responsible for stimulating *BnFT* mRNA

accumulation during darkness, which also suggests that *BnFT* genes are subject to an additional distinct photoperiod-responsive transcriptional regulation.

It is worth recalling from the introduction that the photoperiod-responsive expression of *FT* relies on three conserved blocks situated in its flanking sequences, involving a multitude of *cis*-elements. The gene alignment analysis here showed that the presence and distribution of *cis*-elements within conserved blocks is moderately conserved between *FT* and its homologues in *B. napus* (Fig. 13B). However, the differences are as follows: the uniform existence of two CCAAT-box on Block C in four *BnFT* homologues but only one in *FT*; the presence of an extra CORE motif within Block C and Block A in *BnFT.A2*/C2, and the parallel existence of an E-box and CCAAT-box within Block A in *BnFT.A7*/C6, respectively. These distinct *cis*-elements, which are unique to *BnFT* homologues but not present in *FT, together* with the non-degradation of the CO protein, might account for the high accumulation of *BnFT* gene mRNA during darkness.

4.5 An inverse relationship exists between promoter length and expression level

In plants, most variability in genome size is associated with different repetitive DNA content, which is primarily ascribed to differential amplification of Transposable Elements (TEs), a phenomenon that is ubiquitous among eukaryotic genomes (Hawkins et al., 2006).

Two insertions in the promoter region of *FT.C2* were proposed to be the basis for its silenced expression in *B. oleracea* (Wang et al., 2012), which were identified to have their parallel existence in *BnFT.C2* from both ZS11 and Tapidor cultivars (data not shown). The four *BnFT* genes in ZS11 cultivar possess significantly different promoter length, as exemplified by: the distance from Block C to Block A, which might be the result of TE insertions. Deletions of the sequence between Block C and Block A significantly increased the downstream *LUC* signal, suggesting that *BnFT.C2* promoters with longer deletions can drive gene expression more strongly than those with shorter deletions or no deletions.

One hypothesis for these results is that the deleted/inserted regions might contain repressive *cis*-elements that play a role in recruiting additional TFs and thereby affect the transcription. In *A. thaliana*, *GUS* reporter assays revealed that *FT* expression from a truncated promoter version showed a broader domain of expression in the leaf vein, and it was therefore conducted that the region between Block C and Block A contains sequences that repress *FT* expression (Liu et al., 2014a). Another hypothesis is that the deleted sequences, i.e., the inserted TE itself has a negative effect on gene transcription. TEs are primary targets of cytosine methylation in eukaryotes (Suzuki & Bird, 2008),

and DNA methylation plays a role in silencing genes by blocking transcription initiation, either by preventing protein binding or as a consequence of DNA methylation-induced chromatin remodelling (Curradi et al., 2002).

It is worth noting that the results in this thesis were obtained from the allogenic *N. benthamiana*, which involves the cross-species molecular environment. Different lengths of *BnFT* gene promoter sequences, as well as genes for BnCO and CO proteins were obtained from the original species and used in infiltration assays. However, all the other potential related regulatiory genes were from tobacco, which needs to be considered when analysing the results. For example, BnCO proteins activated both truncated promoter versions of *BnFT* genes more strongly than CO (Fig. 15B). The binding of CO to the *FT* promoter is mediated by the complex containing NF-YB/C and CO (Gnesutta et al., 2017; Tiwari et al., 2010); therefore, NF-YB/C in tobacco might possess a stronger binding with BnCOs compared to CO from *A. thaliana*. In addition, increased protein stability of BnCO proteins compared with CO might also be the reason for the result, either original BnCOs and CO possess different protein characteristics, or the degrading factors in tobacco have stronger interactions with CO than BnCOs, or de-degradation factors are more linked with BnCOs than CO. Furthermore, a previous study using co-bombardment assay revealed that *FT* promoters of different lengths were equally able to drive downstream gene expression, a result that differes from those in this study, which could be caused by the different inner molecular environments of *A. thaliana* and tobacco or by a difference of the association with chromatin between Agrobacterium transfected and bombarded DNA (Adrian et al., 2010).

4.6 Parallel flowering regulatory pathways between *A. thaliana* and *B. napus*

In this study, *B. napus* was shown to have asimilar flowering regulation network to *A. thaliana* on the basis of a high similarity of the distribution of homologous genes within various flowering pathways. A schematic representation of the flowering pathways in *A. thaliana* suggested the presence of *GI*, *CDF1*, and *CO* within the photoperiod pathway, and *FLC* as a component of the vernalization pathway (Kim, 2020). At the convergence point of these pathways were *FT*, *FD*, and *SOC1*, indicating their responsiveness to both photoperiod and vernalization cues. Remarkably, the flowering regulation in *B. napus* mirrors this framework, with the exception that *CO* homologues (*BnCO.A10*, *BnCO.C09*) display responsiveness to both photoperiod and vernalization (Fig. 17).

Specifically, in *A. thaliana*, *FLC* acts as a key repressor of flowering in the vernalization pathway by repressing the transcription of *FT* and *SOC1* (Helliwell et al., 2006; Michaels & Amasino, 1999; Sheldon et al., 1999a), and CO is a key regulatory component of photoperiodic flowering via

transcription activation of *FT* and *TSF* under LD conditions (Imaizumi, 2010; Samach et al., 2000; Song et al., 2012). The CO protein accumulates at dusk under LD conditions but is degraded in SD conditions (Valverde et al., 2004). In *B. napus*, *BnaFLC.A2* and *BnaFLC.C2* among the nine *FLC* homologues have been shown to have conserved and redundant functions in controlling rapeseed flowering by mediating the vernalization response in various near-isogenic lines (NILs). Low temperatures lead to a decrease in *BnFLC* expression and subsequent de-repression of the transcription of *BnFTs* and *BnSOC1s*, therefore allowing the initiation of flowering (Chen et al., 2018). Two *CO* homologues were identified, among which *BnaCO.C9* show high conservation among different ecotypes, and a single amino-acid variation in BnaCO.A10 was found to enhance the flowering promotion and was closely associated with winter-type rapeseed cultivar (Jin et al., 2021).

In this study, both *BnCO.A10* and *BnCO.C9* showed higher expression in LDs and post-vernalization conditions than in the other three conditions. Notably, leaf 6 and leaf 8 were sampled before and after vernalization, respectively. The higher expression of *BnCOs* at post-vernalization compared with pre-vernalization stages might be the result of the cold treatment, as well as changes due to ageing of the meristem between the 6^{th} and 8^{th} leaf. In *A. thaliana*, the transcription of *CO* is dependent on the circadian clock and photoperiod, and is mediated by genes including *FKF1*, *GI* and *CDF1* (Fowler et al., 1999; Imaizumi et al., 2003) although CO has no direct correlation with vernalization and ageing pathways, which are mediated mainly by *FLC* and *miRNAs*, respectively (Aukerman & Sakai, 2003; Sheldon et al., 2000; Wu et al., 2009). In *B. napus*, it was reported that both of the two *BnCOs* from Westar plants were rapidly induced by cold treatment, and were more highly expressed at 4^{o}C than at a normal growth temperature of 22^{o}C, after 5 days treatment at both temperatures (Jin et al., 2021). In addition, *BnCO.A0* showed a constant increase in expression from sowing to flowering, and *BnCO.C9* showed an increase in expression from sowing to the peak expression at 34 days from sowing (Jin et al., 2021). These results indicate that the expression of the two *BnCO* genes is not only affected by light, but is also affected by the cold/vernalization treatment and stage of plant development (ageing); which is consistent with the results obtained from this study. Two insertions were also shown to act as enhancers in the promoter region of *BnCO.C9*, which might possibly be the reason for the vernalization and/or ageing responsiveness, considering possible additional *cis*-elements for corresponding transcription factor binding and subsequent regulation of expression.

5 Conclusion and Perspectives

This study identified four *BnFT* homologues, two *BnNFT* genes, and one *BnCFT* gene by blast searches, phylogeny and synteny analysis in the ZS11 cultivar. Including *TSF* homologues, four groups of genes have four types of synteny relationships among *A. thaliana*, *S. parvula* and *Brassica* species, which provides insights into the possible gene evolution and diversification pathways in the Brassicaceae on the basis of complicated polyploidisation and recombination events. Cross-complementation experiments indirectly verified the weaker complementation abilities of BnFT proteins, which were compensated for the direct expression of their encoding genes at SAM, suggesting the conserved protein functions of FT homologues in molecular interactions with flowering factors; however, BnFT protein stability or their interaction with phloem factors, or both of these might differ between FT and BnFT homologues. Additionally, RNA-seq data revealed conservation of the flowering regulatory network between *A. thaliana* and *B. napus*, with major flowering genes (*FT*, *CO*, *GI*, *CDF1*, *SOC1*, *FLC* homologues) located in the same pathways in both species. However, *BnFTs* share similar photoperiod-responsive expression patterns with each other, but different from the expression pattern of *FT*. Consideration of all these results together, although *B. napus* has conserved gene functions and flowering regulation network compared with *A. thaliana*, *B. napus* also possesses differences in several classes of transcription factors and gene interactions, which require further research.

6. References

Abe, M., Kobayashi, Y., Yamamoto, S., Daimon, Y., Yamaguchi, A., Ikeda, Y. & Araki, T. (2005). FD, a bZIP protein mediating signals from the floral pathway integrator FT at the shoot apex. *Science, 309*(5737), 1052-1056. http://doi.org/10.1126/science.1115983

Adrian, J., Farrona, S., Reimer, J. J., Albani, M. C., Coupland, G. & Turck, F. (2010). Cis-regulatory elements and chromatin state coordinately control temporal and spatial expression of *FLOWERING LOCUS T* in *A. thaliana*. *The Plant Cell, 22*(5), 1425-1440. http://doi.org/10.1105/tpc.110.074682

Allender, C. J. & King, G. J. (2010). Origins of the amphiploid species *Brassica napus* L. investigated by chloroplast and nuclear molecular markers. *BMC Plant Biology, 10*. http://doi.org/10.1186/1471-2229-10-54

Alvarez-Venegas, R., Pien, S., Sadder, M., Witmer, X., Grossniklaus, U. & Avramova, Z. (2003). ATX-1, an *A. thaliana* homolog of TRITHORAX, activates flower homeotic genes. *Current Biology, 13*(8), 627-637. http://doi.org/10.1016/S0960-9822(03)00243-4

Amasino, R. (2010). Seasonal and developmental timing of flowering. *The Plant Journal, 61*(6), 1001-1013. http://doi.org/10.1111/j.1365-313X.2010.04148.x

Amasino, R. M. (1996). Control of flowering time in plants. *Current Opinion in Genetics & Development, 6*(4), 480-487. http://doi.org/10.1016/S0959-437x(96)80071-2

Andres, F. & Coupland, G. (2012). The genetic basis of flowering responses to seasonal cues. *Nature Reviews Genetics, 13*(9), 627-639. http://doi.org/10.1038/nrg3291

Aukerman, M. J. & Sakai, H. (2003). Regulation of flowering time and floral organ identity by a microRNA and its APETALA2-like target genes. *The Plant Cell, 15*(11), 2730-2741. http://doi.org/10.1105/tpc.016238

Baurle, I. & Dean, C. (2008). Differential interactions of the autonomous pathway RRM proteins and chromatin regulators in the silencing of *A. thaliana* targets. *PLoS ONE, 3*(7), e2733. http://doi.org/10.1371/journal.pone.0002733

Blanc, G., Hokamp, K. & Wolfe, K. H. (2003). A recent polyploidy superimposed on older large-scale duplications in the *A. thaliana* genome. *Genome Research, 13*(2), 137-144. http://doi.org/10.1101/gr.751803

Böhlenius, H., Huang, T., Charbonnel-Campaa, L., Brunner, A. M., Jansson, S., Strauss, S. H. & Nilsson, O. (2006). CO/FT regulatory module controls timing of flowering and seasonal growth cessation in trees. *Science, 312*(5776), 1040-1043. http://doi.org/10.1126/science.1126038

Bowers, J. E., Chapman, B. A., Rong, J. K. & Paterson, A. H. (2003). Unravelling angiosperm genome evolution by phylogenetic analysis of chromosomal duplication events. *Nature, 422*(6930), 433-438. http://doi.org/10.1038/nature01521

Bu, Z. Y., Yu, Y., Li, Z. P., Liu, Y. C., Jiang, W., Huang, Y. & Dong, A. W. (2014). Regulation of *A. thaliana* flowering by the histone mark readers MRG1/2 via interaction with CONSTANS to modulate FT expression. *PLoS Genetics, 10*(9):e1004617. http://doi.org/10.1371/journal.pgen.1004617

References

Cai, Y., Chen, L., Liu, X., Guo, C., Sun, S., Wu, C. & Hou, W. (2018). CRISPR/Cas9-mediated targeted mutagenesis of *GmFT2a* delays flowering time in soya bean. *Plant Biotechnology Journal, 16*(1), 176-185. http://doi.org/10.1111/pbi.12758

Cao, S., Kumimoto, R. W., Gnesutta, N., Calogero, A. M., Mantovani, R. & Holt, B. F. (2014). A distal CCAAT/NUCLEAR FACTOR Y complex promotes chromatin looping at the FLOWERING LOCUS T promoter and regulates the timing of flowering in *A. thaliana*. *The Plant Cell, 26*(3), 1009-1017. http://doi.org/10.1105/tpc.113.120352

Cao, S. H., Luo, X. M., Xu, D. A., Tian, X. L., Song, J., Xia, X. C. & He, Z. H. (2021). Genetic architecture underlying light and temperature mediated flowering in *A. thaliana*, rice, and temperate cereals. *New Phytologist, 230*(5), 1731-1745. http://doi.org/10.1111/nph.17276

Capovilla, G., Schmid, M. & Pose, D. (2015). Control of flowering by ambient temperature. *Journal of Experimental Botany, 66*(1), 59-69. http://doi.org/10.1093/jxb/eru416

Castillejo, C. & Pelaz, S. (2008). The balance between CONSTANS and TEMPRANILLO activities determines FT expression to trigger flowering. *Current Biology, 18*(17), 1338-1343. http://doi.org/10.1016/j.cub.2008.07.075

Gómez-Campo C. & Prakash, S. (1999). Origin and domestication. *Development in plant genetics and breeding, 4, 33-58. https://doi.org/10.1016/S0168-7972(99)80003-6.*

Chalhoub, B., Denoeud, F., Liu, S. Y., Parkin, I. A. P., Tang, H. B., Wang, X. Y. & Wincker, P. (2014). Early allopolyploid evolution in the post-Neolithic *Brassica napus* oilseed genome. *Science, 345*(6199), 950-953. http://doi.org/10.1126/science.1253435

Chardon, F. & Damerval, C. (2005). Phylogenomic analysis of the PEBP gene family in cereals. *J Mol Evol, 61*(5), 579-590. http://doi.org/10.1007/s00239-004-0179-4

Chautard, H., Jacquet, M., Schoentgen, F., Bureaud, N. & Benedetti, H. (2004). Tfs1p, a member of the PEBP family, inhibits the Ira2p but not the Ira1p Ras GTPase-activating protein in *Saccharomyces cerevisiae*. *Eukaryot Cell, 3*(2), 459-470. http://doi.org/10.1128/EC.3.2.459-470.2004

Chen, L., Dong, F. M., Cai, J., Xin, Q., Fang, C. C., Liu, L. & Hong, D. F. (2018). A 2.833-kb insertion in *BnFLC.A2* and its homeologous exchange with *BnFLC.C2* during breeding selection generated early-flowering rapeseed. *Molecular Plant, 11*(1), 222-225. http://doi.org/10.1016/j.molp.2017.09.020

Chen, L., Lei, W. X., He, W. F., Wang, Y. F., Tian., J., Gong., J. & Fan., Y. S. a. Z. (2022). Mapping of two major QTLs controlling flowering time in *Brassica napus* using a high-density genetic map. *Plants, 11*(19), 2635. http://doi.org/10.3390 /plants11192635

Chen, M., MacGregor, D. R., Dave, A., Florance, H., Moore, K., Paszkiewicz, K. & Penfield, S. (2014). Maternal temperature history activates *Flowering Locus T* in fruits to control progeny dormancy according to time of year. *Proceedings of the National Academy of Sciences of the United States of America, 111*(52), 18787-18792. http://doi.org/10.1073/pnas.1412274111

Chen, R. Q., Zhang, S. Z., Sun, S. L., Chang, J. H. & Zuo, J. R. (2005). Characterization of a new mutant allele of the *A. thaliana Flowering Locus D* (*FLD*) gene that controls the flowering time by repressing *FLC*. *Chinese Science Bulletin, 50*(23), 2701-2706. http://doi.org/10.1360/982005-1104

Chen, Y. L., Zhang, L. P., Zhang, H. Y., Chen, L. G. & Yu, D. Q. (2021). ERF1 delays flowering through direct inhibition of *FLOWERING LOCUS T* expression in *A. thaliana*. *Journal of Integrative Plant Biology, 63*(10), 1712-1723. http://doi.org/10.1111/jipb.13144

Chen, Y., Song, S. Y., Gan, Y. B., Jiang, L. X., Yu, H. & Shen, L. S. (2020). SHAGGY-like kinase 12 regulates flowering through mediating CONSTANS stability in *Arabidopsis*. *Science Advances, 6*(24), eaaw0413. http://doi.org/10.1126/sciadv.aaw0413

Cheng, F., Mandakova, T., Wu, J., Xie, Q., Lysak, M. A. & Wang, X. W. (2013). Deciphering the diploid ancestral genome of the mesohexaploid *Brassica rapa*. *The Plant Cell, 25*(5), 1541-1554. http://doi.org/10.1105/tpc.113.110486

Cheng, F., Wu, J., Fang, L. & Wang, X. W. (2012). Syntenic gene analysis between *Brassica rapa* and other Brassicaceae species. *Frontiers in Plant Science, 3,* 198. http://doi.org/10.3389/fpls.2012.00198

Cheng, F., Wu, J. & Wang, X. W. (2014). Genome triplication drove the diversification of Brassica plants. *Horticulture Research, 1*,14024. http://doi.org/10.1038/hortres.2014.24

Cheng, J. Z., Zhou, Y. P., Lv, T. X., Xie, C. P. & Tian, C. E. (2017). Research progress on the autonomous flowering time pathway in *A. thaliana*. *Physiology and Molecular Biology of Plants, 23*(3), 477-485. http://doi.org/10.1007/s12298-017-0458-3

Clough, S. J. & Bent, A. F. (1998). Floral dip: a simplified method for Agrobacterium-mediated transformation of *A. thaliana thaliana*. *The Plant Journal, 16*(6), 735-743. http://doi.org/10.1046/j.1365-313x.1998.00343.x

Collani, S., Neumann, M., Yant, L. & Schmid, M. (2019). FT modulates genome-wide DNA-binding of the bZIP transcription factor FD. *Plant Physiology, 180*(1), 367-380. http://doi.org/10.1104/pp.18.01505

Conant, G. C. & Wolfe, K. H. (2008). Turning a hobby into a job: How duplicated genes find new functions. *Nature Reviews Genetics, 9*(12), 938-950. http://doi.org/10.1038/nrg2482

Corbesier, L., Vincent, C., Jang, S. H., Fornara, F., Fan, Q. Z., Searle, I. & Coupland, G. (2007). FT protein movement contributes to long-distance signaling in floral induction of. *Science, 316*(5827), 1030-1033. http://doi.org/10.1126/science.1141752

Curradi, M., Izzo, A., Badaracco, G. & Landsberger, N. (2002). Molecular mechanisms of gene silencing mediated by DNA methylation. *Molecular and Cellular Biology,* 22(9), 3157-3173. http://doi.org/10.1128/Mcb.22.9.3157-3173.2002

D'Aloia, M., Bonhomme, D., Bouché, F., Tamseddak, K., Ormenese, S., Torti, S. & Périlleux, C. (2011). Cytokinin promotes flowering of *A. thaliana* via transcriptional activation of the paralogue. *The Plant Journal, 65*(6), 972-979. http://doi.org/10.1111/j.1365-313X.2011.04482.x

Davis, S. J. (2009). Integrating hormones into the floral-transition pathway of. *The Plant Cell and Environment, 32*(9), 1201-1210. http://doi.org/10.1111/j.1365-3040.2009.01968.x

Dassanayake, M., Oh, D. H., Haas, J. S., Hernandez, A., Hong, H., Ali, S., Yun, D. J., Bressan, R. A., Zhu, J. K., Bohnert, H. J. & Cheeseman, J. M. (2011). The genome of the extremophile crucifer *Thellungiella parvula*. *Nature Genetics*, 43(9), 913–918. https://doi.org/10.1038/ng.889.

Dobin, A., Davis, C. A., Schlesinger, F., Drenkow, J., Zaleski, C., Jha, S., . . . Gingeras, T. R. (2013). STAR: ultrafast universal RNA-seq aligner. *Bioinformatics, 29*(1), 15-21. https://doi:10.1093/bioinformatics/bts635

Fornara, F., Panigrahi, K. C. S., Gissot, L., Sauerbrunn, N., Rühl, M., Jarillo, J. A. & Coupland, G. (2009). Arabidopsis DOF Transcription Factors Act Redundantly to Reduce CONSTANS

Expression and Are Essential for a Photoperiodic Flowering Response. Developmental Cell, 17(1), 75-86. doi:10.1016/j.devcel.2009.06.015

Fowler, S., Lee, K., Onouchi, H., Samach, A., Richardson, K., Coupland, G. & Putterill, J. (1999). GIGANTEA: a circadian clock-controlled gene that regulates photoperiodic flowering in *Arabidopsis* and encodes a protein with several possible membrane-spanning domains. *EMBO Journal, 18*(17), 4679-4688. https://doi.org/10.1093/emboj/18.17.4679

Franzke, A., Lysak, M. A., Al-Shehbaz, I. A., Koch, M. A. & Mummenhoff, K. (2011). Cabbage family affairs: the evolutionary history of Brassicaceae. *Trends in Plant Science, 16*(2), 108-116. https://doi.org/10.1016/j.tplants.2010.11.005

Fu, W., Huang, S., Gao, Y., Zhang, M., Qu, G., Wang, N., Liu, Z. & Feng, H. (2020). Role of *BrSDG8* on bolting in Chinese cabbage (*Brassica rapa*). *Theoretical and Applied Genetics*. 133(10), 2937–2948. https://doi.org/10.1007/s00122-020-03647-4

Garner, W. W. & Allard, H. A. (1919). Effect of the relative length of day and night and other factors of the environment on growth and reproduction in plants. *Journal of Agricultural Research, 18*, 0553-0606.

Gómez-Campo, C; Prakash, S. (1999). Origin and domestication. *Development in Plant Genetics and Breeding*, 4, 33-58. https://doi.org/10.1016/S0168-7972(99)80003-6.

Goretti, D., M. S., Silvestre, M., Collani, S., Langenecker, T., Méndez, C., Madueño, F., Schmid, M. (2020). TERMINAL FLOWER1 functions as a mobile transcriptional cofactor in the shoot apical meristem. *Plant Physiology, 182*(4), 2081–2095.

Gnesutta, N., Kumimoto, R. W., Swain, S., Chiara, M., Siriwardana, C., Horner, D. S. & Mantovani, R. (2017). CONSTANS imparts DNA sequence specificity to the histone fold NF-YB/NF-YC dimer. *The Plant Cell, 29*(6), 1516-1532. http://doi.org/10.1105/tpc.16.00864

Goodrich, J., Puangsomlee, P., Martin, M., Long, D., Meyerowitz, E. M. & Coupland, G. (1997). A polycomb-group gene regulates homeotic gene expression in *A. thaliana*. *Nature, 386*(6620), 44-51. http://doi.org/10.1038/386044a0

Goralogia, G. S., Liu, T. K., Zhao, L., Panipinto, P. M., Groover, E. D., Bains, Y. S. & Imaizumi, T. (2017). CYCLING DOF FACTOR 1 represses transcription through the TOPLESS co-repressor to control photoperiodic flowering in *A. thaliana*. *The Plant Journal, 92*(2), 244-262. http://doi.org/10.1111/tpj.13649

Gu, X. F., Le, C., Wang, Y. Z., Li, Z. C., Jiang, D. H., Wang, Y. Q. & He, Y. H. (2013). FLC clade members form flowering-repressor complexes coordinating responses to endogenous and environmental cues. *Nature Communications, 4*, 1947. http://doi.org/ 10.1038/ncomms2947

Guo, Y., Hans, H., Christian, J. & Molina, C. (2014). Mutations in single FT- and TFL1-paralogs of rapeseed (*Brassica napus L.*) and their impact on flowering time and yield components. *Frontiers in Plant Science, 5*, 282. http://doi.org/ 10.3389/fpls.2014.00282

Hartmann, U., Höhmann, S., Nettesheim, K., Wisman, E., Saedler, H. & Huijser, P. (2000). Molecular cloning of SVP: a negative regulator of the floral transition in *A. thaliana*. *The Plant Journal, 21*(4), 351-360. http://doi.org/10.1046/j.1365-313x.2000.00682.x

Haudry, A., Platts, A. E., Vello, E., Hoen, D. R., Leclercq, M., Williamson, R. J., Forczek, E., Joly-Lopez, Z., Steffen, J. G., Hazzouri, K. M., Dewar, K., Stinchcombe, J. R., Schoen, D. J., Wang, X., Schmutz, J., Town, C. D., Edger, P. P., Pires, J. C., Schumaker, K. S., Jarvis, D. E., … Blanchette, M. (2013). An atlas of over 90,000 conserved noncoding sequences provides insight into crucifer regulatory regions. *Nature Genetics*, 45(8), 891–898. https://doi.org/10.1038/ng.2684

Hawkins, J. S., Kim, H., Nason, J. D., Wing, R. A. & Wendel, J. F. (2006). Differential lineage-specific amplification of transposable elements is responsible for genome size variation in Gossypium. *Genome Research,* 16(10), 1252-1261. https://doi.org/10.1101/gr.5282906

Hedman, H., Kallman, T. & Lagercrantz, U. (2009). Early evolution of the MFT-like gene family in plants. *Plant Molecular Biology, 70*(4), 359-369. http://doi.org/10.1007/s11103-009-9478-x

Helliwell, C. A., Wood, C. C., Robertson, M., Peacock, W. J. & Dennis, E. S. (2006). The *A. thaliana* FLC protein interacts directly in vivo with SOC1 and FT chromatin and is part of a high-molecular-weight protein complex. *The Plant Journal, 46*(2), 183-192. http://doi.org/10.1111/j.1365-313X.2006.02686.x

Hoecker, U., Tepperman, J. M. & Quail, P. H. (1999). SPA1, a WD-repeat protein specific to phytochrome A signal transduction. *Science, 284*(5413), 496-499. http://doi.org/10.1126/science.284.5413.496

Hoecker, U., Xu, Y. & Quail, P. H. (1998). SPA1: A new genetic locus involved in phytochrome A-specific signal transduction. *The Plant Cell, 10*(1), 19-33. http://doi.org/10.1105/tpc.10.1.19

Hsu, C. Y., Adams, J. P., Kim, H. J., No, K., Ma, C. P., Strauss, S. H. & Yuceer, C. (2011). *FLOWERING LOCUS T* duplication coordinates reproductive and vegetative growth in perennial poplar. *Proceedings of the National Academy of Sciences of the United States of America, 108*(26), 10756-10761. http://doi.org/10.1073/pnas.1104713108

Hsu, C. Y., Liu, Y. X., Luthe, D. S. & Yuceer, C. (2006). Poplar FT2 shortens the juvenile phase and promotes seasonal flowering. *The Plant Cell, 18*(8), 1846-1861. http://doi.org/10.1105/tpc.106.041038

Huang, C. H., Sun, R., Hu, Y., Zeng, L., Zhang, N., Cai, L., Zhang, Q., Koch, M. A., Al-Shehbaz, I., Edger, P. P., Pires, J. C., Tan, D. Y., Zhong, Y. & Ma, H. (2016). Resolution of Brassicaceae phylogeny using nuclear genes uncovers nested radiations and supports convergent morphological evolution. *Molecular Biology and Evolution*, 33(2), 394–412. https://doi.org/10.1093/molbev/msv226

Huang, N. C., Jane, W. N., Chen, J., & Yu, T. S. (2012). Arabidopsis thaliana CENTRORADIALIS homologue (ATC) acts systemically to inhibit floral initiation in Arabidopsis. *Plant Journal, 72*(2), 175-184. doi:10.1111/j.1365-313X.2012.05076.x

Imaizumi, T. (2010). *A. thaliana* circadian clock and photoperiodism: time to think about location. *Current Opinion in Plant Biology, 13*(1), 83-89. http://doi.org/10.1016/j.pbi.2009.09.007

Imaizumi, T., Tran, H. G., Swartz, T. E., Briggs, W. R. & Kay, S. A. (2003). FKF1 is essential for photoperiodic-specific light signalling in *Arabidopsis*. *Nature, 426*(6964), 302-306. http://doi.org/10.1038/nature02090

Imaizumi, T. & Kay, S. A. (2006). Photoperiodic control of flowering: not only by coincidence. *Trends in Plant Science, 11*(11), 550-558. http://doi.org/10.1016/j.tplants.2006.09.004

Imaizumi, T., Schultz, T. F., Harmon, F. G., Ho, L. A. & Kay, S. A. (2005). FKF1 F-box protein mediates cyclic degradation of a repressor of CONSTANS in *A. thaliana*. *Science, 309*(5732), 293-297. http://doi.org/10.1126/science.1110586

Inaba, R. & Nishio, T. (2002). Phylogenetic analysis of Brassiceae based on the nucleotide sequences of the S-locus related gene, SLR1. *Theoretical and Applied Genetics, 105*(8), 1159-1165. http://doi.org/10.1007/s00122-002-0968-3

References

Jacobsen, S. E. & Olszewski, N. E. (1993). Mutations at the spindly locus of *A. thaliana* alter gibberellin signal-transduction. *The Plant Cell, 5*(8), 887-896. http://doi.org/10.1105/tpc.5.8.887

Jaeger, K. E. & Wigge, P. A. (2007). FT protein acts as a long-range signal in *A. thaliana*. *Current Biology, 17*(12), 1050-1054. http://doi.org/10.1016/j.cub.2007.05.008

Jahangir, M., Kim, H. K., Choi, Y. H. & Verpoorte, R. (2009). Health-affecting compounds in Brassicaceae. *Comprehensive Reviews in Food Science and Food Safety, 8*(2), 31-43. http://doi.org/10.1111/j.1541-4337.2008.00065.x

Jiang, D. H., Wang, Y. Q., Wang, Y. Z. & He, Y. H. (2008). Repression of FLOWERING LOCUS C and FLOWERING LOCUS T by the *A. thaliana* polycomb repressive complex 2 components. *PLoS ONE, 3*(10), e3404. http://doi.org/10.1371/journal.pone.0003404

Jang, S., Marchal, V., Panigrahi, K. C. S., Wenkel, S., Soppe, W., Deng, X. W. & Coupland, G. (2008). *A. thaliana* COP1 shapes the temporal pattern of CO accumulation conferring a photoperiodic flowering response. *EMBO Journal, 27*(8), 1277-1288. http://doi.org/10.1038/emboj.2008.68

Jang, S., Torti, S. & Coupland, G. (2009). Genetic and spatial interactions between FT, TSF and SVP during the early stages of floral induction in *A. thaliana*. *The Plant Journal, 60*(4), 614-625. http://doi.org/10.1111/j.1365-313X.2009.03986.x

Jia, H. Y., Suzuki, M. & McCarty, D. R. (2014). Regulation of the seed to seedling developmental phase transition by the LAFL and VAL transcription factor networks. *Wiley Interdisciplinary Reviews-Developmental Biology, 3*(1), 135-145. http://doi.org/10.1002/wdev.126

Jin, Q. D., Gao, G. D., Guo, C. C., Yang, T. H., Li, G., Song, J. R. & Zhou, G. S. (2022). Transposon insertions within alleles of *BnaFT.A2* are associated with seasonal crop type in rapeseed. *Theoretical and Applied Genetics, 135*(10), 3469-3483. http://doi.org/10.1007/s00122-022-04193-x

Jin, Q. D., Yin, S., Li, G., Guo, T., Wan, M., Li, H. T. & Zhou, G. S. (2021). Functional homoeologous alleles of *CONSTANS* contribute to seasonal crop type in rapeseed. *Theoretical and Applied Genetics, 134*(10), 3287-3303. http://doi.org/10.1007/s00122-021-03896-x

Jin, S., Jung, H. S., Chung, K. S., Lee, J. H. & Ahn, J. H. (2015). FLOWERING LOCUS T has higher protein mobility than TWIN SISTER OF FT. *Journal of Experimental Botany, 66*(20), 6109-6117. http://doi.org/10.1093/jxb/erv326

Jing, Y. J., Guo, Q. & Lin, R. C. (2019a). The B3-domain transcription factor VAL1 regulates the floral transition by repressing *FLOWERING LOCUS T*. *Plant Physiology, 181*(1), 236-248. http://doi.org/10.1104/pp.19.00642

Jing, Y. J., Guo, Q. & Lin, R. C. (2019b). The chromatin-remodeling factor PICKLE antagonizes polycomb repression of *FT* to promote flowering. *Plant Physiology, 181*(2), 656-668. http://doi.org/10.1104/pp.19.00596

Jing, Y. J., Guo, Q., Zha, P. & Lin, R. C. (2019). The chromatin-remodelling factor PICKLE interacts with CONSTANS to promote flowering in *A. thaliana*. *The Plant Cell and Environment, 42*(8), 2495-2507. http://doi.org/10.1111/pce.13557

Kardailsky, I., Shukla, V. K., Ahn, J. H., Dagenais, N., Christensen, S. K., Nguyen, J. T. & Weigel, D. (1999). Activation tagging of the floral inducer FT. *Science, 286*(5446), 1962-1965. http://doi.org/10.1126/science.286.5446.1962

Karlgren, A., Gyllenstrand, N., Kallman, T., Sundstrom, J. F., Moore, D., Lascoux, M. & Lagercrantz, U. (2011). Evolution of the PEBP gene family in plants: functional diversification in seed plant evolution. *Plant Physiol, 156*(4), 1967-1977. http://doi.org/10.1104/pp.111.176206

Kim, D. H. (2020). Current understanding of flowering pathways in plants: focusing on the vernalization pathway in *A. thaliana* and several vegetable crop plants. *Horticulture Environment and Biotechnology, 61*(2), 209-227. http://doi.org/10.1007/s13580-019-00218-5

Kim, D. H. & Sung, S. (2013). Coordination of the vernalization response through a *VIN3* and *FLC* gene family regulatory network in *A. thaliana*. *The Plant Cell, 25*(2), 454-469. http://doi.org/10.1105/tpc.112.104760

Kim, S. J., Hong, S. M., Yoo, S. J., Moon, S., Jung, H. S. & Ahn, J. H. (2016). Post-Translational Regulation of FLOWERING LOCUS T Protein in Arabidopsis. *Molecular Plant,* 9(2), 308-311. doi:10.1016/j.molp.2015.11.001

Kim, W., Park, T. I., Yoo, S. J., Jun, A. R. & Ahn, J. H. (2013). Generation and analysis of a complete mutant set for the *A. thaliana* FT/TFL1 family shows specific effects on thermo-sensitive flowering regulation. *Journal of Experimental Botany, 64*(6), 1715-1729. http://doi.org/10.1093/jxb/ert036

Kinoshita, T., Ono, N., Hayashi, Y., Morimoto, S., Nakamura, S., Soda, M. & Shimazaki, K. (2011). FLOWERING LOCUS T regulates stomatal opening. *Current Biology, 21*(14), 1232-1238. http://doi.org/10.1016/j.cub.2011.06.025

Kobayashi, Y., Kaya, H., Goto, K., Iwabuchi, M. & Araki, T. (1999). A pair of related genes with antagonistic roles in mediating flowering signals. *Science, 286*(5446), 1960-1962. http://doi.org/10.1126/science.286.5446.1960

Kojima, S., Takahashi, Y., Kobayashi, Y., Monna, L., Sasaki, T., Araki, T. & Yano, M. (2002). Hd3a, a rice ortholog of the *A. thaliana* FT gene, promotes transition to flowering downstream of Hd1 under short-day conditions. *Plant and Cell Physiology, 43*(10), 1096-1105. http://doi.org/10.1093/pcp/pcf156

Komiya, R., Ikegami, A., Tamaki, S., Yokoi, S. & Shimamoto, K. (2008). Hd3a and RFT1 are essential for flowering in rice. *Development, 135*(4), 767-774. http://doi.org/10.1242/dev.008631

Komiya, R., Yokoi, S. & Shimamoto, K. (2009). A gene network for long-day flowering activates RFT1 encoding a mobile flowering signal in rice. *Development, 136*(20), 3443-3450. http://doi.org/10.1242/dev.040170

Kong, F. J., Liu, B. H., Xia, Z. J., Sato, S., Kim, B. M., Watanabe, S. & Abe, J. (2010). Two coordinately regulated homologs of FLOWERING LOCUS T are involved in the control of photoperiodic flowering in soybean. *Plant Physiology, 154*(3), 1220-1231. http://doi.org/10.1104/pp.110.160796

Koornneef, M., Hanhart, C. J. & Vanderveen, J. H. (1991). A genetic and physiological analysis of late flowering mutants in *A. thaliana thaliana*. *Molecular & General Genetics, 229*(1), 57-66. http://doi.org/10.1007/Bf00264213

Chailakhyan, M. Kh. & Krikorian A. D. (1975). Forty years of research on the hormonal basis of plant development: Some personal reflections. *The Botanical Review, 41*, 1-29 http://doi.org/10.1007

Lagercrantz, U. (1998). Comparative mapping between *A. thaliana thaliana* and *Brassica nigra* indicates that Brassica genomes have evolved through extensive genome replication

accompanied by chromosome fusions and frequent rearrangements. *Genetics, 150*(3), 1217-1228. https://doi.org/10.1093/genetics/150.3.1217

Lagercrantz, U. & Lydiate, D. J. (1996). Comparative genome mapping in Brassica. *Genetics, 144*(4), 1903-1910. https://doi.org/10.1093/genetics/144.4.1903

Laubinger, S., Marchal, V., Gentilhomme, J., Wenkel, S., Adrian, J., Jang, S. & Hoecker, U. (2006). *A. thaliana* SPA proteins regulate photoperiodic flowering and interact with the floral inducer CONSTANS to regulate its stability. *Development, 133*(16), 3213-3222. http://doi.org/10.1242/dev.02481

Lee, B. D., Kim, M. R., Kang, M. Y., Cha, J. Y., Han, S. H., Nawkar, G. M. & Paek, N. C. (2017). The F-box protein FKF1 inhibits dimerization of COP1 in the control of photoperiodic flowering. *Nature Communications, 8*, 2259. http://doi.org/10.1038/s41467-017-02476-2

Lee, J. & Amasino, R. M. (2013). Two FLX family members are non-redundantly required to establish the vernalization requirement in *A. thaliana*. *Nature Communications, 4*, 2186. http://doi.org/10.1038/ncomms3186

Lee, J., Oh, M., Park, H. & Lee, I. (2008). SOC1 translocated to the nucleus by interaction with AGL24 directly regulates. *The Plant Journal, 55*(5), 832-843. http://doi.org/10.1111/j.1365-313X.2008.03552.x

Lee, J. H., Ryu, H. S., Chung, K. S., Posé, D., Kim, S., Schmid, M. & Ahn, J. H. (2013). Regulation of temperature-responsive flowering by MADS-box transcription factor repressors. *Science, 342*(6158), 628-632. http://doi.org/10.1126/science.1241097

Lee, J. H., Yoo, S. J., Park, S. H., Hwang, I., Lee, J. S. & Ahn, J. H. (2007). Role of SVP in the control of flowering time by ambient temperature in *A. thaliana*. *Genes & Development, 21*(4), 397-402. http://doi.org/10.1101/gad.1518407

Li, D., Liu, C., Shen, L., Wu, Y., Chen, H., Robertson, M. & Yu, H. (2008). A repressor complex governs the integration of flowering signals in. *Developmental Cell, 15*(1), 110-120. http://doi.org/10.1016/j.devcel.2008.05.002

Li, Z. C., Fu, X., Wang, Y. Z., Liu, R. Y. & He, Y. H. (2018). Polycomb-mediated gene silencing by the BAH-EMF1 complex in plants. *Nature Genetics, 50*(9), 1254-1261 . http://doi.org/10.1038/s41588-018-0190-0

Liao, Y., Smyth, G. K., & Shi, W. (2014). featureCounts: an efficient general purpose program for assigning sequence reads to genomic features. *Bioinformatics, 30*(7), 923-930. http://doi:10.1093/bioinformatics/btt656

Lifschitz, E., Eviatar, T., Rozman, A., Shalit, A., Goldshmidt, A., Amsellem, Z. & Eshed, Y. (2006). The tomato FT ortholog triggers systemic signals that regulate growth and flowering and substitute for diverse environmental stimuli. *Proceedings of the National Academy of Sciences of the United States of America, 103*(16), 6398-6403. http://doi.org/10.1073/pnas.0601620103

Lim, M. H., Kim, J., Kim, Y. S., Chung, K. S., Seo, Y. H., Lee, I. & Park, C. M. (2004). A new *A. thaliana* gene, *FLK*, encodes an RNA binding protein with K homology motifs and regulates flowering time via FLOWERING LOCUS C. *The Plant Cell, 16*(3), 731-740. http://doi.org/10.1105/tpc.019331

Liu, C., Chen, H., Er, H. L., Soo, H. M., Kumar, P. P., Han, J. H. & Yu, H. (2008a). Direct interaction of AGL24 and SOC1 integrates flowering signals in *A. thaliana*. *Development, 135*(8), 1481-1491. http://doi.org/10.1242/dev.020255

Liu, F. Q., Quesada, V., Crevillen, P., Baurle, I., Swiezewski, S. & Dean, C. (2007). The *A. thaliana* RNA-Binding protein FCA requires a lysine-specific demethylase 1 homolog to downregulate FLC. *Molecular Cell, 28*(3), 398-407. http://doi.org/10.1016/j.molcel.2007.10.018

Liu, L., Li, C. Y., Teo, Z. W. N., Zhang, B. & Yu, H. (2019). The MCTP-SNARE nomplex regulates florigen transport in *A. thaliana*. *The Plant Cell, 31*(10), 2475-2490. http://doi.org/10.1105/tpc.18.00960

Liu, L., Liu, C., Hou, X. L., Xi, W. Y., Shen, L. S., Tao, Z. & Yu, H. (2012). FTIP1 is an essential regulator required for florigen transport. *PLoS Biology, 10*(4), e1001313. http://doi.org/10.1371/journal.pbio.1001313

Liu, L., Zhang, Y. & Yu, H. (2020). Florigen trafficking integrates photoperiod and temperature signals in *A. thaliana*. *Journal of Integrative Plant Biology, 62*(9), 1385-1398. http://doi.org/10.1111/jipb.13000

Liu, L. J., Zhang, Y. C., Li, Q. H., Sang, Y., Mao, J., Lian, H. L. & Yang, H. Q. (2008b). COP1-mediated ubiquitination of CONSTANS is implicated in cryptochrome regulation of flowering in *A. thaliana*. *The Plant Cell, 20*(2), 292-306. http://doi.org/10.1105/tpc.107.057281

Liu, L. Y., Adrian, J., Pankin, A., Hu, J. Y., Dong, X., von Korff, M. & Turck, F. (2014a). Induced and natural variation of promoter length modulates the photoperiodic response of FLOWERING LOCUS T. *Nature Communications, 5*, 4558. http://doi.org/10.1038/ncomms5558

Liu, L. Y., Farrona, S., Klemme, S. & Turck, F. K. (2014b). Post-fertilization expression of FLOWERING LOCUS T suppresses reproductive reversion. *Frontiers in Plant Science, 5*. http://doi.org/10.3389/fpls.2014.00164

Liu, W., Jiang, B. J., Ma, L. M., Zhang, S. W., Zhai, H., Xu, X. & Han, T. F. (2018a). Functional diversification of Flowering Locus T homologs in soybean: GmFT1a and GmFT2a/5a have opposite roles in controlling flowering and maturation. *New Phytologist, 217*(3), 1335-1345. http://doi.org/10.1111/nph.14884

Liu, X., Yang, Y. H., Hu, Y. L., Zhou, L. M., Li, Y. G. & Hou, X. L. (2018b). Temporal-specific interaction of NF-YC and CURLY LEAF during the floral transition regulates flowering. *Plant Physiology, 177*(1), 105-114. http://doi.org/10.1104/pp.18.00296

Liu, Y. W., Li, X., Li, K. W., Liu, H. T. & Lin, C. T. (2013). Multiple bHLH proteins form heterodimers to mediate CRY2-dependent regulation of flowering-time in *A. thaliana*. *PLoS Genetics, 9*(10), e1003861. http://doi.org/10.1371/journal.pgen.1003861

Lopez-Vernaza, M., Yang, S. X., Müller, R., Thorpe, F., de Leau, E. & Goodrich, J. (2012). Antagonistic roles of SEPALLATA3, FT and FLC genes as targets of the polycomb group gene CURLY LEAF. *PLoS ONE, 7*(2), e30715. http://doi.org/10.1371/journal.pone.0030715

Love, M. I., Huber, W., & Anders, S. (2014). Moderated estimation of fold change and dispersion for RNA-seq data with DESeq2. *Genome Biology, 15*(12). https://doi.org/10.1186/s13059-014-0550-8

Lu, K., Wei, L. J., Li, X. L., Wang, Y. T., Wu, J., Liu, M. & Li, J. N. (2019). Whole-genome resequencing reveals *Brassica napus* origin and genetic loci involved in its improvement. *Nature Communications, 10*, 1154. http://doi.org/10.1038/s41467-019-09134-9

Lukens, L., Zou, F., Lydiate, D., Parkin, I. & Osborn, T. (2003). Comparison of a *Brassica oleracea* genetic map with the genome of *A. thaliana thaliana*. *Genetics, 164*(1), 359-372. https://doi.org/10.1093/genetics/164.1.359

References

Luo, X., Gao, Z., Wang, Y. Z., Chen, Z. J., Zhang, W. J., Huang, J. R. & He, Y. H. (2018). The NUCLEAR FACTOR-CONSTANS complex antagonizes polycomb repression to de-repress *FLOWERING LOCUS T* expression in response to inductive long days in *A. thaliana*. *The Plant Journal, 95*(1), 17-29. http://doi.org/10.1111/tpj.13926

Lv, X. C., Zeng, X. L., Hu, H. M., Chen, L. X., Zhang, F., Liu, R. & Du, J. M. (2021). Structural insights into the multivalent binding of the *A. thaliana FLOWERING LOCUS T* promoter by the CO-NF-Y master transcription factor complex. *The Plant Cell, 33*(4), 1182-1195. http://doi.org/10.1093/plcell/koab016

Lyons, E. & Freeling, M. (2008). How to usefully compare homologous plant genes and chromosomes as DNA sequences. *The Plant Journal, 53*(4), 661-673. http://doi.org/10.1111/j.1365-313X.2007.03326.x

Lysak, M. A. & Koch, M. A. (2011). Phylogeny, genome, and karyotype evolution of crucifers (Brassicaceae). *Genetics and Genomics of the Brassicaceae, 9*, 1-31. http://doi.org/10.1007/978-1-4419-7118-0_1

Lysak, M. A., Koch, M. A., Pecinka, A. & Schubert, I. (2005). Chromosome triplication found across the tribe Brassiceae. *Genome Research, 15*(4), 516-525. http://doi.org/10.1101/gr.3531105

Koornneef, M., Dellaert. L.W.M. & Van der Veen, J. H. (1982). EMS- and radiation-induced mutation frequencies at individual loci in *A. thaliana thaliana* (L.) Heynh. *Mutation Research, 93*(1), 109-123. http://doi.org/ 10.1016/0027-5107(82)90129-4

Maggioni, L., von Bothmer, R., Poulsen, G. & Lipman, E. (2018). Domestication, diversity and use of *Brassica oleracea* L., based on ancient Greek and Latin texts. *Genetic Resources and Crop Evolution, 65*(1), 137-159. http://doi.org/10.1007/s10722-017-0516-2

Martin, M. (2011). Cutadapt removes adapter sequences from high-throughput sequencing reads. *EMBnet.journal* 17 (1), 10–12. http://doi: 10.14806/ej.17.1.200

Mathieu, J., Warthmann, N., Küttner, F. & Schmid, M. (2007). Export of FT protein from phloem companion cells is sufficient for floral induction in. *Current Biology, 17*(12), 1055-1060. http://doi.org/10.1016/j.cub.2007.05.009

Mathieu, J., Yant, L. J., Mürdter, F., Küttner, F. & Schmid, M. (2009). Repression of flowering by the miR172 Target SMZ. *PLoS Biology, 7*(7), e1000148. http://doi.org/10.1371/journal.pbio.1000148

Michaels, S. D. & Amasino, R. M. (1999). FLOWERING LOCUS C encodes a novel MADS domain protein that acts as a repressor of flowering. *The Plant Cell, 11*(5), 949-956. http://doi.org/10.1105/tpc.11.5.949

Michaels, S. D. & Amasino, R. M. (2001). Loss of FLOWERING LOCUS C activity eliminates the late-flowering phenotype of FRIGIDA and autonomous pathway mutations but not responsiveness to vernalization. *The Plant Cell, 13*(4), 935-941. http://doi.org/10.1105/tpc.13.4.935

Michaels, S. D., Himelblau, E., Kim, S. Y., Schomburg, F. M. & Amasino, R. M. (2005). Integration of flowering signals in winter-annual *A. thaliana*. *Plant Physiology, 137*(1), 149-156. http://doi.org/10.1104/pp.104.052811

Mizoguchi, T., Wright, L., Fujiwara, S., Cremer, F., Lee, K., Onouchi, H. & Coupland, G. (2005). Distinct roles of GIGANTEA in promoting flowering and regulating circadian rhythms in *A. thaliana*. *The Plant Cell, 17*(8), 2255-2270. http://doi.org/10.1105/tpc.105.033464

Mozgova, I. & Hennig, L. (2015). The Polycomb Group Protein Regulatory Network. *Annual Review of Plant Biology, 66*, 269-296. http://doi.org/10.1146/annurev-arplant-043014-115627

Nagaharu, U. (1935). Genome-analysis in Brassica with special reference to the experimental formation of *B. napus* and peculiar mode of fertilization. *Japanese Journal of Botany, 7*, 389–452.

Navarro, C., Abelenda, J. A., Cruz-Oró, E., Cuéllar, C. A., Tamaki, S., Silva, J. & Prat, S. (2011). Control of flowering and storage organ formation in potato by FLOWERING LOCUS T. *Nature, 478*(7367), 119-132. http://doi.org/10.1038/nature10431

Noh, Y. S. & Amasino, R. M. (2003). *PIE1*, an ISWI family gene, is required for *FLC* activation and floral repression in *A. thaliana*. *The Plant Cell, 15*(7), 1671-1682. http://doi.org/10.1105/tpc.012161

Osborn, T. C. (2003). Detection and effects of a homoeologous reciprocal transposition in *Brassica napus*. *Genetics, 165(3),* 1569–1577. http://doi.org/10.1093 /genetics/165.3.1569

Panjabi, P., Jagannath, A., Bisht, N. C., Padmaja, K. L., Sharma, S., Gupta, V. & Pental, D. (2008). Comparative mapping of *Brassica juncea* and *A. thaliana thaliana* using Intron Polymorphism (IP) markers: homoeologous relationships, diversification and evolution of the A, B and C Brassica genomes. *BMC Genomics, 9,* 113. http://doi.org/10.1186/1471-2164-9-113

Parkin, I. A. P., Gulden, S. M., Sharpe, A. G., Lukens, L., Trick, M., Osborn, T. C. & Lydiate, D. J. (2005). Segmental structure of the *Brassica napus* genome based on comparative analysis with *A. thaliana thaliana*. *Genetics, 171*(2), 765-781. http://doi.org/10.1534/genetics.105.042093

Parkin, I. A. P., Sharpe, A. G., Keith, D. J. & Lydiate, D. J. (1995). Identification of the A and C genomes of amphidiploid *Brassica napus* (oilseed rape). *Genome, 38*(6), 1122-1131. http://doi.org/10.1139/g95-149

Pedmale, U. V., Huang, S. S. C., Zander, M., Cole, B. J., Hetzel, J., Ljung, K. & Chory, J. (2016). Cryptochromes interact directly with PIFs to control plant growth in limiting blue light. *Cell, 164*(1-2), 233-245. http://doi.org/10.1016/j.cell.2015.12.018

Pieper, R., Tomé, F., Pankin, A. & von Korff, M. (2021). FLOWERING LOCUS T4 delays flowering and decreases floret fertility in barley. *Journal of Experimental Botany, 72*(1), 107-121. http://doi.org/10.1093/jxb/eraa466

Pin, P. A. & Nilsson, O. (2012). The multifaceted roles of FLOWERING LOCUS T in plant development. *Plant Cell and Environment, 35*(10), 1742-1755. http://doi.org/10.1111/j.1365-3040.2012.02558.x

Pires, J. C., Zhao, J. W., Schranz, M. E., Leon, E. J., Quijada, P. A., Lukens, L. N. & Osborn, T. C. (2004). Flowering time divergence and genomic rearrangements in resynthesized Brassica polyploids (Brassicaceae). *Biological Journal of the Linnean Society, 82*(4), 675-688. http://doi.org/10.1111/j.1095-8312.2004.00350.x

Ponnu, J., Wahl, V. & Schmid, M. (2011). Trehalose-6-phosphate: connecting plant metabolism and development. *Frontiers in Plant Science, 2,* 70. http://doi.org/10.3389/fpls.2011.00070

Putterill, J., Robson, F., Lee, K., Simon, R. & Coupland, G. (1995). The constans gene of *A. thaliana* promotes flowering and encodes a protein showing similarities to zinc-finger transcription factors. *Cell, 80*(6), 847-857. http://doi.org/10.1016/0092-8674(95)90288-0

Qian, W., Meng, J., Li, M., Frauen, M., Sass, O., Noack, J. & Jung, C. (2006). Introgression of genomic components from Chinese *Brassica rapa* contributes to widening the genetic diversity in rapeseed (*B. napus* L.), with emphasis on the evolution of Chinese rapeseed. *Theoretical and Applied Genetics, 113*(1), 49-54. http://doi.org/10.1007/s00122-006-0269-3

References

Qian, W., Sass, O., Meng, J., Li, M., Frauen, M. & Jung, C. (2007). Heterotic patterns in rapeseed (*Brassica napus* L.): I. crosses between spring and Chinese semi-winter lines. *Theoretical and Applied Genetics, 115*(1), 27-34. http://doi.org/10.1007/s00122-007-0537-x

Rajkumar, K., Nichita, A., Anoor, P. K., Raju, S., Singh, S. S. & Burgula, S. (2016). Understanding perspectives of signalling mechanisms regulating PEBP1 function. *Cell Biochem Funct, 34*(6), 394-403. http://doi.org/10.1002/cbf.3198

Rana, D., Boogaart, T., O'Neill, C. M., Hynes, L., Bent, E., Macpherson, L. & Bancroft, I. (2004). Conservation of the microstructure of genome segments in Brassica napus and its diploid relatives. *The Plant Journal, 40*(5), 725-733. http://doi.org/10.1111/j.1365-313X.2004.02244.x

Ratcliffe, O. J., Kumimoto, R. W., Wong, B. J. & Riechmann, J. L. (2003). Analysis of the *A. thaliana* MADS AFFECTING FLOWERING gene family: MAF2 prevents vernalization by short periods of cold. *The Plant Cell, 15*(5), 1159-1169. http://doi.org/10.1105/tpc.009506

Ratcliffe, O. J., Nadzan, G. C., Reuber, T. L. & Riechmann, J. L. (2001). Regulation of flowering in *A. thaliana* by an FLC homologue. *Plant Physiology, 126*(1), 122-132. http://doi.org/10.1104/pp.126.1.122

Reeves, P. H. & Coupland, G. (2001). Analysis of flowering time control in *A. thaliana* by comparison of double and triple mutants. *Plant Physiology, 126*(3), 1085-1091. http://doi.org/10.1104/pp.126.3.1085

Reidt, W., Wohlfarth, T., Ellerström, M., Czihal, A., Tewes, A., Ezcurra, I. & Bäumlein, H. (2000). Gene regulation during late embryogenesis:: the RY motif of maturation-specific gene promoters is a direct target of the FUS3 gene product. *The Plant Journal, 21*(5), 401-408. http://doi.org/10.1046/j.1365-313x.2000.00686.x

Rosso, M. G., Li, Y., Strizhov, N., Reiss, B., Dekker, K. & Weisshaar, B. (2003). An *A. thaliana* thaliana T-DNA mutagenized population (GABI-Kat) for flanking sequence tag-based reverse genetics. *Plant Molecular Biology, 53*(1), 247-259. http://doi.org/10.1023/B:PLAN.0000009297.37235.4a

Rouse, D. T., Sheldon, C. C., Bagnall, D. J., Peacock, W. J. & Dennis, E. S. (2002). FLC, a repressor of flowering, is regulated by genes in different inductive pathways. *The Plant Journal, 29*(2), 183-191. http://doi.org/10.1046/j.0960-7412.2001.01210.x

Samach, A., Onouchi, H., Gold, S. E., Ditta, G. S., Schwarz-Sommer, Z., Yanofsky, M. F. & Coupland, G. (2000). Distinct roles of CONSTANS target genes in reproductive development of *A. thaliana*. *Science, 288*(5471), 1613-1616. http://doi.org/10.1126/science.288.5471.1613

Sanchez, M. D., Aceves-García, P., Petrone, E., Steckenborn, S., Vega-León, R., Alvarez-Buylla, E. R. & García-Ponce, B. (2015). The impact of Polycomb group (PcG) and Trithorax group (TrxG) epigenetic factors in plant plasticity. *New Phytologist, 208*(3), 684-694. http://doi.org/10.1111/nph.13486

Sarid-Krebs, L., Panigrahi, K. C. S., Fornara, F., Takahashi, Y., Hayama, R., Jang, S. & Coupland, G. (2015). Phosphorylation of CONSTANS and its COP1-dependent degradation during photoperiodic flowering of *A. thaliana*. *The Plant Journal, 84*(3), 451-463. http://doi.org/10.1111/tpj.13022

Sawa, M., Kay, S. A. & Imaizumi, T. (2008). Photoperiodic flowering occurs under internal and external coincidence. *Plant Signal Behavior, 3*(4), 269-271. http://doi.org/10.4161/psb.3.4.5219

Sawa, M., Nusinow, D. A., Kay, S. A. & Imaizumi, T. (2007). FKF1 and GIGANTEA complex formation is required for day-length measurement in *A. thaliana*. *Science, 318*(5848), 261-265. http://doi.org/10.1126/science.1146994

Scortecci, K. C., Michaels, S. D. & Amasino, R. M. (2001). Identification of a MADS-box gene, FLOWERING LOCUS M, that represses flowering. *The Plant Journal, 26*(2), 229-236. http://doi.org/10.1046/j.1365-313x.2001.01024.x

Scott D. Michaels, R. M. A. (2001). Loss of FLOWERING LOCUS C activity eliminates the late-flowering phenotype of FRIGADA and autonomous pathway mutations but not responsiveness to vernalization. *Plant Cell and Environment, 13*(4), 935–941. http://doi.org/10.1105 /tpc.13.4.935

Searle, I., He, Y. H., Turck, F., Vincent, C., Fornara, F., Krober, S. & Coupland, G. (2006). The transcription factor FLC confers a flowering response to vernalization by repressing meristem competence and systemic signaling in *A. thaliana*. *Genes & Development, 20*(7), 898-912. http://doi.org/10.1101/gad.373506

Sgamma, T., Jackson, A., Muleo, R., Thomas, B. & Massiah, A. (2014). TEMPRANILLO is a regulator of juvenility in plants. *Scientific Reports, 4*, 3704. http://doi.org/10.1038/srep03704

Sharpe, A. G., Parkin, I. A. P., Keith, D. J. & Lydiate, D. J. (1995). Frequent nonreciprocal translocations in the amphidiploid genome of oilseed rape (*Brassica napus*). *Genome, 38*(6), 1112-1121. http://doi.org/10.1139/g95-148

Sheldon, C. C., Burn, J. E., Perez, P. P., Metzger, J., Edwards, J. A., Peacock, W. J. & Dennis, E. S. (1999). The FLF MADS box gene: A repressor of flowering in *A. thaliana* regulated by vernalization and methylation. *The Plant Cell, 11*(3), 445-458. http://doi.org/10.1105/tpc.11.3.445

Sheldon, C. C., Rouse, D. T., Finnegan, E. J., Peacock, W. J. & Dennis, E. S. (2000). The molecular basis of vernalization: The central role of FLOWERING LOCUS C (FLC). *Proceedings of the National Academy of Sciences of the United States of America, 97*(7), 3753-3758. http://doi.org/10.1073/pnas.060023597

Simpson, G. G. (2004). The autonomous pathway: epigenetic and post-transcriptional gene regulation in the control of *A. thaliana* flowering time. *Current Opinion in Plant Biology, 7*(5), 570-574. http://doi.org/10.1016/j.pbi.2004.07.002

Simpson, G. G. & Dean, C. (2002). Flowering - *A. thaliana*, the rosetta stone of flowering time? *Science, 296*(5566), 285-289. http://doi.org/10.1126/science.296.5566.285

Siriwardana, C. L., Gnesutta, N., Kumimoto, R. W., Jones, D. S., Myers, Z. A., Mantovani, R. & Holt, B. F., 3rd (2016). NUCLEAR FACTOR Y, Subunit A (NF-YA) proteins positively regulate flowering and act through FLOWERING LOCUS T. *PLoS Genetics*, 12(12), e1006496. https://doi.org/10.1371/journal.pgen.1006496

Shu, J., Chen, C., Thapa, R. K., Bian, S., Nguyen, V., Yu, K., Yuan, Z. C., Liu, J., Kohalmi, S. E., Li, C. & Cui, Y. (2019). Genome-wide occupancy of histone H3K27 methyltransferases CURLY LEAF and SWINGER in *Arabidopsis* seedlings. *Plant Direct,* 3(1), e00100. https://doi.org/10.1002/pld3.100

Song, J. M., Guan, Z. L., Hu, J. L., Guo, C. C., Yang, Z. Q., Wang, S., . . . Guo, L. (2020). Eight high-quality genomes reveal pan-genome architecture and ecotype differentiation of. *Nature Plants, 6*(1), 34-45. https://doi:10.1038/s41477-019-0577-7

Song, Y. H., Lee, I., Lee, S. Y., Imaizumi, T. & Hong, J. C. (2012). CONSTANS and ASYMMETRIC LEAVES 1 complex is involved in the induction of FLOWERING LOCUS T in photoperiodic

References

flowering in *A. thaliana*. *The Plant Journal, 69*(2), 332-342. http://doi.org/10.1111/j.1365-313X.2011.04793.x

Song, Y. H., Shim, J. S., Kinmonth-Schultz, H. A. & Imaizumi, T. (2015). Photoperiodic flowering: time measurement mechanisms in leaves. *Annual Review of Plant Biology, 66*, 441-464. http://doi.org/10.1146/annurev-arplant-043014-115555

Spanudakis, E. & Jackson, S. (2014). The role of microRNAs in the control of flowering time. *Journal of Experimental Botany, 65*(2), 365-380. http://doi.org/10.1093/jxb/ert453

Sparkes, I. A., Runions, J., Kearns, A. & Hawes, C. (2006). Rapid, transient expression of fluorescent fusion proteins in tobacco plants and generation of stably transformed plants. *Nature Protocols, 1*(4), 2019-2025. http://doi.org/10.1038/nprot.2006.286

Suárez-López, P., Wheatley, K., Robson, F., Onouchi, H., Valverde, F. & Coupland, G. (2001). CONSTANS mediates between the circadian clock and the control of flowering in *Arabidopsis*. *Nature, 410*(6832), 1116-1120. http://doi.org/10.1038/35074138

Susila, H., Juric, S., Liu, L., Gawarecka, K., Chung, K. S., Jin, S. & Ahn, J. H. (2021). Florigen sequestration in cellular membranes modulates temperature-responsive flowering. *Science, 373*(6559), 1137-1141. http://doi.org/10.1126/science.abh4054

Curradi, M., Izzo, A., Badaracco, G. & Landsberger, N. (2002). Molecular mechanisms of gene silencing mediated by DNA methylation. Molecular and Cellular Biology, 22(9), 3157-3173. http://doi.org/10.1128/Mcb.22.9.3157-3173.2002

Hawkins, J. S., Kim, H., Nason, J. D., Wing, R. A. & Wendel, J. F. (2006). Differential lineage-specific amplification of transposable elements is responsible for genome size variation in Gossypium. Genome Research, 16(10), 1252-1261. http://doi.org/10.1101/gr.5282906

Suzuki, M. M. & Bird, A. (2008). DNA methylation landscapes: provocative insights from epigenomics. *Nature Reviews Genetics*, 9(6), 465-476. http://doi.org/10.1038/nrg2341

Takeshima, R., Nan, H. Y., Harigai, K., Dong, L. D., Zhu, J. H., Lu, S. J. & Abe, J. (2019). Functional divergence between soybean orthologues and in post-flowering stem growth. *Journal of Experimental Botany, 70*(15), 3941-3953. http://doi.org/10.1093/jxb/erz199

Tamaki, S., Matsuo, S., Wong, H. L., Yokoi, S. & Shimamoto, K. (2007). Hd3a protein is a mobile flowering signal in rice. *Science, 316*(5827), 1033-1036. http://doi.org/10.1126/science.1141753

Tang, H., Bowers, J. E., Wang, X., Ming, R., Alam, M. & Paterson, A. H. (2008). Synteny and collinearity in plant genomes. *Science*, 320(5875), 486-488. https://doi.org/10.1126/science

Teotia, S. & Tang, G. (2015). To bloom or not to bloom: role of microRNAs in plant flowering. *Molecular Plant, 8*(3), 359-377. http://doi.org/10.1016/j.molp.2014.12.018

Tian, H., Li, Y., Wang, C., Xu, X., Zhang, Y., Zeb, Q., Zicola, J., Fu, Y., Turck, F., Li, L., Lu, Z. & Liu, L. (2021). Photoperiod-responsive changes in chromatin accessibility in phloem companion and epidermis cells of Arabidopsis leaves. *The Plant Cell*, 33(3), 475-491. https://doi.org/10.1093/plcell/koaa043

Tsuji, H., Taoka, K. & Shimamoto, K. (2011). Regulation of flowering in rice: two florigen genes, a complex gene network, and natural variation. *Current Opinion in Plant Biology, 14*(1), 45-52. http://doi.org/10.1016/j.pbi.2010.08.016

Tsuji, H. & Taoka, K.-i. (2014). Florigen signaling. *The Enzymes*, *35*, 113-144. http://doi.org/10.1016/B978-0-12-801922-1.00005-1

Tsuji, H. & Taoka, K.-i. (2017). Molecular function of forigen. *Breeding Science, 67*(4), 327-332. http://doi.org/10.1270 /jsbbs.17026

Turck, F., Fornara, F. & Coupland, G. (2008). Regulation and identity of florigen: FLOWERING LOCUS T moves center stage. *Annual Review of Plant Biology, 59*, 573-594. http://doi.org/10.1146/annurev.arplant.59.032607.092755

Turck, F., Roudier, F., Farrona, S., Martin-Magniette, M. L., Guillaume, E., Buisine, N., Gagnot, S., Martienssen, R. A., Coupland, G. & Colot, V. (2007). Arabidopsis TFL2/LHP1 specifically associates with genes marked by trimethylation of histone H3 lysine 27. *PLoS Genetics*, 3(6), e86. https://doi.org/10.1371/journal.pgen.0030086

Vale´rie Hecht, a. R. E. L., b Jacqueline K. Vander Schoor,a Stephen Ridge,a Claire L. Knowles,a, & Lim Chee Liew, a. F. C. S., a Ian C. Murfet,a Richard C. Macknight,b and James L. Wellera,1. (2011). The pea GIGAS gene is a FLOWERING LOCUS T homolog necessary for graft-transmissible specification of flowering but not for responsiveness to photoperiod. *The Plant Cell, 23*(1), 147–161. http://doi.org/10.1105/tpc.110.081042

Valverde, F., Mouradov, A., Soppe, W., Ravenscroft, D., Samach, A. & Coupland, G. (2004). Photoreceptor regulation of CONSTANS protein in photoperiodic flowering. *Science, 303*(5660), 1003-1006. http://doi.org/10.1126/science.1091761

Vollrath, P., Chawla, H. S., Schiessl, S. V., Gabur, I., Lee, H., Snowdon, R. & Obermeier, C. (2021). A novel deletion in FLOWERING LOCUS T modulates flowering time in winter oilseed rape. *Theoretical and Applied Genetics, 134*(4), 1217-1231. http://doi.org/10.1007/s00122-021-03768-4

Wang, H. Y., Ma, L. G., Li, J. M., Zhao, H. Y. & Deng, X. W. (2001). Direct interaction of *A. thaliana* cryptochromes with COP1 in light control development. *Science, 294*(5540), 154-158. http://doi.org/10.1126/science.1063630

Wang, J., Hopkins, C. J., Hou, J. N., Zou, X. X., Wang, C. N., Long, Y. & Meng, J. L. (2012). Promoter variation and transcript divergence in Brassicaceae lineages of. *PLoS ONE, 7*(10), e47127. http://doi.org/ 10.1371/journal.pone.0047127

Wang, J., Long, Y., Wu, B. D., Liu, J., Jiang, C. C., Shi, L. & Meng, J. L. (2009). The evolution of *Brassica napus* FLOWERING LOCUST paralogues in the context of inverted chromosomal duplication blocks. *BMC Evolutionary Biology, 9*, 271. http://doi.org/10.1186/1471-2148-9-271

Wang, X. W., Wang, H. Z., Wang, J., Sun, R. F., Wu, J., Liu, S. Y. & Zhang, Z. H. (2011). The genome of the mesopolyploid crop species Brassica rapa. *Nature Genetics, 43*(10), 1035-1157. http://doi.org/10.1038/ng.919

Wang, Y. Z., Gu, X. F., Yuan, W. Y., Schmitz, R. J. & He, Y. H. (2014). Photoperiodic control of the floral transition through a distinct polycomb repressive complex. *Developmental Cell, 28*(6), 727-736. http://doi.org/10.1016/j.devcel.2014.01.029

Wenkel, S., Turck, F., Singer, K., Gissot, L., Le Gourrierec, J., Samach, A. & Coupland, G. (2006). CONSTANS and the CCAAT box binding complex share a functionally important domain and interact to regulate flowering of. *The Plant Cell, 18*(11), 2971-2984. http://doi.org/10.1105/tpc.106.043299

Wickland, D. P. & Hanzawa, Y. (2015). The FLOWERING LOCUS T/TERMINAL FLOWER 1 gene family: functional evolution and molecular mechanisms. *Molecular Plant, 8*(7), 983-997. http://doi.org/10.1016/j.molp.2015.01.007

References

Wigge, P. A. (2011). FT, A mobile developmental signal in plants. *Current Biology, 21*(9), 374-378. http://doi.org/10.1016/j.cub.2011.03.038

Wigge, P. A., Kim, M. C., Jaeger, K. E., Busch, W., Schmid, M., Lohmann, J. U. & Weigel, D. (2005). Integration of spatial and temporal information during floral induction in *A. thaliana*. *Science, 309*(5737), 1056-1059. http://doi.org/10.1126/science.1114358

Wilson, R. N., Heckman, J. W. & Somerville, C. R. (1992). Gibberellin is required for flowering in *A. thaliana thaliana* under short days. *Plant Physiology, 100*(1), 403-408. http://doi.org/10.1104/pp.100.1.403

Woodhouse, S. M. (2021). Unravelling the floral transition in *Brassica oleracea* using transcriptomics. (PhD Thesis).

Wu, G., Park, M. Y., Conway, S. R., Wang, J. W., Weigel, D. & Poethig, R. S. (2009). The sequential action of miR156 and miR172 regulates developmental timing in *A. thaliana*. *Cell, 138*(4), 750-759. http://doi.org/10.1016/j.cell.2009.06.031

Wu, G. & Poethig, R. S. (2006). Temporal regulation of shoot development in *A. thaliana thaliana* by miR156 and its target *SPL3*. *Development, 133*(18), 3539-3547. http://doi.org/10.1242/dev.02521

Xi, W. Y., Liu, C., Hou, X. L. & Yu, H. (2010). Regulates seed germination through a negative feedback loop modulating ABA signaling in *A. thaliana*. *The Plant Cell, 22*(6), 1733-1748. http://doi.org/10.1105/tpc.109.073072

Xu, F., Rong, X. F., Huang, X. H. & Cheng, S. Y. (2012). Recent advances of flowering locus T gene in higher plants. *International Journal of Molecular Sciences, 13*(3), 3773-3781. http://doi.org/10.3390/ijms13033773

Xu, M., Hu, T., Zhao, J., Park, M. Y., Earley, K. W., Wu, G. & Poethig, R. S. (2016). Developmental functions of miR156-regulated SQUAMOSA PROMOTER BINDING PROTEIN-LIKE (SPL) genes in *A. thaliana thaliana*. *PLoS Genetics, 12*(8), e1006263. http://doi.org/10.1371/journal.pgen.1006263

Xu, Y. F., Gan, E. S., Zhou, J., Wee, W. Y., Zhang, X. Y. & Ito, T. (2014). *A. thaliana* MRG domain proteins bridge two histone modifications to elevate expression of flowering genes. *Nucleic Acids Research, 42*(17), 10960-10974. http://doi.org/10.1093/nar/gku781

Yamaguchi, A., Kobayashi, Y., Goto, K., Abe, M. & Araki, T. (2005). TWIN SISTER OF FT (TSF) acts as a floral pathway integrator redundantly with FT. *Plant and Cell Physiology, 46*(8), 1175-1189. http://doi.org/10.1093/pcp/pci151

Yang, H. Q., Wu, Y. J., Tang, R. H., Liu, D. M., Liu, Y. & Cashmore, A. R. (2000). The C termini of *A. thaliana* cryptochromes mediate a constitutive light response. *Cell, 103*(5), 815-827. http://doi.org/Doi 10.1016/S0092-8674(00)00184-7

Yang, Y. W., Lai, K. N., Tai, P. Y. & Li, W. H. (1999). Rates of nucleotide substitution in angiosperm mitochondrial DNA sequences and dates of divergence between Brassica and other angiosperm lineages. *Journal of Molecular Evolution, 48*(5), 597-604. https://doi.org/10.1007/Pl00006502

Yang, Z. L., Qian, S. M., Scheid, R. N., Lu, L., Chen, X. S., Liu, R. & Zhong, X. H. (2018). EBS is a bivalent histone reader that regulates floral phase transition in *A. thaliana*. *Nature Genetics, 50*(9), 1247-1253. http://doi.org/10.1038/s41588-018-0187-8

Yang, Z., Wang, S., Wei, L., Huang, Y., Liu, D., Jia, Y., Luo, C., Lin, Y., Liang, C., Hu, Y., Dai, C., Guo, L., Zhou, Y. & Yang, Q. Y. (2023). BnIR: A multi-omics database with various tools

for *Brassica napus* research and breeding. *Molecular Plant*, 16(4), 775-789. https://doi.org/10.1016/j.molp.2023.03.007

Yuan, L., Song, X., Zhang, L., Yu, Y., Liang, Z., Lei, Y., Ruan, J., Tan, B., Liu, J. & Li, C. (2021). The transcriptional repressors VAL1 and VAL2 recruit PRC2 for genome-wide Polycomb silencing in *Arabidopsis*. *Nucleic Acids Research*, 49(1), 98-113. https://doi.org/10.1093/nar/gkaa1129

Yoo, S. J., Chung, K. S., Jung, S. H., Yoo, S. Y., Lee, J. S., & Ahn, J. H. (2010). BROTHER OF FT AND TFL1 (BFT) has TFL1-like activity and functions redundantly with TFL1 in inflorescence meristem development in Arabidopsis. *Plant Journal*, *63*(2), 241-253. doi:10.1111/j.1365-313X.2010.04234.x

Yoo, S. J., Hong, S. M., Jung, H. S. & Ahn, J. H. (2013). The cotyledons produce sufficient FT protein to induce flowering: Evidence from cotyledon micrografting in *A. thaliana*. *Plant and Cell Physiology, 54*(1), 119-128. http://doi.org/10.1093/pcp/pcs158

Yoo, S. K. (2005). CONSTANS activates SUPPRESSOR OF OVEREXPRESSION OF CONSTANS 1 through FLOWERING LOCUS T to promote flowering in *A. thaliana*. *Plant Physiology, 139*(2), 770–778. http://doi.org/10.1104 /pp.105.066928

Yoo, S. Y., Kardailsky, I., Lee, J. S., Weigel, D. & Ahn, J. H. (2004). Acceleration of flowering by overexpression of *MFT* (*MOTHER OF FT AND TFL1*). *Molecules and Cells*, 17(1), 95–101.

Zeevaart, J. A. D. (1976). Physiology of flower formation. *Annual Review of Plant Physiology and Plant Molecular Biology*, *27*, 321-348. http://doi.org/10.1146/annurev.pp.27.060176.001541

Zhai, H., Lü, S. X., Liang, S., Wu, H. Y., Zhang, X. Z., Liu, B. H. & Xia, Z. J. (2014). GmFT4, a homolog of FLOWERING LOCUS T, is positively regulated by E1 and functions as a flowering repressor in soybean. *PLoS ONE, 9*(2), e89030. http://doi.org/10.1371/journal.pone.0089030

Zhang, B. L., Wang, L., Zeng, L. P., Zhang, C. & Ma, H. (2015a). TOE proteins convey a photoperiodic signal to antagonize CONSTANS and regulate flowering time. *Genes & Development, 29*(9), 975-987. http://doi.org/10.1101/gad.251520.114

Zhang, X., Germann, S., Blus, B. J., Khorasanizadeh, S., Gaudin, V. & Jacobsen, S. E. (2007). The Arabidopsis LHP1 protein colocalizes with histone H3 Lys27 trimethylation. *Nature Structural & Molecular Biology, 14*(9), 869-871. http://doi.org/10.1038/nsmb1283

Zhang, X. H., Wang, C. C., Pang, C. Y., Wei, H. L., Wang, H. T., Song, M. Z. & Yu, S. X. (2016). Characterization and functional analysis of PEBP family genes in upland cotton (*Gossypium hirsutum* L.). *PLoS ONE, 11*(8), e0161080. http://doi.org/10.1371/journal.pone.0161080

Zhang, X. M., Meng, L., Liu, B., Hu, Y. Y., Cheng, F., Liang, J. L. & Wu, J. (2015b). A transposon insertion in FLOWERING LOCUS T is associated with delayed flowering in *Brassica rapa*. *Plant Science, 241,* 211-220. http://doi.org/10.1016/j.plantsci.2015.10.007

Zhu, Y., Klasfeld, S., Jeong, C. W., Jin, R., Goto, K., Yamaguchi, N. & Wagner, D. (2020). TERMINAL FLOWER 1-FD complex target genes and competition with FLOWERING LOCUS T. *Nature Communications, 11*(1), e5118. http://doi.org/10.1038/s41467-020-18782-1

Zhu, Y., Liu, L., Shen, L. S. & Yu, H. (2016). NaKR1 regulates long-distance movement of FLOWERING LOCUS T in *A. thaliana*. *Nature Plants, 2*(6), 16075. http://doi.org/10.1038/nplants.2016.75

References

Zicola, J., Liu, L. Y., Tanzler, P. & Turck, F. (2019). Targeted DNA methylation represses two enhancers of FLOWERING LOCUS T in *A. thaliana thaliana*. *Nature Plants, 5*(3), 300-307. http://doi.org/10.1038/s41477-019-0375-2

Ziolkowski, P. A., Kaczmarek, M., Babula, D. & Sadowski, J. (2006). Genome evolution in *A. thaliana*/Brassica: conservation and divergence of ancient rearranged segments and their breakpoints. *The Plant Journal, 47*(1), 63-74. http://doi.org/10.1111/j.1365-313X.2006.02762.x

Zou, J., Mao, L. F., Qiu, J., Wang, M., Jia, L., Wu, D. Y. & Fan, L. J. (2019). Genome-wide selection footprints and deleterious variations in young Asian allotetraploid rapeseed. *Plant Biotechnology Journal, 17*(10), 1998-2010. http://doi.org/10.1111/pbi.13115

Zuo, Z. C., Liu, H. T., Liu, B., Liu, X. M. & Lin, C. T. (2011). Blue light-dependent interaction of CRY2 with SPA1 regulates COP1 activity and floral initiation in *A. thaliana*. *Current Biology, 21*(10), 841-847. http://doi.org/10.1016/j.cub.2011.03.048

7. Appendix

Table 1 Gene used in this phylogenetic tree construction

Name	Accession Number	Species/Cultivar
FT	*AT1G65480*	*Arabidopsis thaliana*
TSF	*AT4G20370*	
TFL1	*AT5G03840*	
BFT	*AT5G62040*	
MFT	*AT1G18100*	
Sp.FT	*Sp5g20330*	*Schrenkiella parvula*
Sp.TSF	*Sp7g18730*	
Sp.NFT	*Sp5g32040*	
Al.FT	*LOC9322985*	*Arabidopsis lyrata*
Al.TSF	*LOC9306006*	

Table 2. Oligonucleotides used in this study

Application	Primer name	Sequence
RT-qPCR	BnFT.A2-qF	GGTATTCATCGTATCGTGCTCG
	BnFT.A2-qR	CAAGTTATTAAAAGAAGAAGAGGCTC
	BnFT.C2-qF	GGTATTCATCGTATCGTGCTG
	BnFT.C2-qR	GTTATTAAAAGAAGAAGAGGCTCATC
	BnFT.A7-qF	CCACCTCGGGAATTCATCGTC
	BnFT.A7-qR	CCATGACCCATCGATCTAAG
	BnFT.C6-qF	CAAACGGTGTATGAACCAGG
	BnFT.C6-qR	TCTAAGGAAGAAGCCCATCG
	BnNFT.A7-qF	CGAGAGACCCTCTTATCGTAGG
	BnNFT.A7-qR	AATCTCAACCGTTGGTTTGTTC
	BnCFT.C4-qF	CGAGAGATCCTCTTGTGCTTGC
	BnCFT.C4-qR	GATCTCGACCGTTGGTTTATTT
	BnCO.A10-qF	ACGTATGGCTCCTCAGGAAGTCAC
	BnCO.A10-qR	TCTGAATTAGAGGTTCAGGTAGTTTCT
	BnCO.C09-qF	TAAACAAGACTGCATCGTACCAGAGA
	BnCO.C09-qR	GTCAGTTTCCATTGATGGATTGTATG
	BnENTH-qF	GTTTAGACCCGTTGCTGCTC
	BnENTH-qR	TTGTCCATCTCAGCCATTTG

ft-10 complementation with (C+A)p	BnFT.A2C2-pFT-F	TGGTGATATCAAGCTTATGTCTTTAAGTAATAGAGATCCTCTTG
	BnFT.A2-pFT-R	GATCGGGGAAATTCGAGCTCCTAACTTCTTCGTCCTCCG
	BnFT.C2-pFT-R	GATCGGGGAAATTCGAGCTCCTAACTTCTTCGTCCTCCGCAGC
	BnFT.A7C6-pFT-F	TGGTGATATCAAGCTTATGTCTGTAAATAACAGAGATCCTCT
	BnFT.A7-pFT-R	GATCGGGGAAATTCGAGCTCCTAAGTTCTTCGTCCTCCG
	BnFT.C6-pFT-R	GATCGGGGAAATTCGAGCTCCTAACATCTTCGTCCTCCG
	BnNFT.A7-pFT-F	TGGTGATATCAAGCTTATGTCATTAAGTCCGAGAGACCCT
	BnNFT.A7-pFT-R	GATCGGGGAAATTCGAGCTCCTACGAGGTCCTTCTTCCTCCG
	BnCFT.C4-pFT-F	TGGTGATATCAAGCTTATGTCTTTAAGTCCGAGAGATCCTC
	BnCFT.C4-pFT-R	GATCGGGGAAATTCGAGCTCCTATGTTCTTCTTCCTCCACAGCCA
	Plasmid-V-F1	CACAGAGAAACCACCTGTTTGTT
	Plasmid-V-R1	TATGATAATCATCGCAAGACCG
ft-10 complementation with FDp	BnFT.A7C6-pFD-F	AGGTGGTGGAAGTTACCCTTACGATGTGCCTGATTACGCTGGAAGTTCTGTAAATAACAGAGATCCTCTTG
	pFD-2HA-F	CTTCTGTTCTCTTTTCCAATGTACCCATACGATGTGCCTGATTACGCTGGAGGTGGTGGAAGTTACCCTTACG
	BnFT.A7-pFD-R	CAAGGACTTGTAGATTTCCTAAGTTCTTCGTCCTCCG
	BnFT.C6-pFD-R	CAAGGACTTGTAGATTTCCTAACATCTTCGTCCTCCG
	At.FT-pFD-F	AGGTGGTGGAAGTTACCCTTACGATGTGCCTGATTACGCTGGAAGTTCTATAAATATAAGAGACCCTCT
	At.FT-pFD-R	CAAGGACTTGTAGATTTCCTAAAGTCTTCTTCCTCCGCA
	Plasmid-V-F2	ACCGGCTAAAGTCAAGAACCTCT
	Plasmid-V-R2	CCGGGTCTTTTGTTTTACATCTTC
	2HA-tag	TACCCATACGATGTGCCTGATTACGCTGGAGGTGGTGGAAGTTACCCTTACGATGTGCCTGATTACGCT

		CGAATTGGGTACAGTACTGCTATCAATAGTAAT
	pA2-12K-P1-F	TCGATTTCTATGAGC
	pA2-12K-P1-R	ACCAGATGATGCCTGCGTCTATG
	pA2-12K-P2-F	GCAGGCATCATCTGGTGAGAAC
		TCGCGTTTCACCATGGCTTTGATCTAAAACAAA
	pA2-12K-P2-R	CAGGTGG
	pA2-5.7k-P1-R	ACCTTCCGAGCATTACCAAAACACACGTAACCT TG
	pA2-5.7k-P2-F	TTTGGTAATGCTCGGAAGGTAAGTAGTAGTGTA GG
	pA2-2.5k-P1-R	ACCTTCCGAGGCAACCAATTTCCATACACCAC
	pA2-2.5k-P2-F	AATTGGTTGCCTCGGAAGGTAAGTAGTAGTGTA GG
		CGAATTGGGTACAGTACTGTGCTTTAAACTAGT
	pA7-12K-P1-F	GACCAGGAG
	pA7-12K-P1-R	TCCAAACTTCTTTGCAACAGACAAAGG
	pA7-12K-P2-F	GCAAAGAAGTTTGGATTCACTCAG
		TCGCGTTTCACCATGGCTCTGATCTAAAACAAA
	pA7-12K-P2-R	CAGGTTG
Tobacco infiltration	pA7-5.7k-P1-R	CGGTTAGTACTCTCCGACAGCACAAACGC
	pA7-5.7k-P2-F	CTGTCGGAGAGTACTAACCGATTTAGCCTAACG G
	pA7-2.5k-P1-R	TTAATGCTTTCGGTCACCCTTTGTCAAGGAG
	pA7-2.5k-P2-F	AGGGTGACCGAAAGCATTAACTCCAATGCTCCT C
		CGAATTGGGTACAGTACTGCACAAAAGTTACGT
	pC2-5.3K-P1-F	TTTGTTACAGC
	pC2-5.3K-P1-R	ATCTTCTACGGTGTTTGAAGAAGGCGTAACTAC
		CAAACACCGTAGAAGATAAGGAAGATGGAGTT
	pC2-5.3K-P2-F	TGG
	pC2-1.8K-P1-R	GTTACTAGCGTGGATTTCATTTCTTACTTTGTAG
	pC2-1.8K-P2-F	TCCACGCTAGTAACGACGAAACGTGTTTCC
	pFT-Block C-F	CGAATTGGGTACAGTACTGGAGCAGTCAATAAT TTATTTATTCC
	pFT-Block A-R	TCGCGTTTCACCATGGCTTTGATCTTGAACAAAC AGGTG
	V-629-F1	TGAAGCAACTCCTCGAAAAAGC
	V-629-R1	CAATTCCACACAACATACGAGCC
	V-629-F2	GTGCTGCAAGGCGATTAAGTTG
	V-629-R2	ACGAGTGCTTGAGGGAGGTGAC

Appendix

Table 3 Plasmids used in this study

Application	Construct
ft-10 Complementation	C+Ap::FT-pGreen
	Block(C+A)p::BnFT.A2-pGreen
	Block(C+A)p::BnFT.C2-pGreen
	Block(C+A)p::BnFT.A7-pGreen
	Block(C+A)p::BnFT.A7m-pGreen
	Block(C+A)p::BnFT.C6-pGreen
	Block(C+A)p::BnFT.C6m-pGreen
	Block(C+A)p::BnNFT.A7-pGreen
	Block(C+A)p::BnCFT.C4-pGreen
	FDp::FDter-pER8
	FDp::FT-pER8
	FDp::BnFT.A2-pER8
	FDp::BnFT.C2-pER8
	FDp::BnFT.A7-pER8
	FDp::BnFT.C6-pER8
	FDp::BnNFT.A7-pER8
	FDp::BnCFT.C4-pER8
Tobacco infiltration	BlockAp::LUC-pGreen
	BlockAp::LUC-35Sp::RLUC-pGreen
	Block(C+A)p::LUC-35Sp::RLUC-pGreen
	5.7kbFTp::LUC-35Sp:RLUC-pGreen
	12kbBnFT.A2p::LUC-35Sp::RLUC-pGreen
	5.7kbBnFT.A2p::LUC-35Sp::RLUC-pGreen
	2.5kbBnFT.A2p::LUC-35Sp::RLUC-pGreen
	12kbBnFT.A7p::LUC-35Sp::RLUC-pGreen
	5.7kbBnFT.A7p::LUC-35Sp::RLUC-pGreen
	2.5kbBnFT.A7p::LUC-35Sp::RLUC-pGreen
	5.3kbBnFT.C2p::LUC-35Sp::RLUC-pGreen
	1.8kbBnFT.C2p::LUC-35Sp::RLUC-pGreen
	35Sp::BnA10.CO-pGreen
	35Sp::BnC9.CO-pGreen
	35Sp::AtCO-pGreen
	35Sp::LUC-pGreen
	35Sp::H2B-pGreen
	P19

Table 4 Media for seeds germination and microbes

Composition for 1000ml culture media are listed. All media were autoclaved at 121°C for 20 min prior to use, except when specified otherwise

Name	Ingredients	Note
GM medium	4,4g MS-salt including vitamins 0,5g MES 10g Saccharose 9g hytoagar	Adjust pH to 5.7 with 10M KOH
Liquid LB medium	10g Tryptone 5g Yeast Extract 5g NaCl	Adjust pH to 7.2 with 1M NaOH
Solid LB medium	10g Tryptone 5g Yeast Extract 5g NaCl 20g Bacto Agar	Adjust pH to 7.2 with 1M NaOH

Table 5 Antibiotics concentration for selective growth

Antibiotic	Selective concentration
Rifampicin (Rif)	50 µg/mL
Gentamicin (Gent)	25 µg/mL)
Tetracyclin (Tet)	5 µg/mL
Kanamycin (Kan)	40 µg/mL
Carbenicillin (Carb)	100 µg/mL
Hygromicin B (Hyg)	26.25 µg/mL
Phosphinotricin (PPT)	12 µg/mL

Appendix

Table 6 Gene studied in heatmap

Name	Gene Name	Gene Accession
BnFT	*BnFT.A2*	*BnaA02G0156900ZS*
	BnFT.C2	*BnaC02G0200600ZS*
	BnFT.A7	*BnaA07G0282700ZS*
	BnFT.C6	*BnaC06G0323800ZS*
BnNFT	*BnNFT.A7*	*BnaA07G0365100ZS*
BnCFT	*BnCFT.C4*	*BnaC04G0181400ZS*
BnCO	*BnCO.A10*	*BnaA10G0206200ZS*
	BnCO.C9	*BnaC09G0505500ZS*
BnADO2	*BnADO2.A7*	*BnaA07G0015400ZS*
	BnADO2.A7A	*BnaA07G0015500ZS*
	BnADO2.A7B	*BnaA07G0015600ZS*
	BnADO2.C7	*BnaC07G0032700ZS*
	BnADO2.C7A	*BnaC07G0032800ZS*
	BnADO2.C7B	*BnaC07G0033600ZS*
BnGI	*BnGI.A9*	*BnaA09G0458700ZS*
	BnGI.C5	*BnaC05G0198400ZS*
BnCDF1	*BnCDF1.A2*	*BnaA02G0400200ZS*
	BnCDF1.C2	*BnaC02G0532300ZS*
	BnCDF1.A6	*BnaA06G0277300ZS*
	BnCDF1.C3	*BnaC03G0554300ZS*
BnFLC	*BnFLC.A2*	*BnaA02G0035100ZS*
	BnFLC.C2	*BnaC02G0039100ZS*
	BnFLC.A3	*BnaA03G0039200ZS*
	BnFLC.C3	*BnaC03G0046300ZS*
	BnFLC.A3A	*BnaA03G0144400ZS*
	BnFLC.C3A	*BnaC03G0167700ZS*
	BnFLC.A10	*BnaA10G0244800ZS*
	BnFLC.C9	*BnaC09G0556700ZS*
BnSVP	*BnSVP.A4*	*BnaA04G0147200ZS*
	BnSVP.C4	*BnaC04G0438900ZS*
	BnSVP.A9	*BnaA09T0591400ZS*
	BnSVP.C8	*BnaC08G0443200ZS*
BnTEM1	*BnTEM1.A8*	*BnaA08G0227400ZS*
	BnTEM1.A9	*BnaA09G0438500ZS*
	BnTEM1.C5	*BnaC05G0225100ZS*
BnFD	*BnFD.A1*	*BnaA01G0026200ZS*
	BnFD.C1	*BnaC01G0031000ZS*
	BnFD.A3	*BnaA03G0552500ZS*
	BnFD.C3	*BnaC03G0701500ZS*
	BnFD.A8	*BnaA08G0176900ZS*

	BnFD.C7	*BnaC07G0528800ZS*
BnSOC1	*BnSOC1.A3*	*BnaA03G0221300ZS*
	BnSOC1.C3	*BnaC03G0260300ZS*
	BnSOC1.A4	*BnaC04G0606600ZS*
	BnSOC1.C4	*BnaC04G0060400ZS*
	BnSOC1.A5	*BnaA05G0054300ZS*
	BnSOC1.A4A	*BnaA04G0287900ZS*

8. Abbreviations

General abbreviations

%	percentage
:	fused to (in the context of gene fusion constructs)
°C	Degree Celsius
3´	three prime end of DNA fragment
35S	promoter of the Cauliflower Mosaic virus
5´	five prime end of DNA fragment
µ	micro
A	Adenine
A. thaliana	*A. thaliana thaliana*
AS	Acetosyringone
ATPases	Adenosine 5'-TriPhosphatase
BAC	Bacterial Artificial Chromosome
bHLH	basic Helix Loop Helix
BiFC	Bi-molecular Fluorescent Complementation
bp	base pair
C	Cytosine
C+A	Block C + Block A
C175	Cysteine 175
CCT	CONSTANS, CO-like, and TOC1 domain
cDNA	complementary DNA
CDS	Coding sequences
Col-0	*A. thaliana thaliana* ecotype Columbia-0
CORE	CO-responsive element
C-terminal	Carboxyterminal

Cq	Quantification Cycle
D	Aspartate
DEGs	Differentially Expressed Genes
DH	Doubled Haploid
DNA	Deoxyribonucleic acid
DNase	Deoxyribonuclease
dNTP	Deoxyribonucleic triphosphate
E	Glutamate
E. coli	*Escherichia coli*
FAC	Florigen Activation Complex
FC	Fold Change
Fig.	Figure
G	Guanine
g	gram
GA	Gibberellic Acid
gDNA	genomic DNA
GM	½ strength Murashige and Skoog medium
GTFs	General Transcription Factors
h	hour
Hyg	Hygromicin B
H3K4me3	Histone H3 lysine 4 trimethylation
H3K27me3	Histone H3 lysine 27 trimethylation
IR	Inverted Repeats
k	kilo
kb	kilobase pair

Abbreviations

L	Liter
LD	Long Day
Ler	Landsberg erecta
m	milli
M	Molar (mol/l)
MgCl2	Magnesium chloride
min	Minute (s)
MITE	Miniature Inverted-repeat Transposable Element
ml	milliliter
mM	millimolar
mm	millimeter
mol	mole
mRNA	messenger RNA
N	Asparagine
n	nano
N-	amino-terminal
NGS	Next Generation Sequencing
NOS	*Nopaline Synthase*
NOSmin	minimal promoter of the *NOS* gene
NOSterm	*NOS* terminator
p	pico
PCA	Principal Component Analysis
PCR	Polymerase Chain Reaction
PG	Phosphatidylglycerol
PPT	Phosphinotricin

PRC	Polycomb repressive complex
QTL	Quantitative Trait Locus
Rif	Rifampicin
RNA	Ribonucleic acid
RNase	Ribonuclease
RNA-seq	RNA-sequencing
rpm	rounds per minute
rRNA	ribosomal RNA
RT	Room Temperature
RT-qPCR	Reverse Transcription quantitative PCR
S	Arginine
SAM	Shoot Apical Meristem
SD	Short Day
SE	Standard error for statistical analysis
SEs	Sieve Elements
sgRNA	single guide RNA
s/sec	seconds
T	Thymine
T1, T2, T3	First, second, third generation after transformation
T-DNA	Transferred DNA
TFBS	Transcription Factor Binding Sites
TFs	Transcription Factors
TrxG	Trithorax group proteins
TSS	Transcription Start Site
UTR	Untranslated region

Abbreviations

μg	Microgram
μM	Micromolar
V	Volts
ZT	Zeitgeber Time

Abbreviations of gene names

AG	*AGAMOUS*
AP1	*APETALA 1*
AP2	*APETALA 2*
ATC	*A. THALIANA THALIANA CENTRORADIALIS*
ATX1	*A. THALIANA HOMOLOG OF TRITHORAX 1*
BFT	*BROTHER OF FT AND TFL1*
bHLH	*BASIC HELIX-LOOP-HELIX*
bZIP	*BASIC LEUCINE ZIPPER*
CCA1	*CIRCADIAN CLOCK-ASSOCIATED 1*
CDFs	*CYCLING DOF FACTORs*
CIB1	*CRYPTOCHROME-INTERACTING bHLH 1*
CLF	*CURLY LEAF*
CO	*CONSTANS*
COL	*CO-LIKE*
COP1	*CONSTITUTIVE PHOTOMORPHOGENESIS 1*
CORE	*CONSTANS RESPONSIVE ELEMENT*
CRY2	*CRYPTOCHROME 2*
EBS	*EARLY BOLTING IN SHORT DAYS*
EMF1	*EMBRYONIC FLOWER1*

ERF	*ETHYLENE RESPONSIVE ELEMENT BINDING FACTOR*
FCA	*FLOWERING CONTROL LOCUS A*
FD	*FLOWERING LOCUS D*
FKF1	*FLAVIN-BINDING, KELCH REPEAT, F-BOX1*
FLC	*FLOWERING LOCUS C*
FLD	*FLOWERING LOCUS D*
FLK	*FLOWERING LOCUS K*
FLM	*FLOWERING LOCUS M*
FRI	*FRIGIDA*
FT	*FLOWERING LOCUS T*
FTIP1	*FT-INTERACTING PROTEIN 1*
FUL	*FRUITFULL*
FY	*FLOWERING LOCUS Y*
GFP	*GREEN FLUORESCENT PROTEIN*
GI	*GIGANTEA*
GUS	*β-GLUCURONIDASE*
Hd3a	*HEADING DATE 3a*
HFD	*HISTONE FOLD DOMAIN*
HMA	*HEAVY METAL ASSOCIATED*
HOS1	*HIGH EXPRESSION OF OSMOTICALLY RESPONSIVE GENE 1*
LB	*LYSOGENY BROTH*
LD	*LUMINIDEPENDENS*
LFY	*LEAFY*
LHP1	*LIKE HETEROCHOMATON PROTEIN1 (also known as TFL2)*
LUC	*LUCIFERASE*
MAF	*MADS AFFECTING FLOWERING*

Abbreviations

MFT	*MOTHER OF FT AND TFL1*
MRG	*MORF RELATED GENE*
miR156	*microRNA156*
miR172	*microRNA172*
NaKR1	*SODIUM POTASSIUM ROOT DEFECTIVE 1*
NF-Y	*NUCLEAR FACTOR-Y*
PcG	*POLYCOMB GROUP GENES*
PEPB	*PHOSPHATIDYLETHANOLAMINE-BINDING PROTEIN*
PHYA	*PHYTOCHROME A*
PHYB	*PHYTOCHROME B*
PIF	*PHYTOCHROME-INTERACTING FACTOR*
PKL	*PICKLE*
PRC	*POLYCOMB RERPRESSIVE COMPLEX*
QKY	*QUIRKY*
RAV	*RELATED TO ABI3/VP*
RFT1	*RICE FLOWERING LOCUS T 1*
SHL	*SHORT LIFE*
SFT	*SINGLE FLOWER TRUSS*
SMZ	*SCHLAFMUTZE*
SNZ	*SCHNARCHZAPFEN*
SOC1	*SUPPRESSOR OF OVEREXPRESSION OF CONSTANS1*
SPA	*SUPPRESSOR OF PHYA-105*
SPL	*SQUAMOSA PROMOTER BINDING PROTEIN-LIKE*
SP3D	*SELF PRUNING 3D*
SP6A	*SELF-PRUNING 6A*

SUC2	*SUCROSE TRANSPORTER2*
SVP	*SHORT VEGETATIVE PHASE*
SYP121	*SYNTAXIN OF PLANTS121*
TEM	*TEMPPANILLO*
TFL1	*TERMINAL FLOWER1*
TFL2	*TERMINAL FLOWER 2 (also known as LHP1)*
TOC1	*TIMING OF CAB EXPRESSION 1*
TOE	*TARGET OF EAT*
TPL	*TOPLESS*
TSF	*TWIN SISTER OF FT*
VAL1	*VIVIPAROUS1/ABSCISIC ACID INSENSITIVE3-LIKE1*
YFP	*YELLOW FLUORESCENT PROTEIN*

Erklärung zur Dissertation

gemäß der Promotionsordnung vom 12. März 2020

Hiermit versichere ich an Eides statt, dass ich die vorliegende Dissertation selbstständig und ohne die Benutzung anderer als der angegebenen Hilfsmittel und Literatur angefertigt habe. Alle Stellen, die wörtlich oder sinngemäß aus veröffentlichten und nicht veröffentlichten Werken dem Wortlaut oder dem Sinn nach entnommen wurden, sind als solche kenntlich gemacht. Ich versichere an Eides statt, dass diese Dissertation noch keiner anderen Fakultät oder Universität zur Prüfung vorgelegen hat; dass sie - abgesehen von unten angegebenen Teilpublikationen und eingebundenen Artikeln und Manuskripten - noch nicht veröffentlicht worden ist sowie, dass ich eine Veröffentlichung der Dissertation vor Abschluss der Promotion nicht ohne Genehmigung des Promotionsausschusses vornehmen werde. Die Bestimmungen dieser Ordnung sind mir bekannt. Darüber hinaus erkläre ich hiermit, dass ich die Ordnung zur Sicherung guter wissenschaftlicher Praxis und zum Umgang mit wissenschaftlichem Fehlverhalten der Universität zu Köln gelesen und sie bei der Durchführung der Dissertation zugrundeliegenden Arbeiten und der schriftlich verfassten Dissertation beachtet habe und verpflichte mich hiermit, die dort genannten Vorgaben bei allen wissenschaftlichen Tätigkeiten zu beachten und umzusetzen. Ich versichere, dass die eingereichte elektronische Fassung der eingereichten Druckfassung vollständig entspricht.

Datum: 18.12.2023

Name: Juanjuan Wang

Unterschrift:

Delimitation of own contribution

I independently acquired the results presented in this study without any assistance other than that stated here. The specific experimental contributions of other individuals who participated in this study are listed below:

As the supervisor of this study, Prof. Dr. Franziska Turck provided valuable guidance and support throughout the project. She also performed the lastal blast, synteny analysis and most of the RNA-Seq data analysis.

Petra Taenzler helped with some of the seeds harvest in *ft-10* complementation experiments.

Acknowledgements

First of all, I would like to thank my supervisor **Dr. Franziska Turck** for her guidance and support, and discussion with her helped me so much not only in the project progress but also for my improvement in scientific training and understanding.

I would also like to thank:

Prof. Dr. George Coupland for giving me the opportunity to work in his department with great facilities provided by the Max Planck Institute for Plant Breeding Research. His advice helped me focus on the key objectives of the project.

Prof. Dr. Ute Höcker for being my Thesis Advisory Committee (TAC) member and the reviewer and examiner of my thesis

Prof. Dr. Stanislav Kopriva for being the chair of my thesis committee

Dr. Haoran Zhou for being my TAC member, and for his advice and discussion during my PhD study, which helped me a lot.

Dr. Simone Zündorf for being my best friend and the "neighbor" in the lab and her suggestions and support when I was under stress.

Petra Taenzler for her help with my projects and many basic lab work

Maik Mendler, Dema Alhajturki, Cristina Alcaide, Na Ding, Kang Wang, He Gao for their collaboration, support and advice.

Everybody in the Coupland department for a wonderful working atmosphere.

The China Scholarship Council (CSC) for providing financial assistance during my PhD period

The lab of Jing Wang from Huazhong Agricultural University, China for introducing the project background and providing *B. napus* seeds

The IT centre, greenhouse staff, the media kitchen for providing solid support to my PhD project

Chinese community in MPIPZ for all your discussion and help.

My family and friends for their love and support.

Curriculum Vitae

Name: Juanjuan Wang

Date of birth: January 18th, 1991

Place of birth: Jiangxi, China

Nationality: Chinese

E-mail: jwang2@mpipz.mpg.de

Education

10/2019-04/2024: Doctoral studies at the University of Cologne, Cologne, Germany

Max Planck Institute for Plant Breeding Research (MPIZ) in Cologne, Germany, under the supervision of Prof. Dr. G. Coupland

Scholarship of the China Scholarship Council (CSC)

09/2015-07/2019: Master of Institute of Botany, The Chinese Academy of Science, China

09/2009-07/2015: Bachelor of Jiangxi Agricultural University, China